unesco
Intergovernmental Oceanographic Commission

WORKSHOP REPORTS, 318

Expert meeting on seismic sources of tsunamis in the NW Caribbean and non-seismic sources in the Caribbean Region

HEREDIA, COSTA RICA | 3–5 DECEMBER 2024

Tsunami Ready

Published in 2026 by the United Nations Educational,
7, place de Fontenoy, 75352 Paris 07 SP, France

For bibliographic purposes this document should be cited as follows:

IOC-UNESCO. 2026. *Expert meeting on seismic sources of tsunamis in the NW Caribbean and non-seismic sources in the Caribbean Region, Heredia, Costa Rica, 3–5 December 2024*. Paris: UNESCO, (Workshop Reports, 318).

Cover: © Erik Lukas_Ocean Image Bank

Layout: UNESCO workshop

Printed in France

(IOC/2026/WR/318)

Intergovernmental Oceanographic Commission
Workshop Report No. 318

EXPERT MEETING ON SEISMIC SOURCES OF TSUNAMIS IN THE NW CARIBBEAN AND NON-SEISMIC SOURCES IN THE CARIBBEAN REGION

Heredia, Costa Rica | 3–5 December 2024

We would like to express our gratitude to our colleagues from the Universidad Nacional of Costa Rica, SINAMOT (Sistema Nacional de Monitoreo de Tsunamis), and OVSICORI (Observatorio Vulcanológico y Sismológico de Costa Rica) for their invaluable help in preparing this expert meeting, and all experts who have not only participated but also contributed to the preparation and validation of this report.

Table of contents

Executive Summary

The Expert Meeting on Seismic Sources of Tsunamis in the Northwest (NW) Caribbean and Non-Seismic Sources in the Caribbean Region was convened by the Intergovernmental Oceanographic Commission (IOC) of UNESCO in Heredia, Costa Rica, from 3–5 December 2024. The meeting brought together regional and international experts to improve understanding, characterization, and numerical modelling of tsunami sources in the Caribbean Basin, with a particular focus on the NW Caribbean and non-seismic mechanisms such as landslides and volcanic activity.

The meeting aimed to support Member States of the Tsunami and Other Coastal Hazards Warning System for the Caribbean and Adjacent Regions (CARIBE-EWS) in refining tsunami source databases, hazard assessments, and community preparedness initiatives under the Tsunami Ready Recognition Programme. It filled two key knowledge gaps: (1) The lack of validated seismic tsunami source models for the NW Caribbean (from the Gulf of Honduras to southern Cuba); and (2) The absence of a comprehensive review of non-seismic tsunami sources (landslides and volcanic events) across the entire Caribbean region.

Experts reviewed geological, geophysical, geodetic, and historical data to define 21 new seismic tsunami scenarios for the NW Caribbean. These scenarios are linked to known fault systems such as the Motagua–Polochic Fault Zone (Guatemala–Honduras), the Swan Island Fault Zone (Honduras–Cayman Trough), the Walton and Oriente Fault Zones (Jamaica–Cuba), and the Cayman Trough. Recent major earthquakes (e.g., 2009, 2018, 2020, 2025) were used to constrain rupture dimensions and slip parameters. Scenarios integrate realistic strike-slip and normal faulting geometries without assuming extreme, low-probability "mega-events."

Regarding non-seismic tsunamis, the experts proposed 9 new submarine landslide scenarios and 5 new volcanic tsunami scenarios. The new landslide tsunamis scenarios include 3 each in the Muertos Trough (Dominican Republic), Cariaco Basin (Venezuela), and Désirade–Barracuda Ridge (Guadeloupe) areas, with variable volumes (1–10 km^3). The volcanic tsunamis scenarios include updated Kick'Em Jenny volcano (Grenada) flank-collapse scenario, a tsunami generated by underwater explosion at Kick'Em Jenny, pyroclastic flow at the Soufriere St Vincent, and dome-collapses at Soufriere Hills (Montserrat) and Soufrière (Guadeloupe).

The results of numerical simulations of the 21 seismic and 9 landslide tsunami scenarios are included in the report, together with 3 additional scenarios in the SW Caribbean (San Andres Rift and Hess Escarpment).

Participants also endorsed recommendations on future works such as additional simulations of volcanic tsunamis, the implementation of the new scenarios proposed here in the CATSAM database, and the feasibility of a probabilistic tsunami hazard assessment (PTHA) for the Caribbean (noting the need for better input data).

1. Background and Objectives

1.1 Purpose

The Intergovernmental Oceanographic Commission (IOC) of UNESCO supported the Member States of the Tsunami and Other Coastal Hazards Warning System for the Caribbean and Adjacent Regions (CARIBE-EWS) to better understand and quantify earthquake sources in the Northwest Caribbean and non-seismic sources in the whole Caribbean and Adjacent Regions that can generate dangerous tsunamis. The purpose of the meeting was also to directly support community hazard assessments and holistic risk management, including contributing to the evacuation planning that are part of the implementation of the Tsunami Ready Recognition Program in the Caribbean and its Adjacent regions.

1.2 Objectives

The meeting aimed to deliver a number of outcomes which are summarised in this IOC Technical Report. All participants endorsed and supported the report. The objectives can be summarized as follows, in agreement with key objectives of ICG/CARIBE-EWS. The expert meeting fills two gaps: the first one in terms of geographical coverage for seismic sources of tsunamis, the second one in terms of non-seismic sources for the entire Caribbean. Previous meetings have specifically covered the following areas:

- Earthquake and Tsunami Hazard in Northern Haiti- Historical Events and Potential Sources (IOC, 2013, WR-255, in red on Fig. 1).
- Sources of tsunamis in the Caribbean with possibility to impact the southern coast of the Dominican Republic (IOC, 2016, WR-276).
- Tsunami Hazard in Central America- Historical Events and Potential Sources (IOC, 2018, WR-278, in blue on Fig. 1).
- Sources of Tsunamis in the Lesser Antilles (IOC, 2019, WR-291, in green on Fig. 1).

The main geographical gap in terms of seismic sources thus extends from the Gulf of Honduras to southern Cuba (in orange on Fig. 1). In the online database of tsunami sources for the Caribbean (CATSAM - Caribbean and Adjacent Regions Tsunamis Sources and Models : https://www.ncei.noaa.gov/maps/CATSAM/) there are currently one scenario for the southern coast of Cuba (CUBA scenario, used for the CaribeWave17 exercise), one scenario between Jamaica and Haiti (JAMAICA scenario, used in CaribeWave20), and two scenarios for the Gulf of Honduras (ROATAN and GULF OF HONDURAS, this latter having been used for CaribeWave23). None of these scenarios has been validated at an expert meeting. The scenarios in the Gulf of Honduras were used for a training meeting in Honduras in 2016.

Figure 1. Map of the Caribbean showing areas covered by previous ICG/CARIBE-EWS expert meetings. The study area (NW Caribbean) is in orange.

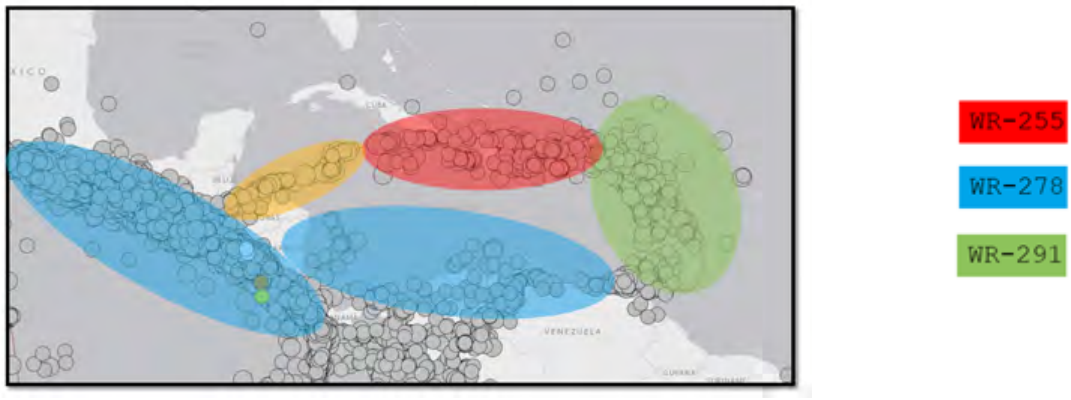

Non-seismic sources of tsunamis (landslides and volcanic eruptions) were previously discussed at an expert meeting on tsunami sources in the Lesser Antilles (IOC-UNESCO, 2020, WR-291, Martinique, 2019). The meeting's report includes a list of volcanic tsunamis observed in the Lesser Antilles since 1902, a list of potentially tsunamigenic volcanoes in the Antilles, and a table of scenarios of volcanic sources of tsunamis proposed by the experts.

This new meeting addresses non-seismic sources for the entire Caribbean. Volcanic tsunami sources were used for CaribeWave exercises in 2019 (Kick'Em Jenny volcano) and in 2023 (Mount Pelée). Considering the great uncertainty on such complex sources, it was simplified to a point source with a magnitude M_w 6.0 (which is not relevant for a volcanic source, but this is mandatory to trigger an alert), originated from Kick'em Jenny submarine volcano (Grenada). Following the expert meeting in Martinique, it was decided to add a better-defined landslide source from Kick'em Jenny, based on the numerical simulations of Harbitz et al. (2012). This is so far the only non-seismic source of tsunami listed in CATSAM and it was selected for the CaribeWave exercice to be organized in 2026.

1.3 Meeting Overview

Two separate meetings were initially recommended, one on non-seismic sources for the whole Caribbean, the other on non-seismic sources in the north-western Caribbean. For ecological and logistical reasons, it was decided to merge them. The meeting was organized in a hybrid format (Annex V).

During the first day, the first session involved all participants (joint session) and was devoted to presenting the objectives of the meeting (Frédéric Dondin and Raphaël Paris), the CATSAM scenario database (Nicolas Arcos), and the Tsunami Ready Recognition Program (Silvia Chacon-Barrantes). Participants were also able to take advantage of presentations illustrating the latest advances of the Global Tsunami Model project for the ICG/NEAMTWS (Tsunami Early Warning and Mitigation System in the North-Eastern Atlantic), the Mediterranean and Connected Seas, particularly in terms of PTHA and its applicability to the Caribbean (Finn Lovholt, Natalia Zamora, Hong Kie Thio, and Stefano Lorito). The second part of the first day was devoted to general presentations on the seismic sources of tsunamis in the NW Caribbean Region, tectonic setting and historical events (Emile Okal), and the non-seismic sources in the Caribbean Region (Raphaël Paris). During the second day, the experts split into two groups (parallel sessions) to discuss possible scenarios and recommended parameters for numerical simulations. Discussions also focused on the relevance and feasibility of a probabilistic approach, particularly for non-seismic sources. At the final joint session (Day 3), participants took stock of the parallel discussions, and preliminary results were presented. The final discussion also included a proposal for a hybrid earthquake-landslide scenario to be used for a future CaribeWave exercise.

2. Regional Overview

In this section we briefly review on one side the tectonic setting, the historical seismicity and tsunamis in the Northwest Caribbean region, and on the other side the non-seismic (landslide and volcanic) sources of tsunamis in the whole Caribbean region.

2.1 The Northwest Caribbean Region

2.1.1 Tectonic setting of the NW Caribbean

The northwest Caribbean region, as defined in this report, extends from the Gulf of Honduras to Cuba and Jamaica, with a southern extension to the Hess escarpment off Nicaragua (Fig. 2). From a tectonic point of view, this region is at the crossroads between the wedge-shaped triple junction of the North America, Cocos and Caribbean plates to the West (green rectangle on Fig. 2), and the subduction of the Antilles to the East. The deformation associated with the relative motion of the three plates is largely accommodated by a 1500 km long system of left-lateral, strike slip (transform) faults (red lines on Fig. 2) (Lyon-Caen et al., 2006; Authemayou et al., 2011; Guzman-Speziale, 2022; Calais et al., 2023). The North American plate moves westward relative to the Caribbean plate at an overall velocity of 18-20 mm per year (DeMets et al., 2000; Symithe et al., 2015).

Figure 2. Map of the general tectonic setting of the Caribbean, showing the North-America – Cocos -Caribbean triple junction (green rectangle) and the system of transform faults (red lines) accommodating the deformation associated with the relative motion of the three plates, as indicated by the values of plate velocity in cm/yr. (Guzman-Speziale, 2022). MAT – Middle America trench; MP – Motagua-Polochic fault zone; CT – Cayman trough; E-PG – Enriquillo – Plantain Garden fault zone; O – Oriente fault zone; S – Septentrional fault zone; SI – Swan Island fault zone; W – Walton fault zone. Orange triangles are volcanoes with historic activity of the Central America volcanic arc (CAVA) and the Trans Mexican volcanic belt (TMVB).

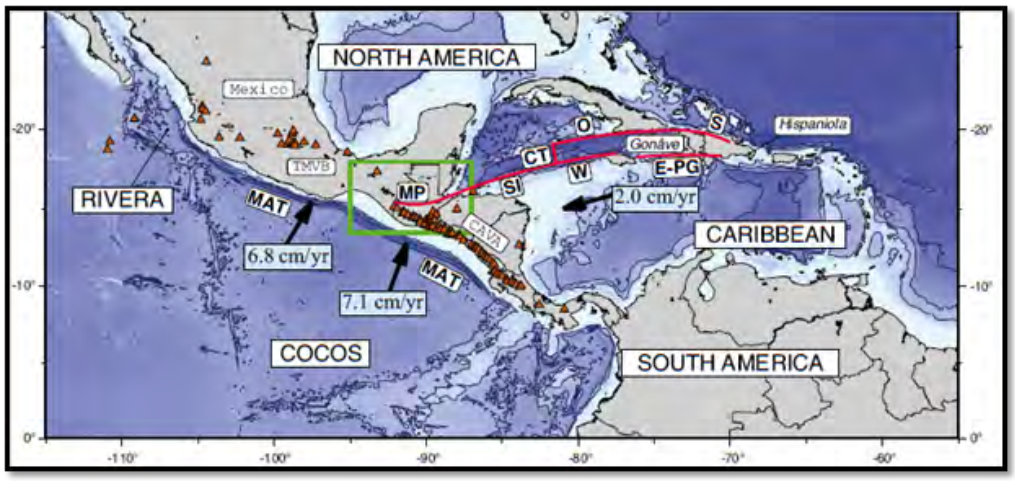

Figure 3. Map of the seismicity and geodesy of the NW Caribbean, showing the earthquakes with a magnitude M > 3, the focal mechanisms of earthquakes with M > 6, and the GPS velocities (Calais et al. 2023). The region of interest for this study is circled in black.

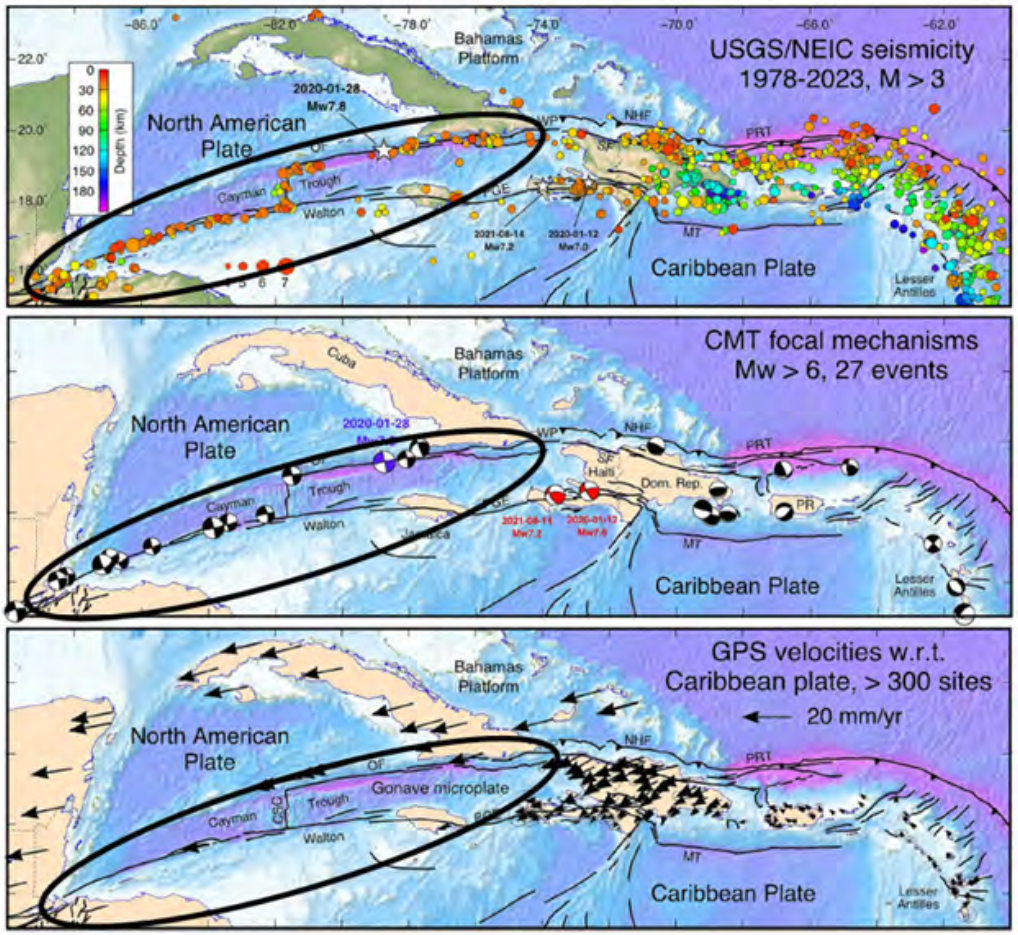

West of the Cayman Islands, the plate boundary appears to be a single strike-slip fault zone (Swan Island fault), whereas to the East it becomes dual or multi-branched and especially wide, with a seismogenic zone up to 250 km wide at the longitude of Hispaniola (Mann et al., 1995). Indeed, different microplates appear to partition the deformation at the boundary between the North America and Caribbean plates, the largest one being the Gonâve microplate between Cuba, Hispaniola and Jamaica (Rosencrantz and Mann, 1991). The exact extent and boundaries of these microplates are not very well defined, especially between Hispaniola and Puerto Rico (e.g., Benford et al., 2012). The transition from a single to a dual-branched strike-slip system is characterized by a small extensional pull-apart basin, known as the Cayman Trough. The basin measures 100 km from the NNW to the SSE and is bounded to the SW by the Swan Island fault, to the SE by the Walton fault, and to the NE by the Oriente fault (Rosencrantz and Mann, 1991). Gravity and magnetic data (ten Brink et al. 2002) suggest that 2–3-km-thick oceanic crust, formed at the ultraslow spreading Mid-Cayman Spreading Centre (15-17 mm/yr after DeMets et al. 2007), is juxtaposed against the 20–30-km-thick continental crust (Peirce et al., 2019).

Models of GPS velocities show that east of the Cayman Trough, the Oriente northern strike-slip branch, extending from the Cayman Islands to Hispaniola, accommodates about 10 mm/year of the overall plate motion (Symithe et al., 2015; Calais et al., 2023). A similar slip rate is deduced for the southern Walton - Plantain-Garden branch. On the western side of the study area, most of the relative motion of the tectonic plates is accommodated by the Motagua fault at slip rates that decrease westwards from 14 mm/year in eastern Guatemala to < 2 mm/year in western Guatemala (Ellis et al., 2019).

From West to East, the main tectonic features of interest for the purpose of this study are:

- the Motagua-Polochic continental faults (MP), crossing Guatemala and ending to the East in the Gulf of Honduras, with an overall W-E orientation;
- the Swan Island submarine fault zone (SI), connecting the Gulf of Honduras to the Cayman Trough, with a WSW-ENE orientation;
- the Cayman Trough (CT), oriented NNW-SSE between the Swan Island fault to the West, and the Oriente and Walton faults to the East;
- the Walton fault zone (W), extending W-E from the southern tip of the Cayman Trough to the North of Jamaica;
- and the Oriente fault zone (O), from the northern tip of the Cayman Trough to the southern coast of Cuba.

Figure 4. Map of major historical earthquakes in the Northwest Caribbean region, showing the earthquake epicentres (red stars for well-located earthquakes, pink stars for poorly located earthquakes), the surface ruptures of recent earthquakes (red ellipses), and the main faults (yellow lines).

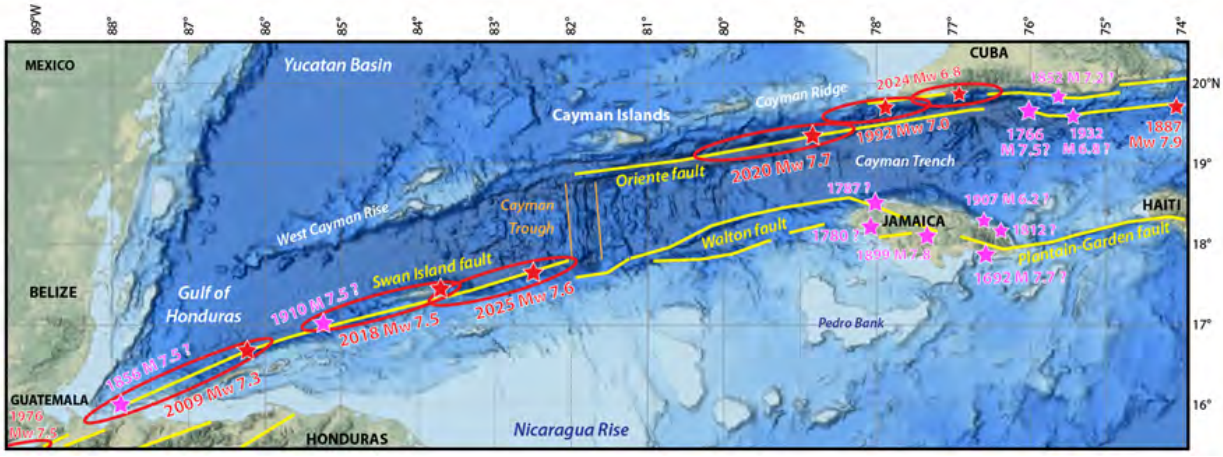

2.1.2 Historical earthquakes in the NW Caribbean

In the NW Caribbean, 15 earthquakes with $M_w > 6$ were recorded since 1978, all with a strike-slip focal mechanism and a depth < 30 km (Fig. 3). In the NCEI database of significant earthquakes, i.e. large enough to have a destructive impact on human societies at a local to regional level (https://www.ngdc.noaa.gov/hazel/view/hazards/earthquake/search), 43 earthquakes are listed for the 1539-2025 period in the NW Caribbean, with very limited information on about half of these events, particularly before 1692. There are no earthquakes with M > 8, but at least 7 events with M ≥ 7. Historical earthquakes are distributed along the main tectonic features (Fig. 4) such as the strike-slip fault zones of Swan Island (M > 7 earthquakes in 1856, 1910, 2009, 2018, and 2025), and Oriente (M > 7 in 1775, 1992, and 2020). At the junction between the Walton and Plantain-Garden strike-slip fault zones, Jamaica island is crossed by several major active faults and thus heavily impacted by earthquakes. The deadliest events in the NW Caribbean were the 1692 M = 7.7 (~3000 fatalities), 1780 (~300) and 1907 M = 6.2 (~1000) earthquakes, all three in Jamaica. The 1957 M = 6.2 was the strongest felt earthquake since 1907 in Jamaica.

Interestingly, the main seismic ruptures (M > 7) of the Motagua-Swan Island fault zone are regularly spaced, with epicentres 150 to 200 km apart, and a migration from west to east involving the earthquakes of 1976, 2009, 2018, and 2025 (Fig. 4). This time-space distribution illustrates the strain partitioning along a relatively regular segmentation of the fault zone. However, it remains difficult to develop any recurrence model because the ruptures are relatively well constrained only for the instrumental period. The four recent left-lateral strike-slip earthquakes on steeply dipping (>80°) fault planes have been well-characterized in terms of rupture extent and slip distribution (Graham et al., 2012; Cheng and Wang, 2020; Ye et al., 2025), providing examples of possible scenarios of rupture for the different segments of the Swan Island fault zone.

As an example, the M_W = 7.3 2009 earthquake had a 250 km long rupture zone with patchy slip of 1 to 6 m (Graham et al., 2012; Ye et al., 2025), with rupture along two segments of the Swan Island fault zone, the westernmost of which extends to the Motagua fault (later we designate this as the Motagua offshore fault, to distinguish it from the further westward extent of the Swan Island fault). The previous onland Motagua fault ruptured in the 1976 MS = 7.5 earthquake (Fig. 4). The 2009 event was followed by the 2018 M_w = 7.5 and 2025 M_w = 7.6 Swan Island fault earthquakes, located respectively 300 km and 450 km to the east (Fig. 4). The January 10, 2018 event involved slip of up to 10-25 m distributed along an 80 km rupture length north of eastern Honduras, while the February 8, 2025 event had comparable peak slip along a 72 km rupture length extending to near the Cayman Trough (USGS-NEIC; Ye et al., 2025). These are very large slip values for strike-slip ruptures of these lengths but slip is not uniform along the fault. Cheng and Wang (2020) calculated that one of the strike-slip subfaults that ruptured during the 2018 earthquake had a rupture speed slightly faster than the local shear wave velocity, implying a supershear process. Unlike these recent events, our knowledge of the earthquakes of 1856 and 1910 (both M ~ 7.5) is much more limited.

Large earthquake trends are less clear for the Oriente fault zone compared to the Swan Island fault zone, although there is also a fairly regular spacing (~100 km) between epicenters of the large ruptures of 2020, 1992, 2024 and 1766 (from west to east). With a magnitude M_W = 7.7, the January 28, 2020 Cayman Islands earthquake is the largest event in the NW Caribbean since the 1692 earthquake in Jamaica, but its impact was much more limited (300 buildings damaged in Cuba) because the epicentre was located at least 120 km from any populated land. The rupture propagated westward along a 300 km section of the steeply dipping (~82°) Oriente fault zone with patchy slip of up to 12 m (Ye et al., 2025), possibly with two successive supershear episodes (Tadapansawut et al., 2021). The May 25, 1992 M_W 6.8 event ruptured on a northward dipping (~53°) left-lateral Oriente fault (USGS-NEIC; Perrot et al., 1997). The adjacent November 10, 2024 M_W 6.8 event to the east ruptured bilaterally over a 40 km stretch of the northward dipping (~52°) fault south of western Cuba with peak slip of up to 1.5 m (Ye et al., 2025). These three recent ruptures do not appear to have any overlap of their slip zones.

Moving eastward along the Oriente fault zone, the focal mechanisms become more complex and the depth of the earthquakes also increases (Cotilla Rodriguez et al., 2007). On the southern coast of Cuba, there is a cluster of seismicity south of Santiago de Cuba, with 12 earthquakes M > 6 since 1578 (Calais et al., 1998; Cotilla Rodriguez et al., 2007; NCEI database). At least two of these earthquakes were deadly: the 1766 M = 7.5 and the 1932 M = 6.8 earthquakes killed 120 and 14 people respectively.

In this seismic "landscape", there are two seismic gaps east of the Cayman Trough (Fig. 3). The first one is located on the western part of the Oriente fault zone (Cayman Ridge segment), and the other one is on the western part of the Walton fault zone, as confirmed by the geographical distribution of earthquakes with M > 3 during the last 50 years (Fig. 3). The gap of the western Oriente fault zone is consistent with GPS models assuming a full creeping of the Cayman Ridge segment (Calais et al., 2023).

2.1.3 Historical tsunamis in the NW Caribbean

We have examined the information compiled in the NCEI database of tsunami events and runups (https://www.ngdc.noaa.gov/hazard/tsu_db.shtml), in which 16 tsunamis are listed for the NW Caribbean, and additional information gathered from available publications. Relevant information is summarized event by event below.

- 24 November 1539: an earthquake referred to as the "Cabo de Higueras earthquake" occurred in the Gulf of Honduras and may have produced a tsunami. Sailors accounts mention a "sea quake", ground shaking, and landslides.
- 7 June 1692: the M = 7.7 earthquake destroyed Port-Royal, the capital of Jamaica, built on a small peninsula, connected to the mainland by a thin sand ridge in the middle of the bay. The site was thus highly vulnerable. A 1.8 m wave crossed the bay (this is thus not really a runup), ships were overturned, and 90% of the building were destroyed. 45 km^2 of the peninsula were inundated by the tsunami. Landslide were observed in the harbour. The earthquake killed ~1000 people, and the tsunami ~2000. Following the disaster, the capital of Jamaica was moved further north to Kingston.
- 11 February 1775: a large earthquake south of Santiago de Cuba, also felt in Hispaniola, generated waves that caused extensive destruction on the southern coast of Cuba.
- 27 October 1787: an earthquake in NW Jamaica produced sea level agitation in the harbour of St James, Montego Bay.
- 11 November 1812: On the northern coast of Jamaica, the sea was much agitated following an earthquake. A landslide may have occurred in the Bay of Annotto, where the anchorage ground sank.
- 17 July 1852: a questionable earthquake located south of Santiago de Cuba, was associated to a wave that engulfed the bay, affecting vessels and port structures.
- 4 August 1856: the M = 7.5 earthquake in the Gulf of Honduras generated a tsunami that impacted all coasts of the gulf from Belize to Trujillo in Honduras. The waves reached the base of the Fortaleza de San Fernando at Omoa, 550 m inland (runup of 5 m a.s.l.), on the north-western coast of Honduras (probably very close to the epicentre). The tsunami was well observed in the rivers as a bore propagating inland, sometimes preceded by a water withdrawal.
- 23 September 1887: a M 7.9 earthquake in the Windward Passage, eastern part of the Oriente fault zone generated a tsunami that is reported on the south-eastern coast of Cuba and the western coast of Hispaniola (Haiti), but very limited information is available.
- 19 February 1893: an earthquake was felt in Kingston, Jamaica, followed by large ripples crossing the harbour.
- 14 January 1907: the M = 6.2 earthquake located north of Jamaica generated a tsunami with an initial sea withdrawal of 3 m and runups up to 2.5 m on the northern coast of Jamaica. The tsunami was also observed on the southern coast in Kingston, which was extensively damaged by the earthquake.
- 3 February 1932: the M = 6.7 earthquake south of Santiago de Cuba generated a minor tsunami (according to tide gauge records and reports from a ship).
- 4 February 1976: this M_s = 7.5 earthquake in Guatemala (Plafker, 1976) was particularly disastrous but since its epicentre was located 70 km inland it produced a very small tsunami in the Gulf of Honduras, recorded by a nearby tide gauge in Honduras (12 cm).
- 28 May 2009: the M_W = 7.3 earthquake on the western part of the Swan Island fault zone produced a tsunami whose effects were described at the mouth of the river Motagua in Guatemala. The retreat of the water was followed by a surge carrying debris that damned the exit of the river. As a result, the river level rose by 2 to 4 m over a distance of 1 km, flooding 500 m on either side of the bed. The flood lasted 24 hours and was observed up to 25 km inland.
- 10 January 2018: the M_W = 7.5 earthquake on the Swan Island fault generated a small tsunami that was recorded on tide gauges in Belize and Mexico, with amplitudes from 1 to 8 cm. A runup of 40 cm was observed on Roatan Island, at 330 km from the epicentre.
- 28 January 2020: following the M_W = 7.7 earthquake on the Oriente fault zone, the Pacific Tsunami Warning Center (PTWC) issued a tsunami warning message, forecasting that the earthquake could generate a small tsunami with a maximum wave amplitude of 0.3 to 1 m in Cuba, Jamaica, Cayman Islands, Honduras, Mexico and Belize (Xu et al., 2022). A small tsunami was indeed recorded by the tide gauge in George Town (Cayman Islands, 290 km from the epicentre), with an amplitude of 12 cm 11 minutes after the earthquake.
- 8 February 2025: the M_w = 7.6 earthquake on the eastern part of Swan Island fault zone prompted the PTWC to trigger an alert indicating possible hazardous waves for all the countries around, later restricted to the Cayman Islands, Cuba, and Honduras. A very small tsunami (max 4 cm) was recorded by the Isla de Mujeres tide gauge in Mexico. This event represents an example of a tsunami detected only by current instrumental means, which clearly illustrates the difference with historical event catalogs.

Table 1. List of historical tsunamis in the Northwest Caribbean region (compiled from a review of available publications and the NCEI database: https://www.ngdc.noaa.gov/hazard/tsu_db.shtml).

Date	Source		Tsunami size		Tsunami location
yr-mm-dd	***Type***	***Fault zone***	***Observations***	***Tide gauge***	***countries***
1539-11-24	earthquake	Swan Island (Gulf of Honduras)			Guatemala, Belize, Honduras
1692-06-07	M = 7.7 earthquake	South Jamaica and/or Garden-Plantain	1.8 m (wave height)		Jamaica, Haiti (?)
1775-02-11	earthquake	Oriente (Cuba)			Cuba
1787-10-27	earthquake	Walton? (Jamaica)			Jamaica
1812-11-11	earthquake	Blue Mountains? (Jamaica)			Jamaica
1852-07-17	earthquake	Oriente (Cuba)			Cuba
1856-08-04	M = 7.5 earthquake	Swan Island (Gulf of Honduras)	5 m (runup)		Guatemala, Belize, Honduras
1887-09-23	M = 7.9 earthquake	Oriente (between Cuba and Hispaniola)			Cuba, Haiti
1893-02-19	earthquake	South Jamaica			Jamaica
1907-01-14	M = 6.2 earthquake	Blue Mountains (Jamaica)	2.5 m (runup)		Jamaica
1932-02-03	M = 6.7 earthquake	Oriente (Cuba)		yes, but not quantified	Cuba
1976-02-04	M_s = 7.5 earthquake	Motagua (Guatemala)		12 cm (amplitude)	Guatemala, Honduras
2009-05-28	M_W = 7.3 earthquake	Swan Island (Gulf of Honduras)			Guatemala, Honduras
2018-01-10	M_W = 7.5 earthquake	Swan Island	40 cm (runup)	1-8 cm (amplitude)	Guatemala, Honduras, Belize, Mexico
2020-01-28	M_W = 7.7 earthquake	Oriente		12 cm (amplitude)	Cayman Islands
2025-02-08	M_w = 7.6 earthquake	Swan Island		4 cm (amplitude)	Mexico

All tsunami listed in Table 1 were generated by earthquakes. It is interesting to note that some very powerful earthquakes were apparently not tsunamigenic (e.g., 1766 Cuba, 1780 Jamaica), and many others produced tsunamis of very low amplitude (e.g., 1976, 2009, 2018, 2020, 2025). Admittedly, catalogues of recent tsunamis are much more complete (thanks to tide gauge data) than historical catalogues. The strike-slip nature of the plate boundary is generally not conducive to the generation of large tsunamis (i.e. with waves > 1 m at the shoreline). An additional landslide source was proposed to explain some local observations (e.g., the 5 m runup in Honduras during the 1856 tsunami). Xu et al. (2022) argued that the January 28, 2020 tsunami was not generated solely by coseismic seafloor deformation from the M_w = 7.7 strike-slip earthquake, but that a submarine landslide was the primary cause. The September 28, 2018 earthquake along the Palu-Koro strike-slip fault (Sulawesi, Indonesia) was associated with a devastating tsunami in Palu Bay. Many publications concluded that the local tsunami was generated by multiple landslides in the bay (e.g., Nakata et al., 2020; Williamson et al., 2020). However, Elbanna et al. (2021) demonstrated that the length and high velocity of the rupture (supershear) in a narrow and shallow bay could explain the unexpected tsunami in Palu, without requiring co-seismic landslides. They indicated, the presence of an apex at the tip of the bay represents an aggravating factor, since it results in a strike-normal horizontal displacement combined with wave focusing, reflection, and refraction. However, other more comprehensive simulations by Schambach et al. (2021) of dual EQ-landslide sources, using more advanced models, reached the opposite conclusion that the landslides were major contributors to the observed tsunami runups and inundation. The Gulf of Honduras presents a somewhat similar, albeit less narrow, context to Palu Bay, in the Bahia de Amatique (Guatemala) and Bahia de Omoa (Honduras).

Figure 5. Vintage view of the 1856 tsunami in Honduras (De Ballore, F. de M., 1888, Tremblements de Terre et éruptions volcaniques au Centre Amérique, depuis la conquête espagnole jusqu'à nos jours. Imprimerie et Lithographie Eugène Jobard, Paris).

2.1.4 Paleotsunamis in the NW Caribbean

Tsunamis can also be described in terms of their morphological impact (erosion marks) and sedimentological impact (sedimentary deposits), which sometimes enables us to extend the catalog of historical tsunamis. Traces of paleotsunamis have been described in several places in the Caribbean (Engel et al., 2016, and references therein). Work carried out in the NW Caribbean has shown the existence of coarse-grained littoral deposits (boulders, pebble ridges, berms of gravel deposits) on the Yucatán coast of Mexico (Shaw and Benson, 2015), on Grand Cayman (Jones and Hunter, 1992; Robinson et al., 2006), and in Jamaica (Rowe et al., 2009), but their origin - hurricane versus tsunami - is still debated. To date, there is no unequivocal evidence of paleotsunami deposits in the NW Caribbean. In-depth studies in coastal marshes could prove very useful in identifying tsunamigenic events on a Holocene scale.

2.2 Non-Seismic Sources Of Tsunamis in the Caribbean Region

Non-seismic tsunami sources include gravitational, volcanic-gravitational and purely volcanic (i.e. directly linked to eruptive phenomena). For the purposes of this study, tsunamis linked to meteorite impacts will not be considered. When distinguishing landslide and volcanic tsunamis, there is always an overlap linked to landslides in a volcanic context. On volcanic islands, some landslides are directly linked to volcanic activity (e.g. collapse of an active lava dome, landslides caused by magmatic intrusion), while others are linked to meteorological events or earthquakes. We have chosen to group together all landslide sources of tsunamis, whatever their geological context (volcanic islands, carbonated shelf, river deltas, etc.). We have not included remote sources such as a tsunami generated by a massive flank collapse of La Palma in the Canary Islands, as this scenario and its possible impact on the Antilles have already been widely discussed (e.g., Tehranirad et al., 2015).

2.2.1 Landslide sources of tsunamis

The Caribbean Basin is exposed to tsunamis generated by landslides, which are identified by the scars and submarine mass-wasting deposits they formed. Landslides were most particularly frequent in the volcanic arc of the Lesser Antilles, with 47 main events during the last 1.2 million years, including 15 during the last 12 thousand years (Boudon et al., 2007). Volcanic island flank failures typically involve volumes ranging from a few hundred million m^3 to several tens of km^3. As an example, Lebas et al. (2011) detected seven major mass-wasting events off Martinique, the oldest one being dated at ~2.5 Myrs ago). Detailed record at the island scale reveals more frequent but less voluminous events in the northern part of the volcanic arc (Coussens et al., 2016). IODP expedition 340 carried out in 2012 led to numerous publications on mass-transport deposits offshore Montserrat and Martinique islands (Le Friant et al., 2020 and references therein). One of the main advances concerns the source of material involved in these large landslides. Indeed, the proximal volcanic debris avalanche deposits are usually restricted to the slopes of the volcanic islands, but their emplacement can trigger voluminous failures of seafloor sediment in the deep-sea basin (Watt et al., 2012; Le Friant et al., 2015). As an example, Brunet et al. (2016) observed three large-scaled subaerial flank collapses of Mount Pelée, Martinique, that remobilized seafloor sediment and certainly caused a large local or even regional tsunami.

Figure 6. Schematic figure of the processes acting during the emplacement of a large volcanic debris avalanche offshore a volcanic island (Le Friant et al., 2015).

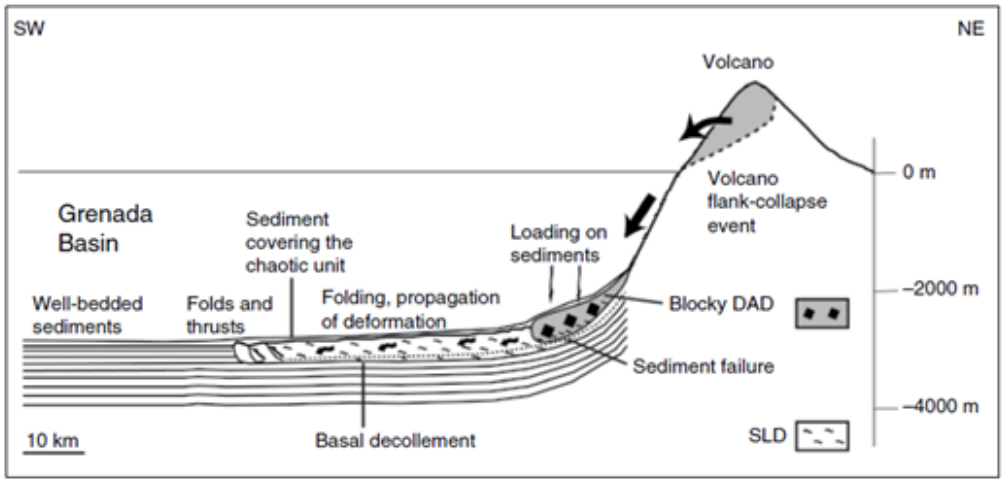

The multi-stage and multi-process nature of volcanic island slope failures complicates the parameterization of numerical simulations. In terms of tsunami generation, landslides composed of mainly seafloor sediments may generate smaller tsunamis than equivalent volumes of subaerial block-rich mass flows rapidly entering water (Le Friant et al., 2015). When a subaerial landslide enters the water it generates an impulsive wave, which receives most of the energy transferred from the landslide, and then propagates away from the source. The water in front of the landslide is pushed forward, and the water above is pushed upward. The height of the leading and largest wave is positively correlated to landslide Froude number, relative thickness, mass flux and volume (Fritz et al., 2004; Yavari-Ramshe and Ataie-Ashtiani, 2016). In the case of a submarine landslide, the main parameters controlling the tsunamigenic potential are the volume of the sliding mass, its initial acceleration, and its maximum velocity (e.g., Harbitz et al. 2006, Yavari-Ramshe and Ataie-Ashtiani 2016; Roger et al., 2024).

There is also evidence of non-volcanic large submarine landslides everywhere in the Caribbean Basin, as evidenced by bathymetric surveys and seismic profiling on island slopes and shelf margins (e.g., Moscardelli et al., 2006; ten Brink et al., 2006; Chaytor et al., 2016; Leslie and Mann, 2016). As an example, Tarazona et al. (2023) identified 220 submarine landslides on the slopes of the continental shelf off Colombia, with areas ranging between 0.1 and 209 km^2 (Fig. 7).

Many studies on submarine landslides are aimed at defining laws of landslide size distribution (e.g., ten Brink et al., 2006, 2009), and assessing landslide susceptibility (e.g., Grilli et al., 2009; Collico et al., 2020; Tarazona et al., 2023). On the northern edge of the carbonate shelf north of Puerto Rico, ten Brink et al. (2006) found that the cumulative distribution of slope failure volumes follows a power-law distribution. Large submarine landslide scars (> 1 km^3) are "surprisingly" less abundant in active margins that experience frequent earthquakes compared to passive margins (Urgeles and Camerlenghi, 2013). The common explanation for this observation is that, in active margins, frequent co-seismic small failures allow the slopes to be regularly purged. There is also a possible effect of sediment densification induced by repeated seismic shaking, resulting in a slope stability increase with increasing earthquake frequency and decreasing sedimentation rates (ten Brink et al., 2016). The influence of high sedimentation rates on landslide susceptibility is well-illustrated by the numerous submarine slope failures observed on the deltas of the Magdalena River in Colombia (Leslie and Mann, 2016) and Orinoco River in Venezuela (Moscardelli et al., 2006).

Figure 7. Map of the northwest of Colombia showing different types of submarine landslide deposits associated with different environments, from canyon walls and channel-levee systems, to tectonically controlled ridges and continental shelf break (Tarazona et al., 2023).

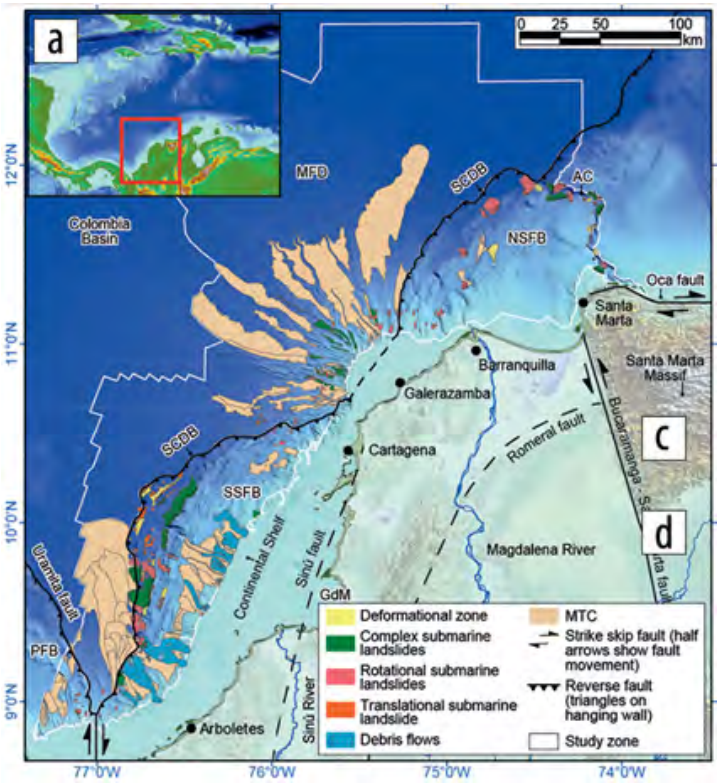

In terms of landslide tsunami hazard, even a small landslide on the order of tens of millions m^3 can produce local tsunamis that could threaten nearby communities (e.g., landslide tsunami at Stromboli volcano in 2002: Bonaccorso et al., 2003). During an earthquake, slope failures of all size may be produced, from large slumps > 1 km^3 (e.g., Papua New Guinea1998: Tappin et al., 2001) to coastal cliff collapses < 10 million m^3, which locally augment the height of tsunami waves produced by the earthquake itself. In the Caribbean, there are discussions about possible co-seismic landslides during the 1692 (Kingston, Jamaica), 1856 (Gulf of Honduras), and 1882 (Panama) earthquakes, and their contribution to local tsunami runup, as mentioned in the NCEI database. However, there is no direct (and published) evidence of these landslides. López-Venegas et al. (2008) documented a fresh submarine landslide with an estimated volume of 10 km^3 in northwestern Puerto Rico, and they demonstrated that a landslide source better reproduces the wave heights observed on the western coast of Puerto Rico after the October 11, 1918 M_L = 7.5 earthquake in the Mona Passage, rather than the earthquake itself. Submarine telegraph cables were reported to be cut in this area following the earthquake. The January 12, 2010 M_w = 7.1 Haiti earthquake ruptured an inland segment of the Enriquillo-Plantain Garden strike-slip fault zone, but it produced local tsunamis with wave runups up to 3 m on both sides of the Southwestern Peninsula of Haiti (Fritz et al., 2013). The tsunamis could not be related to the rupture velocity, which was typical at 2.6 km/s (de Lépinay et al., 2011), and they were convincingly attributed to multiple landslides on the northern and southern coasts of the peninsula (Hornbach et al., 2010; Poupardin et al., 2020).

Figure 8. Map of submarine landslides triggered by the January 12, 2010 M_w = 7.1 strike-slip earthquake, southwestern coast of Haiti, and maximum computed tsunami wave heights, which are in agreement with observed runups inland (Poupardin et al., 2020).

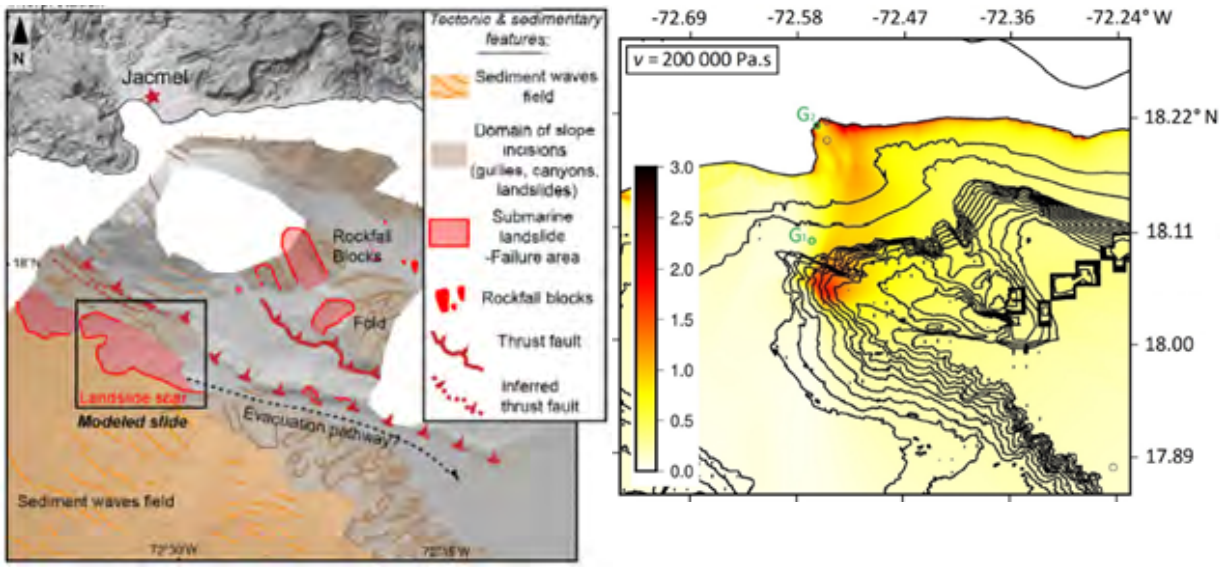

2.2.2 Volcanic sources of tsunamis

In addition to landslides, the activity of volcanoes can generate tsunamis through various processes, such as pyroclastic flows, eruptive column collapse, underwater explosions, caldera collapse, volcano-tectonic earthquakes, or atmospheric waves following major explosions (Paris, 2015; Schindelé et al., 2024). All these source mechanisms differ in terms of volume, mass flux, duration, and interaction with water. The complexity of the physical processes at work during the generation of volcanic tsunamis makes their numerical modelling a challenge. This is why, first and foremost, it is important to understand the links between the different types of volcanoes and the different types of eruptions on the one hand, and the different mechanisms that generate volcanic tsunamis on the other (Schindelé et al., 2024).

Figure 9. Source mechanisms of volcanic tsunamis, including gravitational (subaerial and submarine landslides, pyroclastic flows, eruptive column collapse), explosive (underwater explosions, atmospheric forcing), and volcano-tectonic processes (caldera collapse, volcano-tectonic earthquakes). Modified from Paris et al. (2014).

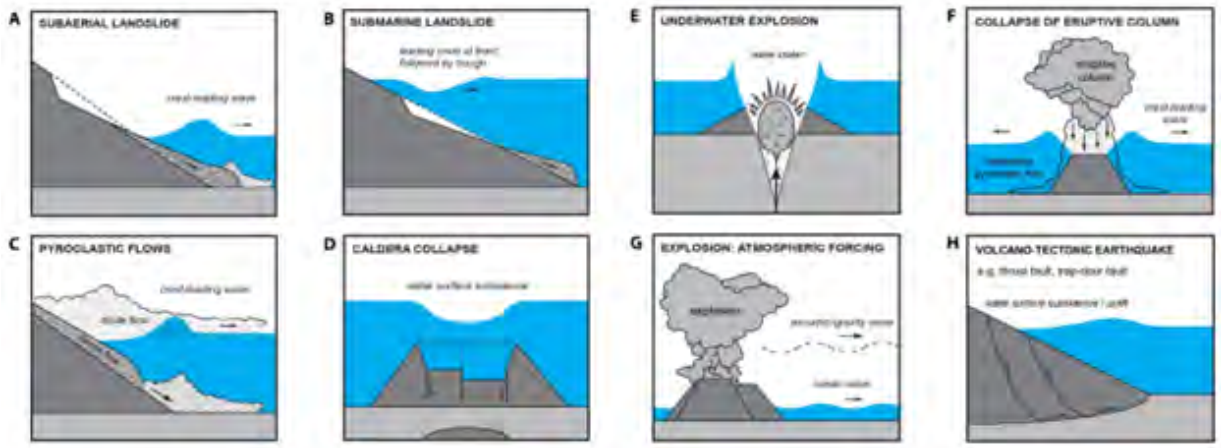

Two major events have alerted the scientific community to the need to better understand volcanic tsunamis and integrate them into local and regional warning systems, in connection with volcano observatories: the December 22, 2018 tsunami in Sunda Strait, Indonesia, triggered by the collapse of Anak Krakatau volcano (e.g., Grilli et al., 2019; Muhari et al., 2019), and the January 15, 2022 worldwide tsunami produced by atmospheric waves of the Hunga Tonga explosions (e.g., Borrero et al., 2022; Carvajal et al., 2022; Omira et al., 2022). As a response, the IOC-UNESCO Working group on TOWS (Tsunamis and Other hazards related to sea level Warning and mitigation Systems) created an *Ad Hoc* team on Tsunamis generated by Volcanoes (TGV) under its Task Team on Tsunami Watch Operations (TT-TWO). The TGV team aimed to specifically document the processes of tsunami generation during volcanic eruptions, the modelling techniques, examples of monitoring and warning systems designed for volcanic tsunamis, establish a list of priority volcanoes to watch, a list of contacts in volcano observatories, and to provide guidance to Member States and IOC-UNESCO. For detailed background information on volcanic tsunamis, we thus refer the reader to the Technical Series report n° 183 (IOC-UNESCO, 2023).

In the Caribbean, 11 volcanic tsunamis occurred during the XXth and XXIst centuries (Table 2). All these tsunamis were generated by volcanoes of the Lesser Antilles and their impact was limited to nearby islands (i.e., typically within tens of kilometers). The activity of volcanoes in the Lesser Antilles certainly generated tsunamis before 1902, but there is no available information on this subject, apart from publications on past landslides on the slopes of the islands (see previous section). Apart from the Lesser Antilles, there are no other active volcanoes in the Caribbean that could pose a tsunami threat.

Two volcanic eruptions were particularly tsunamigenic: the 1902 eruption of Mount Pelée in Martinique (France), and the 1997-2010 eruption of Soufrière Hills in. The majority of the tsunamis observed during these two eruptions were related to pyroclastic flows entering the sea, except for the May 5, 1902 tsunami in St Pierre (Martinique), which was caused by a huge debris flow (Lacroix, 1904). On the night of the Boxing Day December 26, 1997, eruption at Montserrat, waves inundated the Old Road Bay, western coast, 4 km from the impact site of the pyroclastic flow with the water. The initial sea retreat was followed by inundation up to 80 m inland and a local runup of 3 m a.s.l. (Pelinovsky et al., 2004). There was no clear evidence of waves elsewhere. A major collapse of the volcanic dome on July 12, 2003, produced massive pyroclastic flows that reached the sea and caused a tsunami on the eastern coast, with a maximum runup of 4 m a.s.l. in Farm Bay, 4 km from the impact, and a noticeable runup (< 1 m) on the northwestern coast of Guadeloupe Island, 60 km from the volcano (Pelinovsky et al., 2004). We should also mention that shorth-length waves were observed on the coasts of Grenada, the southern grenadines and Barbados during the 1939 eruption of Kick'em Jenny submarine volcano, north of Grenada, but their exact height is highly uncertain (Smith and Shepherd, 1993, 1995; O'Loughlin and Lander, 2003; Lindsay et al., 2005).

Table 2. List of volcanic tsunamis observed in the Caribbean since 1902 (updated from IOC-UNESCO, 2020, and Lacroix, 1904). The worldwide tsunami due to atmospheric waves of the Hunga – Tonga volcanic explosions on January 15, 2022 was of course observed in the Caribbean (Sostre-Cortés et al., 2025), but it is not included in this list since it was not generated by a volcano in the Caribbean. Note that the 1965 tsunami in Grenada is ranked as "doubtful" in the NCEI database.

yr-mm-dd	Lat	Long	Country	Volcano	Tsunami source	Runup
1902-05-05	14.82	-61.17	Martinique, France	Mount Pelée	Debris flow	5 m
1902-07-05	13.33	-61.18	St Vincent and the Grenadines	Soufriere	Pyroclastic flow ?	1 m
1902-05-08	14.82	-61.17	Martinique, France	Mount Pelée	Pyroclastic flow	> 2 m
1902-05-20	14.82	-61.17	Martinique, France	Mount Pelée	Pyroclastic flow	> 3.5 m
1902-08-30	14.82	-61.17	Martinique, France	Mount Pelée	Pyroclastic flow	1 m
1939-07-24	12.30	-61.63	Grenada	Kick'em Jenny	Submarine explosion?	2 m
1965-10-24	12.30	-61.63	Grenada	Kick'em Jenny	Submarine explosion?	
1997-12-26	16.72	-62.18	Montserrat	Soufriere Hills	Pyroclastic flow	3 m
1999-01-20	16.72	-62.18	Montserrat	Soufriere Hills	Pyroclastic flow	2 m
2003-07-12	16.72	-62.18	Montserrat	Soufriere Hills	Pyroclastic flow	4 m
2006-05-20	16.72	-62.18	Montserrat	Soufriere Hills	Pyroclastic flow	1 m

3. Workshop Outcomes

3.1 Definition of the Earthquake Sources

The experts examined all available publications on the tectonic setting, historical seismicity and geodesy, and tsunami catalogues, to build a list of 21 new scenarios of tsunamis produced by seismic ruptures in the NW Caribbean region (Fig. 10 and Table 3). It is not the aim of this report to detail how each of the scenarios was defined, but Table 3 provides the main earthquake parameters required for numerical simulations: extent (length and width) and geometry of the rupture (strike, dip, rake), vertical slip, seismic moment (M_o), and moment magnitude (M_w).

Figure 10. Fault segments selected as seismic sources of tsunamis in the NW Caribbean region. Numbers refer to the seismic rupture ID as defined in Table 3. Seismicity catalogues : 1904-1964 M5+ events from ISC-GEM (Storchak et al. 2013) and 1964-2017 M3.6+ events from ISC-EHB (Di Giacomo and Storchak, 2016). Epicenters colors are function of depth : red for z from 0 to 29 km, orange 29-74, yellow 74-151 km.

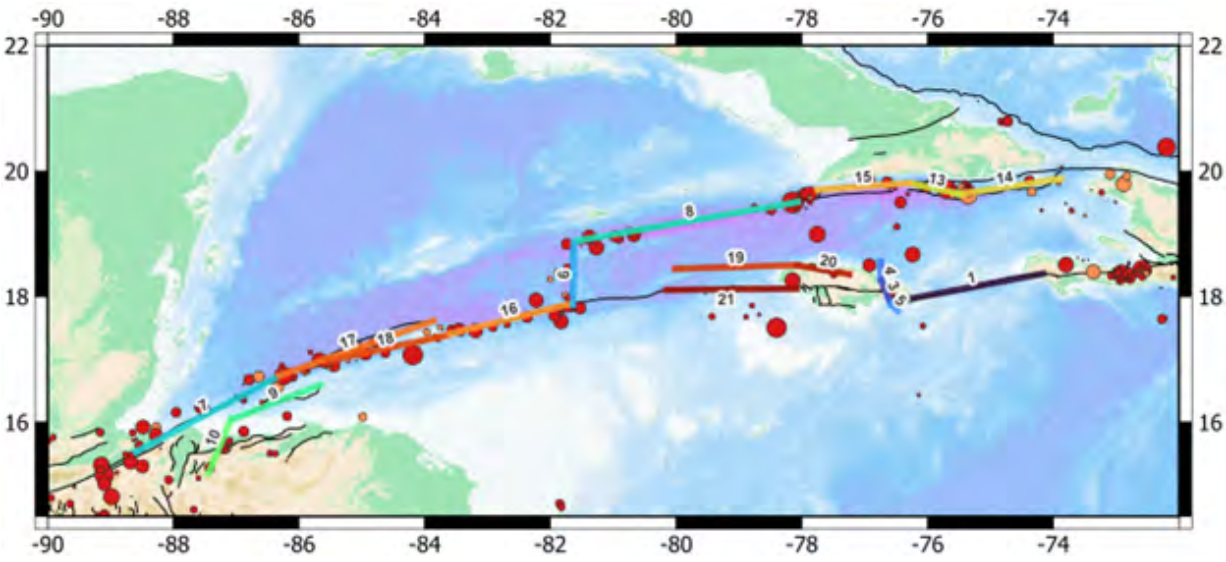

Table 3. Seismic source parameters of tsunami in the NW Caribbean. Scenario 22 is a combination of scenarios 3, 4 and 5, thus corresponding to a combined rupture of the three Jamaica segments. Same for scenario 23 (South Deformation Belt scenarios 13 and 14 combined). Each scenario has its own ID for numerical simulations. Scenarios 2, 11 and 12 are presented in section 4.1. (Hess Escarpment and San Andres Rift).

ID	Name	Length (km)	Azimut (°)	LongMin (°)	LongMax (°)	LatMin (°)	LatMax (°)	Strike (°)	Dip (°)	Rake (°)	Width (m)	Sismogenic depth (km)	Slip (m)	Mo	Mw
1	Enriquillo Plantain	242.5	79.30	-76.41	-74.161	17.938	18.363	262	70	35	22.5	20	2.6	4.257E+10	7.7
3	Jamaica Central	45.6	157.81	-76.74	-76.582	17.876	18.260	13	36	126	31	20	2.1	8.912E+10	7.2
4	Jamaica North	32.6	178.70	-76.75	-76.739	18.261	18.555	0	36	126	31	20	2.1	6.359E+10	7.1
5	Jamaica South	16.2	134.07	-76.58	-76.474	17.771	17.876	282	33	23	31	20	2.1	3.173E+10	6.9
6	Mid Cayman	108.4	0.73	-81.64	-81.632	17.868	18.847	0	45	-90	42	30	2.6	3.55E+10	7.6
7	Motagua offshore	279.1	62.12	-88.60	-86.309	15.527	16.738	46	52	15	25	20	3.1	6.489E+10	7.8
8	Oriente	374.7	80.03	-81.58	-78.071	18.889	19.504	375	90	-180	20	20	3.3	7.419E+10	7.8
9	Roatan offshore	161.2	68.68	-87.06	-85.659	16.047	16.592	254	45	-90	42	30	3.2	6.498E+10	7.8
10	Roatan onshore	102.7	22.58	-87.44	-87.083	15.194	16.055	20	50	-110	42	30	2.5	3.236E+10	7.6
13	South Def Belt Central	84.6	102.21	-76.28	-75.488	19.633	19.803	285	43	30	44	30	2.4	2.681E+10	7.6
14	South Def Belt East	169.4	81.28	-75.48	-73.882	19.632	19.877	260	36	90	50	30	3.6	9.148E+10	7.9
15	South Def Belt West	153.8	85.68	-77.75	-76.287	19.697	19.808	264	53	7	25	20	2.3	2.653E+10	7.5
16	Swan Island East	212.5	76.09	-83.60	-81.657	17.406	17.886	255	90	0	20	20	2.4	3.06E+10	7.6
17	Swan Island North	278.6	70.44	-86.31	-83.858	16.739	17.612	76	90	0	20	20	2.8	4.681E+10	7.7
18	Swan Island South	206.7	77.75	-85.55	-83.652	16.970	17.381	75	90	0	20	20	2.4	2.977E+10	7.6
19	Walton North	204.7	88.28	-80.02	-78.081	18.438	18.499	88	90	0	20	20	2.4	2.948E+10	7.6
20	Walton onshore	87.2	99.70	-78.06	-77.25	18.355	18.494	99	82	11	20	20	1.6	8.372E+10	7.2
21	Walton South	219.5	269.50	-76.75	-76.474	17.772	18.554	269	90	0	20	20	2.4	3.161E+10	7.6
22	Jamaica (3+4+5)														
23	South Def Belt (13+14)														
24	Motagua offshore (bis)	279.1	62.12	-88.60	-86.309	15.527	16.738	46	52	15	25	19	2.7	6.489E+10	7.8

The selection of the earthquake scenarios was largely guided by the documented earthquake history, which fills in extensive portions of the plate boundary system in the northwest Caribbean. For example, the 2009 Honduras earthquake helped to define the Motagua offshore (7, 24) scenario; the 2018 Swan Island earthquake the Swan Island North (17) scenario along with viable rupture of the Swan Island South (18) scenario; the 2025 earthquake the Swan Island East (16) scenario; the 2020 Cayman earthquake the Oriente (8) scenario; the 1992 and 2024 Cuba events the South Def Belt West (15) scenario; historic events off southern Cuba the South Def Belt Central (13,23) and South Def Belt East (14, 23) scenarios. While oceanic crust is very thin in most of these areas, juxtaposition against thicker continental crust along Honduras and Cuba suggests a possible fault depth extent of up to 20 to 30 km, although available slip models indicate slip may be concentrated at less than 10 km depths in some recent events (e.g., 2018 Swan Islands). The depth extent couples with the assumed uniform slip to control the scenario event size, with larger, but patchy slip of 10 to 24 m estimated for some recent events on the Swan Island and Oriente fault, so earthquake moments are comparable to those for observed events. An average crustal rigidity of 30 GPa is assumed, but this has uncertainty and likely varies laterally and with depth but details are not known. Scenarios around Jamaica (1-4, 19-22) are based on fault maps and reports of historic events lacking specific quantification. The Mid Cayman (6) scenario is a highly speculative normal faulting ridge extension model for completeness. The Roatan (9, 10) scenarios are based on uplift rates observed on the offshore island and are quite poorly constrained. The degree of segmentation of the major faults and lack of historic great earthquakes lead us not to consider 'worst-case' scenarios where the entire plate boundary system ruptures in a mega event, as this is such a low probability scenario that it does not provide useful guidance on tsunami mitigation.

3.2 Definition Of The Non-Seismic Sources

3.2.1 Review of available scenarios

Discussions focused first on a review of available publications with simulated scenarios of non-seismic tsunamis in the Caribbean (Table 4). We found more than 20 published landslide scenarios ranging from subaerial debris flows and small submarine landslide (several million m^3) to island flank collapse (several km^3). Most of these scenarios concern landslides of volcanic edifices, including an exhaustive study on Mount Pelée in Martinique (Poulain et al., 2023), but there are also simulations of tsunamis generated by river delta collapse (Magdalena River, Colombia: Leslie and Mann, 2016) and carbonated shelf collapse (North Puerto Rico: ten Brink et al., 2006), as well as simulations aiming at reproducing co-seismic landslides during the 2010 Haiti (Hornbach et al., 2010: Poupardin et al., 2020) and 1918 Mona Passage earthquakes (López-Venegas et al., 2008). Among all scenarios, only one was recently added to the CATSAM database as a case-study of non-seismic tsunami: a 0.6 km^3 submarine landslide of the western flank of Kick'em Jenny volcano, simulated by Harbitz et al. (2012).

There are also published simulations of tsunamis generated by eruptive phenomena such as a pyroclastic flow entering the sea at Soufrière Hills volcano, Montserrat (Heinrich et al., 1998; Poisson and Pedreros, 2010), a dome collapse at Mount Pelée volcano, Martinique (Poulain et al., 2023), and a large submarine explosion of Kick'em Jenny volcano (Smith and Shepherd, 1993, 1995).

Table 4. List of non-seismic scenarios of tsunamis in the Caribbean, for which a numerical simulation is published. For gravitational sources (landslides, pyroclastic flows) we indicate the volume (V) and for explosions the energy (E).

Location	Country	Lat	Long	Cause	Parameter	Reference
Volcanic landslides						
Soufrière Hills volcano	Montserrat	16.711	-62.175	subaerial landslide	V = 0.17 km^3	Harbitz et al. (2012)
Mount Pelée volcano	Martinique - France	14.809	-61.166	debris flow	V = 5 x 10^6 m^3	Poisson & Pedreros (2010)
Mount Pelée volcano	Martinique - France	14.809	-61.166	submarine landslide	V = 0.01 km^3	Poulain et al. (2023)
Mount Pelée volcano	Martinique - France	14.809	-61.166	submarine landslide	V = 0.05 km^3	Poulain et al. (2023)
Mount Pelée volcano	Martinique - France	14.809	-61.166	submarine landslide	V = 0.6 km^3	Poulain et al. (2023)
Mount Pelée volcano	Martinique - France	14.809	-61.166	massive flank collapse	V = 1.2 km^3	Poulain et al. (2023)
Mount Pelée volcano	Martinique - France	14.809	-61.166	massive flank collapse	V = 1.8 km^3	Poulain et al. (2023)
Mount Pelée volcano	Martinique - France	14.809	-61.166	massive flank collapse	V = 12.8 km^3	Poulain et al. (2023)
Mount Pelée volcano	Martinique - France	14.809	-61.166	massive flank collapse	V = 16.2 km^3	Poulain et al. (2023)
Mount Pelée volcano	Martinique - France	14.809	-61.166	multistage flank collapse	0.6 + 0.6 + 0.6 km^3	Poulain et al. (2023)
Mount Pelée volcano	Martinique - France	14.809	-61.166	multistage flank collapse	6.9 + 5.9 + 3.7 km^3	Poulain et al. (2023)
Mount Pelée volcano	Martinique - France	14.809	-61.166	dome collapse	V = 9.8 x 10^6 m^3	Poulain et al. (2023)
Mount Pelée volcano	Martinique - France	14.809	-61.166	dome collapse	V = 57 x 10^6 m^3	Poulain et al. (2023)
Oualibou volcano	St Lucia	13.828	-61.049	subaerial landslide	V = 0.25 km^3	Harbitz et al. (2012)
Oualibou volcano	St Lucia	13.828	-61.049	subaerial landslide	V = 0.1 km^3	Le Roy et al. (2017)
Kick'em Jenny volcano	Grenada	12.300	-61.640	submarine landslide	V = 0.6 km^3	Harbitz et al. (2012)
Kick'em Jenny volcano	Grenada	12.300	-61.640	massive flank collapse	V = 4.5 km^3	Dondin et al. (2012)
La Soufrière	St Vincent	13.300	-61.250	massive flank collapse	V = 9 km^3	Le Friant et al. (2009)
Eruptive processes						
Kick'em Jenny volcano	Grenada	12.300	-61.640	underwater explosion	E = 10^{12} J	Smith & Shepherd (1993, 1995)
Kick'em Jenny volcano	Grenada	12.300	-61.640	underwater explosion	E = 10^{14} J	Smith & Shepherd (1993, 1995)
Soufrière Hills volcano	Montserrat	16.711	-62.175	pyroclastic flow	V = 16 x 10^6 m^3	Poisson & Pedreros (2010)
Non-volcanic landslides						
Yucatan Shelf	Mexico	23.170	-90.220	submarine landslide	V = 17 km^3	Chaytor et al. (2016)
Magdalena River Fan	Colombia	11.400	-75.600	submarine landslide	V = 680 km^3	Leslie & Mann (2016)
Mona Canyon	Puerto Rico	18.560	-67.440	submarine landslide	V = 10 km^3	López-Venegas et al. (2008)
Southern Peninsula, south coast	Haïti	17.900	-72.550	submarine landslide	V = 2 km^3	Poupardin et al. (2020)
Southern Peninsula, north coast	Haïti	18.507	-72.809	submarine landslide		Hornbach et al. (2010)
Northern Shelf, Puerto Rico	Puerto Rico	18.783	-66.740	submarine landslide	V = 22 km^3	ten Brink et al. (2006)

Figure 11. Non-seismic sources of tsunamis in the Caribbean.

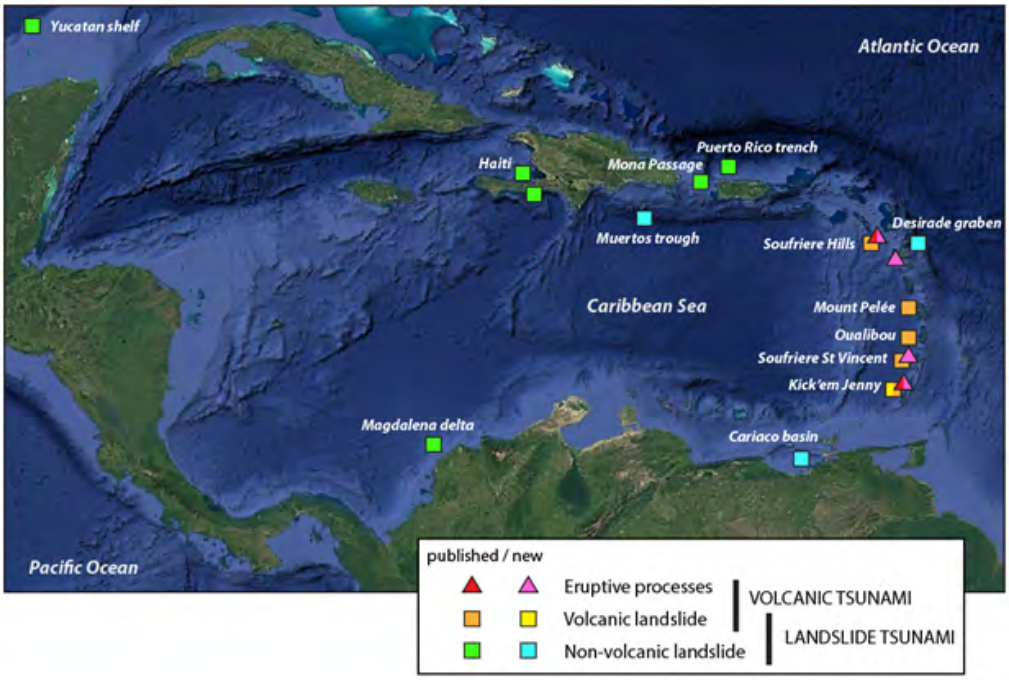

3.2.2 New scenarios of non-volcanic landslide tsunamis

Submarine landslides are likely to occur throughout the Caribbean basin. In the absence of a probabilistic approach, at least for the time being, we have reasoned in terms of spatial distribution of existing scenarios (Table 4). Different locations of submarine landslides were discussed during the 2019 expert meeting in Martinique (IOC-UNESCO, 2020) and three of them perfectly fill the gaps identified: Muertos Trough in the northern part of the Caribbean Sea, Cariaco Basin in the southern part of the Caribbean Sea, and Désirade Graben on the eastern side of the Lesser Antilles. Each landslide location is broken down into three scenarios of different volumes (1, 5, and 10 km^3), summing up a total of 9 new scenarios (Table 5). The range of volumes was selected on the basis of landslide deposits described in the literature, especially those that were caused by historical earthquakes such as the 1918 Mona Passage and 2010 Haiti earthquakes (López-Venegas et al., 2008; Hornbach et al., 2010; Poupardin et al., 2020).

The first case of submarine landslide is located on the northern slopes of the ***Muertos Trough***, south of Puerto Rico and the Dominican Republic (Figs. 11 & 12). The Muertos Trough is a West-East elongated and asymmetrical basin formed at the foot of the thrust belt between the Caribbean Sea plateau to the south and the island arc to the north (Granja Bruña et al., 2009). The Muertos Trough is characterized by steep slopes to the north and gentle slopes to the south. Over the instrumental period, seismicity is moderate compared to the main faults bordering the Caribbean plate, but some recent earthquakes had magnitudes M > 6 (M_s = 6.7 in 1984 south of the Dominican Republic, M_w = 6.4 in 2020 south of Puerto Rico), i.e., magnitudes high enough to trigger submarine landslides on the submarine slopes of the trough. Although there is no proven example of landslide tsunami in this area, this set of scenarios aims at illustrating an example of underestimated tsunami hazard due to moderate earthquake magnitudes (M ~ 6), but possibly locally amplified due to a submarine landslide. Granja-Bruña et al. (2022) provided a list of tsunami sources related to new estimations of the Muertos Trough seismic potential with worst case scenarios up to M8 and identified a ~30 km^3 slump failure in the Muertos Mega-splay at longitude 69.5°W.

Figure 12. Potential tsunami sources along the Muertos Trough (Granja Bruña et al., 2022). MFT: Muertos Frontal Thrust. MMS: Muertos Mega-splay. MRT: Muertos Rear Thrust. CS: Complutense slump. MTFZ: Muertos Trough Fault Zone. BRFZ: Beata Ridge Fault Zone. (a) Map of the tsunami sources, showing the most populated cities (BARH: Barahona; BHAI: Bajos de Haina ; SDOM: Santo Domingo; SPMAC: San Pedro de Macorís; LROM: La Romana; BYUM: Boca de Yuma; PCAN: Punta Cana). (b) Conceptual cross-section of the Muertos margin).

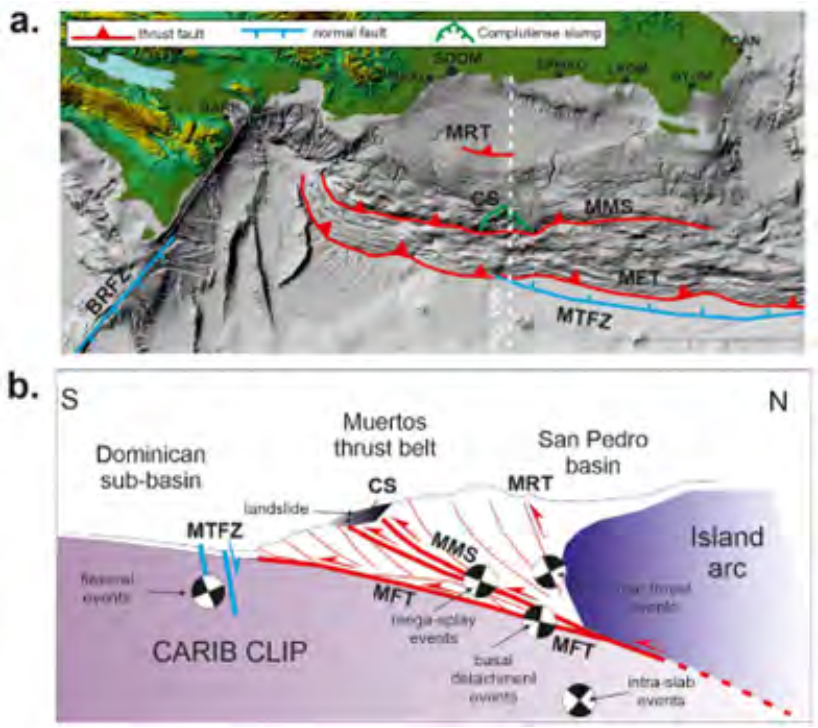

Three volumes of landslide are proposed for the numerical simulations (1, 5, and 10 km^3), all three initiated from the same location (Table 5) and moving southward from the Muertos Trough. The selected source area (Fig. 12) is characterized by steep slopes on anticline ridges of the compressional front of the thrust belt (Granja Bruña et al., 2009) and it falls in the middle of the four scenarios of seismic rupture discussed during the expert meeting in Dominican Republic (IOC-UNESCO, 2016) and listed in the CATSAM database (https://www.ncei.noaa.gov/maps/CATSAM/) along the western part of the Muertos Trough.

Figure 13. Main tectonic features and earthquake focal mechanisms in and around the Cariaco Basin, North Venezuela. The yellow circle indicates the submarine landslide location proposed in this report. Modified from Escalona et al. (2011).

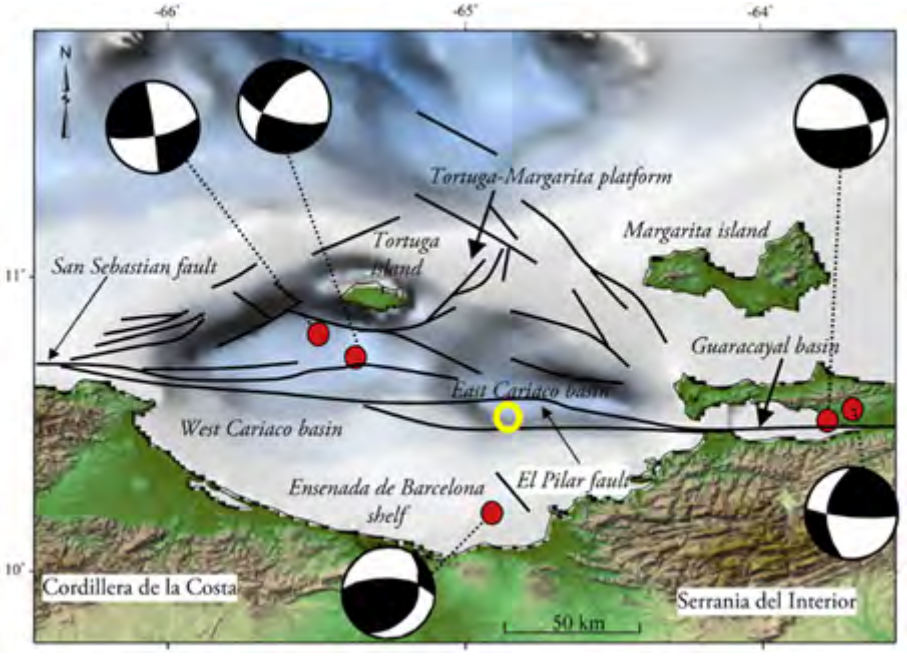

The scenarios of submarine landslide in the ***Cariaco Basin*** follows the same idea, but in a different tectonic setting. The Cariaco Basin is an east-west trending 180 km long, 40 km large and 1400 m deep depression composed of two sub-basins on the continental shelf off the northern coast of Venezuela (Figs. 11 & 13). It is a pull-apart basin formed along the El Pilar - San Sebastian right-lateral strike-slip fault system, located in the obliquely-convergent Caribbean and South American plate boundary (Audemard et al., 2005; Escalona et al., 2011). Like its northern counterpart, this plate boundary is frequently the site of earthquakes of magnitude M > 6.5 up to 7.7 (e.g. October 29, 1900 Macuto earthquake, west the Cariaco Basin). The July 15, 1853 M = 6.7 and January 17, 1929 M_s = 6.9 earthquakes caused great damage, including a tsunami, in the Cumana area, at the eastern end of the Cariaco Basin. There is limited information on the tsunami that followed the October 29, 1900 M = 7.7 Mancuto earthquake, one of the largest historical earthquakes along this system of faults, with an epicenter close to the northwestern corner of the Cariaco Basin.

For the Cariaco Basin, we propose three scenarios of submarine landslide (1, 5, and 10 km^3) on the southern slope of the eastern sub-basin (Fig. 13), all three initiated from the same location (Table 5) and slid northward. In the CATSAM database, there is one scenario of rupture centered in the Cariaco Basin, with a magnitude M_w = 8.17, thus corresponding to a worst-case scenario. It could be interesting to combine this scenario with one of the landslide scenarios proposed here for a future Caribe Wave exercise.

Figure 14. Bathymetric map of the forearc between Guadeloupe and Barbuda (Seibert et al., 2020), with a close-up view on a landslide headscarp and fan deposit south of the Barracuda ridge.

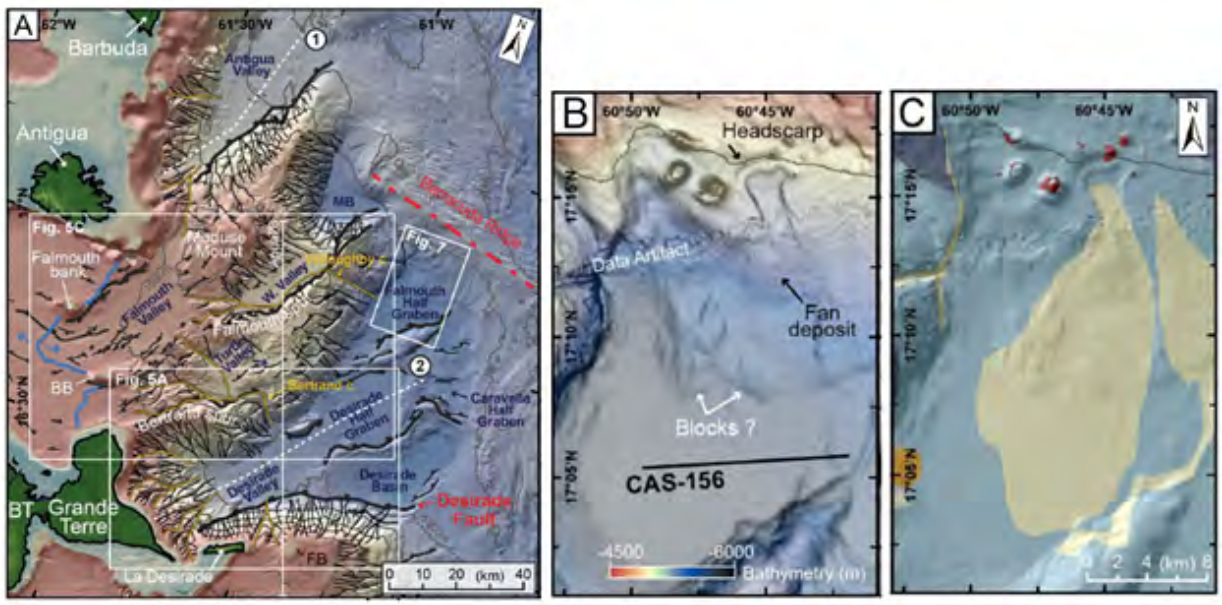

The third location proposed for a submarine landslide is located 100 km east of Antigua, between the ***Désirade*** Valley and the Barracuda Ridge (Fig. 14), i.e. on the eastern slopes of the Lesser Antilles islands arc. The advantage of this location is that it is opposite to the numerous volcanic landslides that occurred on the western slopes of the islands (and for which several simulations were already published, as listed in Table 4). We selected this area because there is published evidence of landslide headscarps and fan deposits, especially on the southern side of the Barracuda Ridge (Seibert et al., 2020). Furthermore, sediment cores studies revealed the existence of turbidites formed by large megathrust earthquakes during the Quaternary (Seibert et al., 2024). As for the other landslide scenarios, three different volumes are proposed (1, 5, and 10 km^3).

Table 5. List of new scenarios of non-volcanic submarine landslide sources of tsunamis in the Caribbean.

Location	Country	Lat	Long	Direction	Cause	Volume
Muertos Trough	Dominican Republic	17.547	-69.298	southward	submarine landslide	1 km^3
Muertos Trough	Dominican Republic	17.547	-69.298	southward	submarine landslide	5 km^3
Muertos Trough	Dominican Republic	17.547	-69.298	southward	submarine landslide	10 km^3
Cariaco Basin	Venezuela	10.463	-64.776	northward	submarine landslide	1 km^3
Cariaco Basin	Venezuela	10.463	-64.776	northward	submarine landslide	5 km^3
Cariaco Basin	Venezuela	10.463	-64.776	northward	submarine landslide	10 km^3
Désirade -Barracuda	Guadeloupe (France)	17.253	-60.752	southward	submarine landslide	1 km^3
Désirade -Barracuda	Guadeloupe (France)	17.253	-60.752	southward	submarine landslide	5 km^3
Désirade -Barracuda	Guadeloupe (France)	17.253	-60.752	southward	submarine landslide	10 km^3

3.2.2 New scenarios of volcanic tsunamis

The selection of new scenarios of volcanic tsunamis aims at completing and improving the list of available (and published) scenarios of volcanic tsunamis listed in Table 4. The meeting was attended by representatives of the main institutions responsible for monitoring active volcanoes in the Lesser Antilles, i.e., the SCR-UWI (Seismic Research Center, University of the West Indies) and IPGP (Institut de Physique du Globe de Paris, France). We here propose five new scenarios of volcanic tsunamis, including both landslide and eruptive sources, as listed in Table 6.

Table 6. List of new scenarios of volcanic sources of tsunamis in the Caribbean. For volcanic landslide sources, we indicate the volume (V), for pyroclastic flows the mass flux (Q), and for underwater explosions the explosion energy (E).

Volcano	Country	Lat	Long	Cause	Parameter
Kick'em Jenny	Grenada	12.300	-61.640	underwater explosion in summit crater	E = 2.8 x 10^{16} J
Kick'em Jenny	Grenada	12.300	-61.640	submarine landslide on north-western flank	V = 0.1 km^3
Soufrière	St Vincent	13.334	-61.182	pyroclastic flow on western flank	Q = 10^5–10^8 m^3/s
Soufriere Hills	Montserrat	16.711	-62.175	dome collapse on eastern flank	V = 0.1 km^3
Soufrière	Guadeloupe (France)	16.042	-61.663	dome collapse on western flank	V = 0.1 km^3

Kick'em Jenny submarine volcano, located north of Grenada, has been recognized as a potential source of tsunamis for several decades, thanks to the work of Smith and Shepherd (1993, 1995) and Dondin et al. (2012). Kick'em Jenny is the most active volcano in the Caribbean, with at least 14 eruptions between 1939 and 2017. A tsunami was observed during the 1939 eruption, and possibly in 1965. The horse-shoe shaped morphology of the volcano provides evidence of past flank instability, which motivated previous works on flank collapses and resulting tsunamis. Dondin et al. (2012) simulated a 4.5 km^3 flank collapse, which represents a worst-case scenario, whereas Harbitz et al. (2012) used a volume of 0.6 km^3. The simulation of Harbitz et al. (2012) is so far the only volcanic tsunami scenario implemented in CATSAM. In the case of volcanic unrest, magmatic intrusions may destabilize the flanks of the volcano, thus causing small landslides typically on the order of a few million m^3, as occurred at Stromboli in 2002 (Bonaccorso et al., 2003). We thus recommend also considering a volume of 0.1 km^3 in order to see how much it impacts the islands around (Grenada, Carriacou, Grenadines). Considering that the summit of Kick'em jenny volcano is now at a water depth of 160-180 m, we cannot rule out the possibility of a tsunami generated by a submarine explosion. Based on previous work by Smith and Shepherd (1993, 1995), we estimate that an explosion with an energy of 2.8 x 10^{16} J (equivalent to 4.37 x 106 tons TNT) would represent a worst-case scenario. A first order approach to simulate tsunamis generated by underwater explosions was applied to volcanoes such as Kolumbo submarine volcano in Greece, Karymskoye Lake in Russia (Torsvik et al., 2010), and Lake Taal in the Philippines (Paris and Ulvrova, 2019). This method could easily be applied to Kick'em Jenny volcano.

In Montserrat, the summit dome of ***Soufrière Hills volcano*** shows signs of instability, as explained by Erouscilla Joseph, Head of the SRC-UWI, during the meeting. During the 1995-2013 eruption, dome collapses produced pyroclastic flows that reached the sea (Herd et al., 2005) and generated tsunamis, the 2003 event being observed in Guadeloupe (Pelinovsky et al., 2004). In September 2023, the Montserrat volcano observatory (MVO, operated by SRC-UWI) reported increased seismicity, gas emissions, and rockfalls. These signs raise concern about a possible collapse of the summit dome, especially in the case of an earthquake. At the end of the 1995-2013 eruption, the lava dome had a volume of ~120 x 106 m^3 (Arnold et al., 2016), which represents about half the volume of the 2003 dome collapse that produced a tsunami (Herd et al., 2005). It would therefore be interesting to plan new simulations of dome collapse, testing several volumes, to see if the flows reach the sea.

Figure 15. Map of the pyroclastic flow deposits from 1902 eruption of Soufriere, St Vincent, and simulation of pyroclastic flows on the western flank of the volcano (Gueugneau et al., 2024).

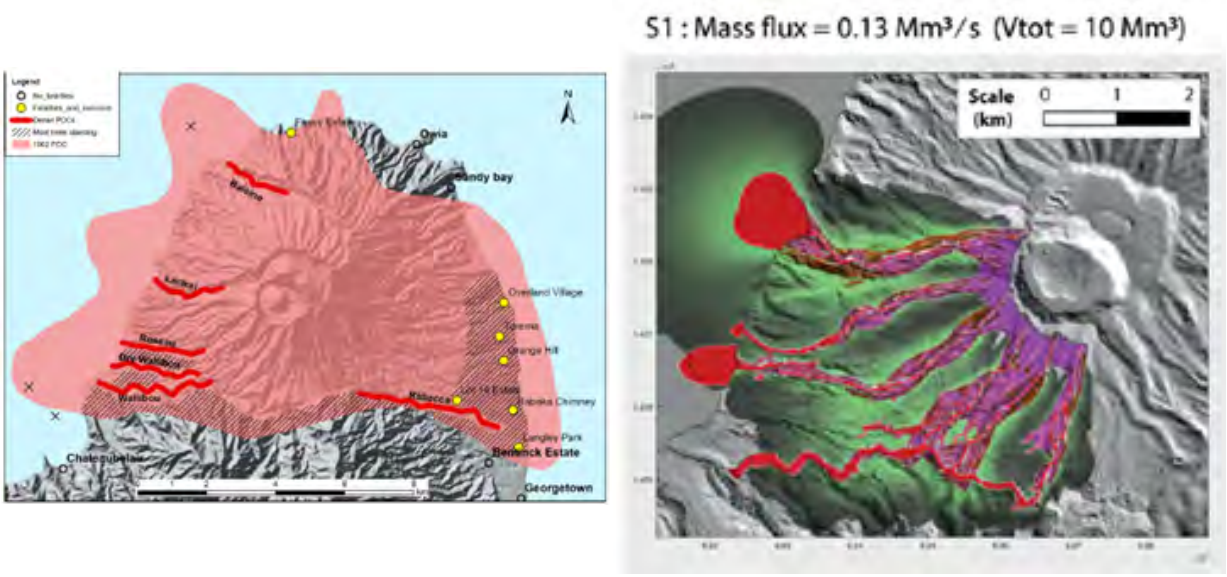

During the 2020-2021 eruption of ***Soufrière volcano at St Vincent***, pyroclastic flows confined in the deep valleys of the western flank of the volcano reached the sea, thus giving rise to some concerns about possible tsunamis. The ICG/CARIBE-EWS recommended installing a new sea level station during the eruption, in agreement with SRC-UWI, to detect any sea level disturbance related to the entrance of pyroclastic flows into the sea on the western flank of the volcano. The new station was finally installed in Chateau Bel-Air in February 2022 and is now connected to the IOC network. Fortunately, no tsunamis were recorded during the 2020-2021 eruption, but a tsunami with a maximum runup of 1 m at Saint Lucia and Barbados was observed during the 1902 eruption (NCEI database: https://www.ngdc.noaa.gov/hazel/view/hazards/tsunami/runup-search/). Numerical simulations by Gueugneau et al. (2024) show that pyroclastic flows produced by collapsing volume of 10 x 106 m^3/s, i.e. similar to the inferred volume of the 1902 eruption, reach the sea with a mass flux of 105 m^3/s and a front thickness of ~10 m (for the dense part of the flow) in the Larikai and Roseau valleys (Fig. 15). These two valleys on the western flank of the volcano are those for which the distance from the eruptive center to the sea is the shortest. We thus recommend using the input parameters provided by Gueugneau et al. (2024) to run future simulations of tsunami generated by pyroclastic flows at Soufrière St Vincent volcano.

Although there is no published evidence of past tsunami related to the eruptions of ***Soufrière volcano in Guadeloupe***, the experts suggested testing the tsunamigenic potential of a major dome collapse. Over the last 9150 years, at least 9 dome and flank collapses occurred, mostly on the south-western flank of the volcano. The last magmatic eruption, in 1530 CE, started with a partial flank-collapse of 80 ± 40 × 106 m3 (Boudon et al., 2008; Komorowski et al., 2008). Peruzzetto et al. (2019) simulated debris avalanches produced by dome collapse with volumes ranging from 1 to 100 x 106 m3. With runouts of 15 km, the largest dome collapses are able to disturb the sea but we did not simulated the resulting tsunami. As suggested by Anne Le Friant, Head of monitoring activities at IPGP, the experts agreed to use the 100 x 106 m3 dome collapse scenario of Peruzzetto et al. (2019) as an input for a future tsunami simulation.

3.3 Tsunami Simulations

3.3.1 Seismic sources

To produce the new simulations included in the report, we used COMCOT (Cornell Multi-grid Coupled Tsunami) simulation model to model the generation of tsunami from various sources, tsunami propagation and coastal runup. This model was initially developed during the mid-90s at Cornell University (Liu et al. 1995;1998), and since then has been progressively developed at Cornell University (Wang and Liu, 2006; Wang 2008) and subsequently at GNS Science, New Zealand (Wang and Power 2011). It has been carefully tested and widely applied to numerous tsunami studies (e.g. Liu et al. 1995; Wang & Power, 2011; Roger et al. 2023). The model computes tsunami generation, propagation, and coastal interaction by solving both linear and non-linear shallow water equations using a modified explicit leap-frog finite difference scheme and considering the weak dispersion effect (Wang, 2008; Wang and Liu, 2011). For earthquake sources, the initial sea surface deformation is calculated using Okada (1985)'s formulae with the fault plane geometry and either a uniform or non-uniform slip distribution. Water surface elevation and horizontal velocities are calculated at the center and at the edge centers of each grid cell within the computational domain, respectively. Absorbing boundary schemes are used at the boundaries of the computational domain to dampen the incoming waves, avoiding reflection from the domain boundaries (Wang and Power 2011).

GEBCO (2024) was used to create a single numerical grid covering the whole region of interest between 270° and 301°E and 7° and 24°N. It has a spatial resolution of one arcmin. Friction between the tsunami and the terrain surface it moves over is modelled through a bottom friction model with n as the Manning's coefficient of roughness (Wang and Power 2011). The bottom friction is calculated as a function of gravitational acceleration, Manning's *n*, current velocity and water depth (Wang and Power 2011). The higher the roughness coefficient, the higher the friction; the deeper the water, the smaller the friction. Various Manning's roughness coefficients have been proposed for different types of land cover types and water areas (Wang et al. 2017). In this study Manning's n = 0.013 is used for water areas which is within the range of roughness values commonly used for relatively smooth water channel and flood plains, but toward the smaller end of the range for those environments (Arcement and Schneider,1989; Wang et al. 2017).

An array of virtual sea-level sensors has been designed for this project, notably to check the stability of the numerical model and the simulation results. The outputs of the simulations are maximum wave amplitude maps, tsunami travel time maps (TTT) and time series at virtual sensors' location calculated over a propagation time of 24 hours at Mean Sea Level (MSL; GEBCO bathymetry data is referenced to MSL, meaning that the depths are measured to an average sea level as MSL value is different from one region to another one [GEBCO, 2024]).

Table 7. Impact of the scenario of tsunamis generated by seismic ruptures in the NW Caribbean, inferred from numerical simulations (see Annex I for complete results).

ID	Name	Impact	Areas	H_{max} (m)
1	Enriquillo Plantain	regional	East Jamaica, West Haiti, South Cuba	2.34
3	Jamaica Central	local	SE Jamaica (Kingston Bay)	1.29
4	Jamaica North	local	NE Jamaica	2.43
5	Jamaica South	local	SE Jamaica (Albion)	0.78
6	Mid Cayman	local	West Jamaica, North Honduras	2.22
7	Motagua offshore	regional	Guatemala, North Honduras, East Belize, SE Mexico, NW Cuba, West Jamaica	8.16
8	Oriente	very limited	H_{max} < 0.5 m everywhere	0.26
9	Roatan offshore	regional	Guatemala, North Honduras, East Belize, SE Mexico, NW Cuba	3.07
10	Roatan onshore	local	North Honduras	3.04
13	South Def Belt Central	regional	South Cuba, NE Jamaica, SW Haiti	1.43
14	South Def Belt East	regional	South Cuba, West Haiti, Jamaica, South Inagua (Bahamas), NW Venezuela	4.90
15	South Def Belt West	local	SW Cuba (Cape Cruz)	0.66

16	Swan Island East	very limited	H_{max} < 0.5 m everywhere	0.23
17	Swan Island North	very limited	H_{max} < 0.5 m everywhere	0.29
18	Swan Island South	very limited	H_{max} < 0.5 m everywhere	0.20
19	Walton North	very limited	H_{max} < 0.5 m everywhere	0.24
20	Walton onshore	very limited	H_{max} < 0.5 m everywhere	0.24
21	Walton South	very limited	H_{max} < 0.5 m everywhere	0.32
22	Jamaica (3+4+5)	local	East Jamaica	2.65
23	South Def Belt (13+14)	regional	South Cuba, West Haiti, Jamaica, South Inagua (Bahamas), NW Venezuela	4.64
24	Motagua offshore (bis)	local	NW Honduras	0.83

Maximum wave amplitude (H_{max}) and tsunami travel times (TTT) for all simulations are compiled in Annex I and Annex II. Table 7 summarizes the impact that each scenario of tsunami might have on the coasts of the Caribbean. Seven scenarios have a very limited impact, with wave heights less than 0.5 m (measured on the close 1 arcmin pixel to the shoreline) everywhere in the Caribbean, including in near-field locations. Other scenarios show essentially a localized impact, focusing on a particular stretch of coastline. As an example, scenario 4 (Jamaica North) shows a significant impact on all coasts of NE Jamaica, with a maximum wave amplitude of 2.43 m close to the seismic rupture zone, but elsewhere wave maximum amplitude are lower than 0.5 m. Scenarios described as "regional" produce waves of over 0.5 m along the coasts of several countries.

As illustrated on figure 16, the most impacting scenarios are :

- A tsunami generated by a M_w = 7.7 earthquake on the Enriquillo - Plantain Garden strike-slip fault system between Jamaica and Haiti (scenario #1 in tables 3 and 7), producing wave amplitudes above 0.5 m along the coasts of Jamaica (East coast) and Haiti (West coast).
- A M_w = 7.6 normal faulting event on the Mid-Cayman spreading center (scenario #6 in tables 3 and 7), which generates a tsunami wave amplitudes above 1 m on the western coast of Jamaica, and locally above 0.5 m along the northern coast of Honduras.
- Following a M_w = 7.8 strike-slip earthquake on the offshore extension of the Motagua fault (scenario #7 in tables 3 and 7), a tsunami propagates in all of the Gulf of Honduras, producing wave amplitudes above 2 m along the coasts of Guatemala and Honduras (even reaching ~8 m in Roatan), more than 1 m along the coasts of Belize and Mexico (east coast of Yucatán), and more than 0.5 m in some areas of Jamaica (northwestern coast) and Cuba (northwestern coast). This is the most impactful scenario simulated herein. The results of the simulation are concordant with observations of the 1856 M = 7.5 earthquake in the Gulf of Honduras. Figure 17 illustrates the duration of the tsunami trapped in the gulf for more than 20 hours.
- A M_w = 7.8 strike-slip earthquake near Roatan Island, on the western segment of the Swan Island fault (scenario #9 in tables 3 and 7), causing a tsunami with wave amplitudes above 0.5 m on the coasts Guatemala, Honduras, Belize, Mexico, and some areas in NW Cuba, with a maximum wave amplitude of ~3 m on the northern coast of Honduras.
- Rupture models on the central and eastern segments of the Southern Deformation Belt (scenario #13 and #14 in tables 3 and 7) both generate regional tsunamis impacting the southern coast of Cuba, Jamaica, and Haiti, the eastern segment scenario being more tsunamigenic (up to 4.9 m in NW Haiti), with a significant impact on Inagua (Bahamas) and even the northern coast of Venezuela. Scenario #23 combining ruptures of both the eastern and central segments is a localized worst-case scenario.

Figure 16. Most impactful scenarios of tsunamis generated by seismic ruptures in the NW Caribbean, based on numerical simulations. Each scenario has an ID listed in the title, identical to that shown in tables 3, 7 and 9. The color scale represents the maximum water surface elevation recorded during the simulation. The purple value corresponds to the highest wave amplitude recorded locally. Red dots indicate virtual tide gauges where surface elevation profiles were computed.

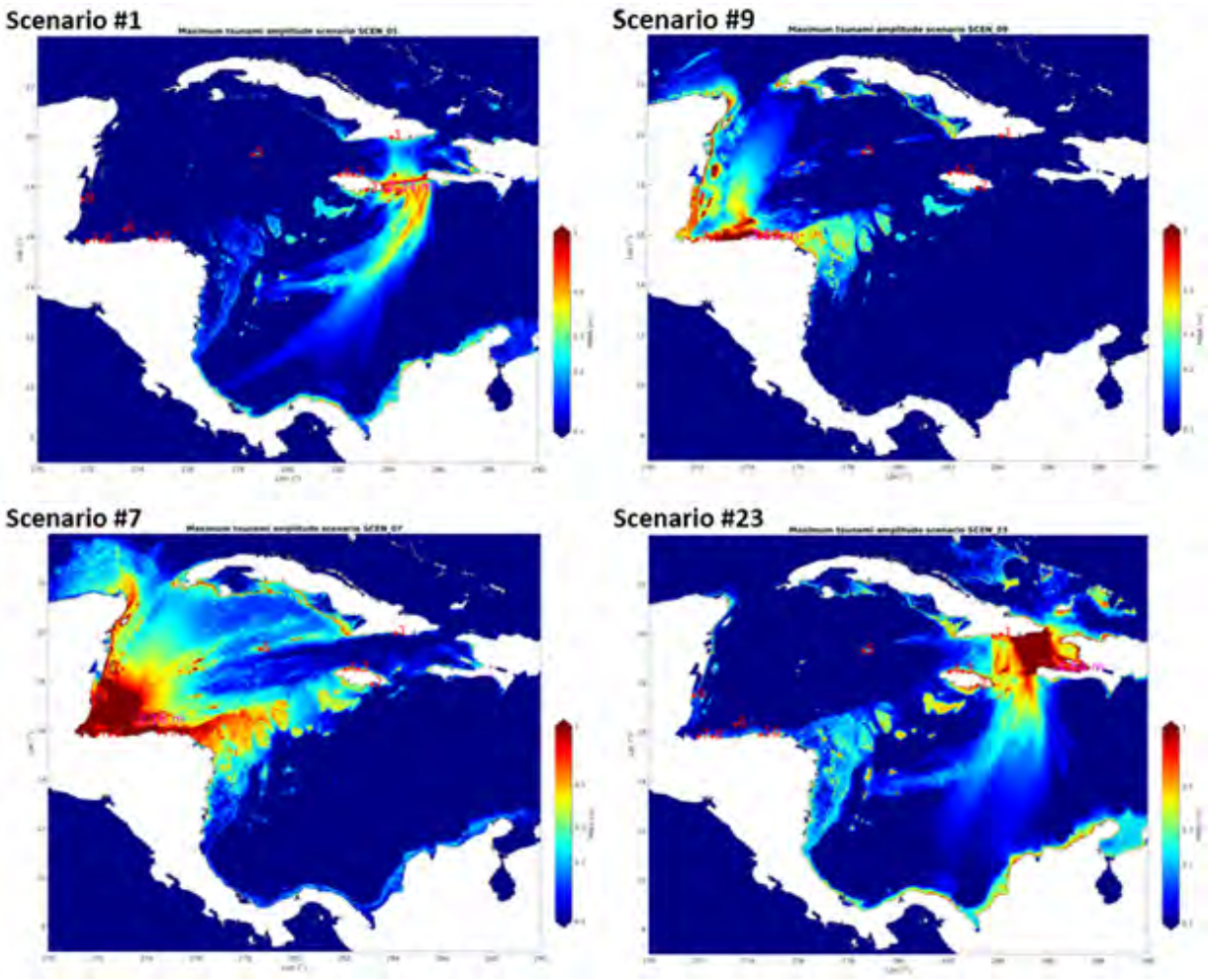

Figure 17. Water surface elevation profile recorded on the eastern coast of Belize following a $M_w = 7.8$ earthquake on Motagua fault (scenario #7 in tables 3 and 7).

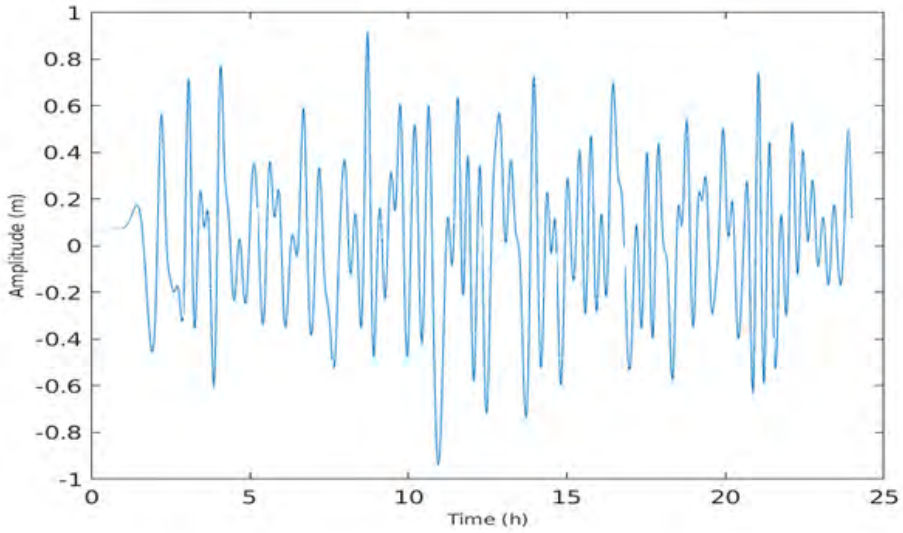

Maps of Tsunami Travel Times (TTT) are essential documents for implementing procedures of early warning and evacuation. The impact of tsunamis described here as "local" is limited to nearby areas which are affected in a matter of minutes after the earthquake. Regional tsunamis initiated from Cuba and Jamaica propagate in all the Caribbean basin in 3-4 hours (Fig. 18: scenarios #1 and #23), while those initiated in the Gulf of Honduras (Fig. 18: scenarios #7 and #9) reach the Lesser Antilles in 7-9 hours. However, for all regional tsunamis, the main areas affected (i.e. wave amplitudes over 0.5 m) are struck in less than 1 hour, except for the northern coast of Venezuela that is struck in 2 hours in the case of ruptures along the Enriquillo - Plantain Garden Fault (scenario #1) or the Southern Deformation Belt (scenario #23).

Figure 18. Example of Tsunami Travel Time (TTT) maps following seismic ruptures in the NW Caribbean (same scenarios as on Fig. 16). Each scenario has an ID listed in the title, identical to that shown in tables 3, 7 and 9. The color scale represents the tsunami travel times recorded by the simulation with a detection threshold of 1 cm (i.e., if the simulated amplitude is less than 1 cm, the TTT is not shown on the figure).

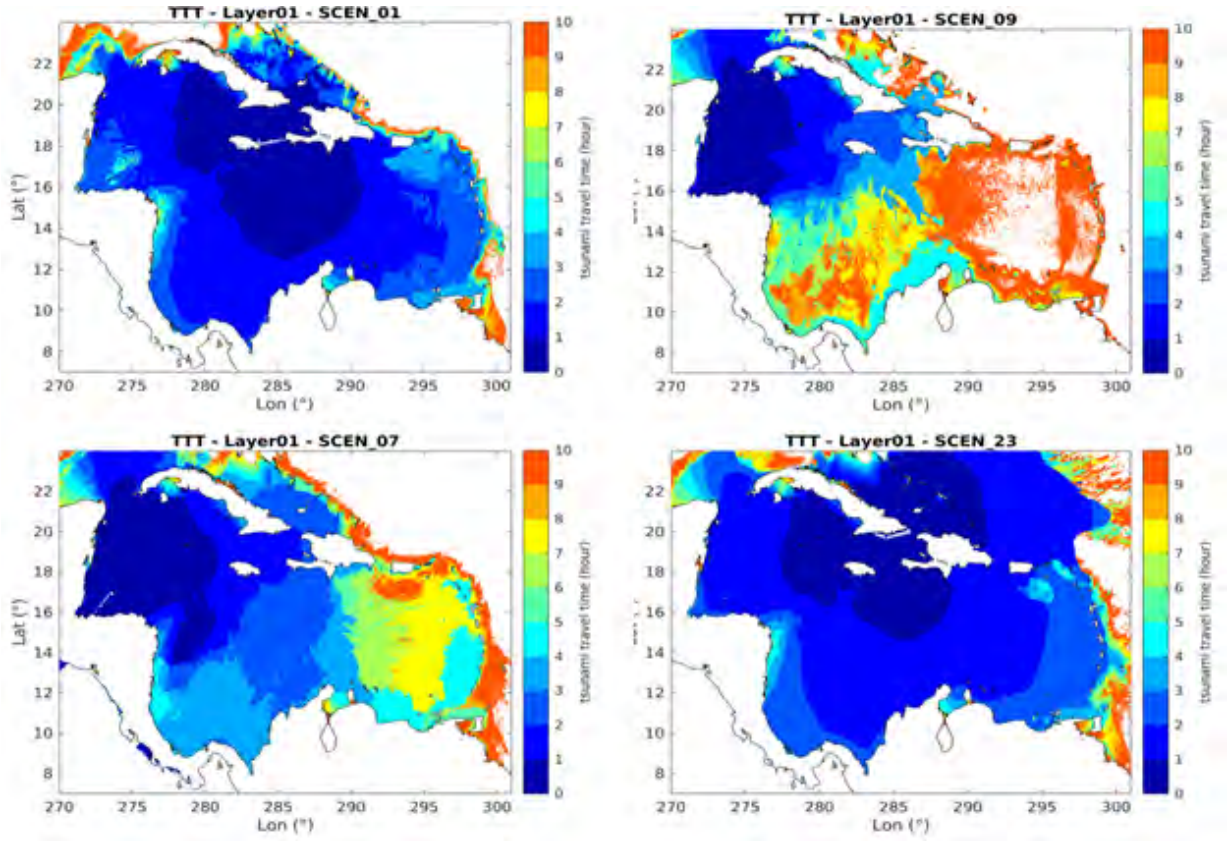

3.3.2 Non-seismic sources

For the three case-studies of non-volcanic submarine landslides (Table 5), the numerical simulations were produced with Landslide-HySEA code (Macías et al., 2015; González-Vida et al., 2019), a non-dispersive code implementing a strong coupling between the granular material and the water layer. We also provide a comparison with two other models, the Multilayer-HySEA code (Macías et al, 2021a, b) and a non-hydrostatic weakly coupled version of Landslide-HySEA. A comparative study of these models for a rigid slide laboratory experiment was realized by Macías et al. (2021a). For the three case-studies, namely Cariaco Basin, Muertos Trough and Desirade-Barracuda, three different volumes of submarine landslide are simulated (1, 5 and 10 km^3) as recommended in the previous section. The aim here is not to reproduce mapped landslides, so there is limited information available for the simulations. The location, rough extent and volume being the only input parameters together with the bathymetry, we used the ***calibrated submarine landslide*** (CSL) method to model the initial conditions of the simulations (see Annex I for detailed information of the CSL method). The results obtained using the CSL method for a landslide volume of 10 km^3 are illustrated as topographic profiles on Figure S3. The different parameters used for the simulations are summarized in Table 8. Figure S2 shows an example of initial and final distribution of thickness of the sliding mass in 2D and 3D (Muertos Trough submarine landslide, volume V = 10 km^3). The results of the 9 simulations (3 locations, 3 volumes) are illustrated as maps of maximum wave amplitudes (Fig. 20) and tsunami arrival times (Fig. 22) at the scale of the Caribbean Sea, but also by zooming in on the nearest populated areas (Fig. 21).

Table 8. Parameters of numerical simulations of non-volcanic submarine landslides using Landslide-HySEA code.

Bathymetry Data	• Source: GEBCO (2024) • Resolution: 450 m
Mesh Information	• Grid Size: 2,619 x 2,066 = 5,410,854 volumes • Extent in X: [233,033, 1,399,010] m • Extent in Y: [1,109,980, 2,068,710] m
Configuration set-up	• Initialization: From file • CFL Condition: 0.5 • Ratio of densities between water and granular material: 0.45 • Pouliquen angles (degrees): 1, 3, 1.5 º • Friction Coefficient on water-Bottom: 0.01 (Manning coefficient)

Physical Constraints	• Maximum Allowed Velocity:
	  • Water: 25 m/s
	  • Granular Material: 150 m/s
	• Epsilon h: 0.005 m (Minimum water depth)

Simulation Time	• Total Time: 10800.1 seconds (3 hours) • Total Runtime (1GPU): 4.436782e+02 sec (~8 min)

We also performed a comparison between three different numerical models for the Muertos Trough landslide scenario (volume V = 10 km^3): (1) Landslide-HySEA, which is used for all the submarine landslide simulations presented in this report, (2) the non-hydrostatic version of Landslide-HySEA, with a weak coupling between the water and the slide, and (3) the multilayer version of HySEA code (Macías et al., 2021a, 2021b). The Multilayer-HySEA model implements a two-phase model intended to reproduce the interactions between the landslide and the water. The motion of the landslide is represented by the lower phase, consisting of a Savage–Hutter model. The upper phase describes the hydrodynamic component using a stratified vertical structure that includes non-hydrostatic terms in order to account for dispersive effects in the propagation of the waves. The multilayer version is thus dispersive and provides a richer vertical structure. As first approach, the non-dispersive Landslide-HySea model gives reliable results, even if the height of the leading wave is slightly overestimated (Fig. 19). If any of these scenarios were to be implemented in the CATSAM database, we recommend running new simulations using the multilayer version of HySEA or another validated (Kirby et al., 2022) landslide tsunami model such as the multilayer non-hydrostatic NHWAVE model, that features strong coupling between granular slide motion and stresses with the overlying water (Zhang et al., 2021a,b).

Figure 19. A comparison between Landslide-HySEA model (left), the multilayer-HySEA dispersive model (middle), and a non-hydrostatic version of Landslide-HySEA (right) for the Muertos Trough submarine landslide scenario (volume V = 10 km^3).

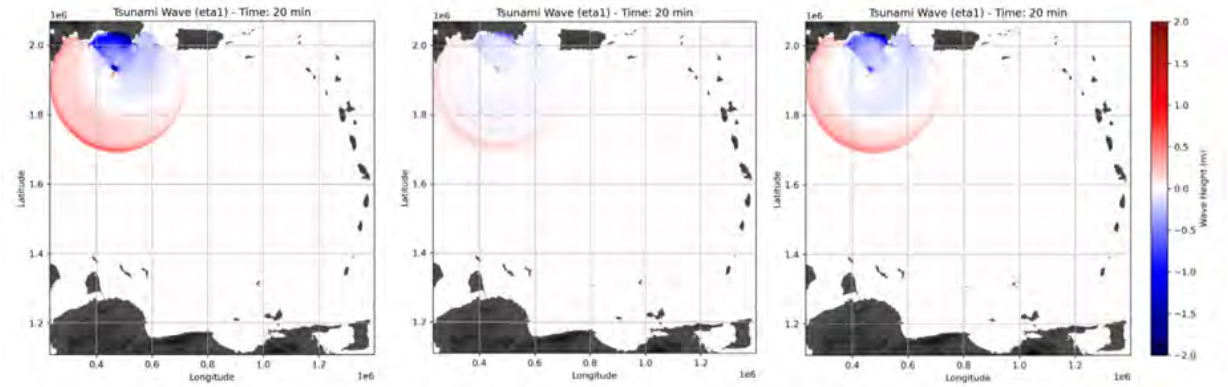

The results presented here with the non-dispersive HySEA model provide a first-order estimate of the areas that could be impacted by significant tsunami waves, i.e. waves higher than 0.5 m at the shoreline (which is sufficient to carry people away). The first conclusion is that the smallest landslide (V = 1 km^3) scenarios produce very low waves (< 0.1 m high), with a very limited impact on the nearest coasts, except for the Cariaco Basin scenario that locally generates waves up to 0.5 m high on the western coast of Isla de Margarita (Fig. 21). Increasing the volume of the landslide enlarges the extent of the area impacted by the tsunami. The 5 km^3 Desirade-Barracuda landslide generates waves higher than 0.5 m on the eastern coasts of Antigua and Guadeloupe, with local maxima up to 1 m, but it has no impact on the other islands. Although it is directed to the South, the 5 km^3 Muertos Trough landslide produces waves up to 0.5 high on the southern coast of the Dominican Republic, with very localized maxima exceeding 1 m. The tsunami hits the Dominican Republic in 20 minutes, and Puerto Rico in 30 minutes. The tsunami then traverses the deep part of the Caribbean Sea to reach the southern Dutch Antilles (Aruba, Curaçao and Bonaire) in 50 minutes with wave amplitudes between 0.5 and 2 m. Note that these far-field values are probably slightly overestimated by the non-dispersive model. The 5 km^3 Cariaco Basin scenario has a significant impact (waves > 0.5 m) over 550 km of the southern coast of Venezuela, which is characterized by shallow waters. Some populated areas such as the western coast of Isla de Margarita and Araya are severely impacted (waves 3-5 m) 10-15 minutes after the landslide. These wave amplitudes are doubled in the case of a 10 km^3 landslide that is also clearly recorded (waves ~0.5 m) on the southern coast of Saint Lucia, and western coasts of Dominica, Guadeloupe, Montserrat, Nevis, and Saint Kitts. Note that the densely populated area of Barcelona and Puerto La Cruz in Venezuela receives waves 2-3 m high, even if the energy of the tsunami is reduced by the islands of Chimana Grande and La Boracha (Fig. 21).
The 10 km^3 Cariaco Basin scenario has no consequences on the northern and western part of the Caribbean. On the contrary, the tsunami generated by the 10 km^3 Muertos Trough landslide propagates easily in the deep waters of the Caribbean Sea and produces waves 1-2 m high on the southern Dutch Antilles. This scenario has a major impact in the near-field, with waves more than 1 m high on all the southern coast of Hispaniola (Dominican Republic and Haiti), and more than 2 m up to 3 m between Santo Domingo and La Romana (Fig. 21). The 10 km^3 Desirade-Barracuda scenario has no far-field impact in the Caribbean Sea because it is generated on the eastern side of the Lesser Antilles arc, but all the islands nearby record significant waves (> 0.5 m) 10-20 minutes after the landslide, especially the eastern coasts of Guadeloupe and Antigua (with local maxima exceeding 2 m).

Figure 20. Maximum wave amplitude (in meters) computed for the three cases of submarine landslides: Muertos Trough, Cariaco Basin, and Desirade-Barracuda (see parameters in Table 5), considering three different volumes (1, 5, and 10 km^3). The scale of wave amplitude is saturated to 0.5 m, but larger wave amplitudes are locally observed (see Fig. 20 for close-up views).

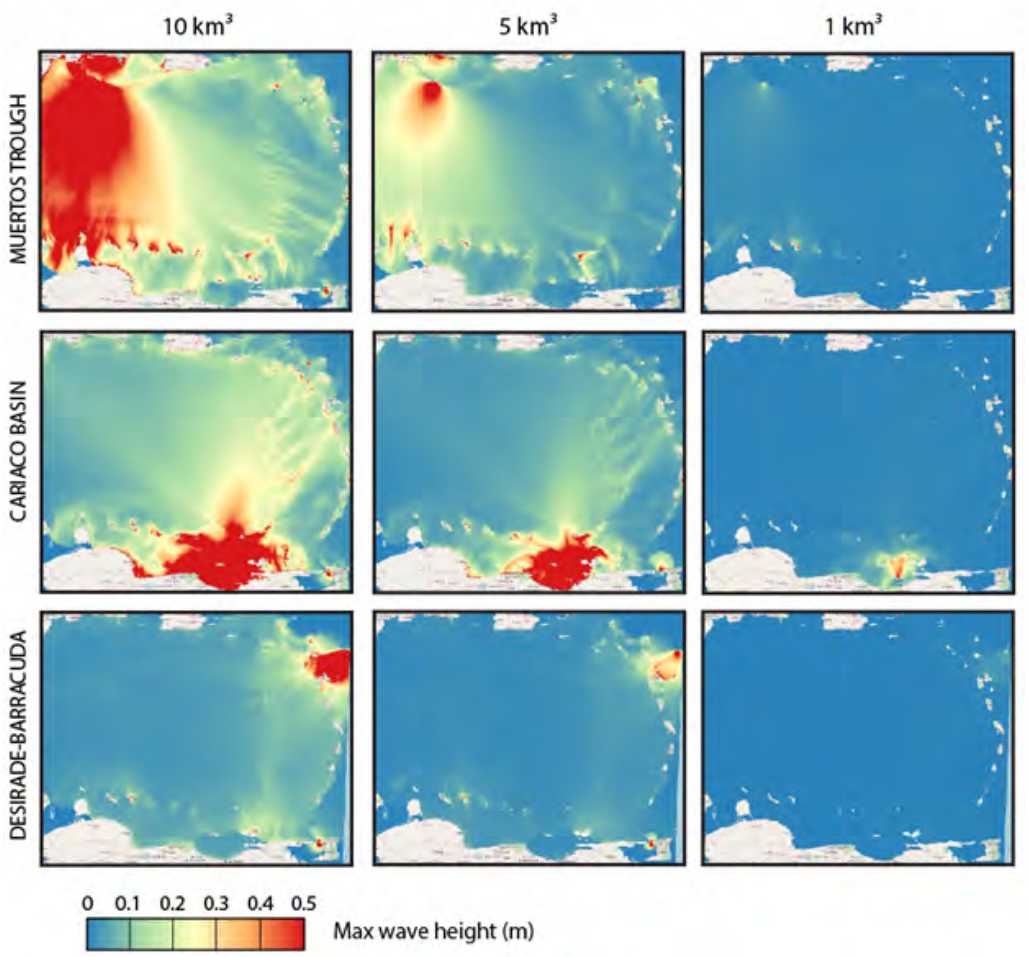

Figure 21. Maximum wave amplitude (in meters) computed for the three cases of submarine landslides: Muertos Trough, Cariaco Basin, and Desirade-Barracuda (see parameters in Table 5), considering a landslide volume V = 10 km^3. The scale of wave amplitude is saturated to 2.5 m.

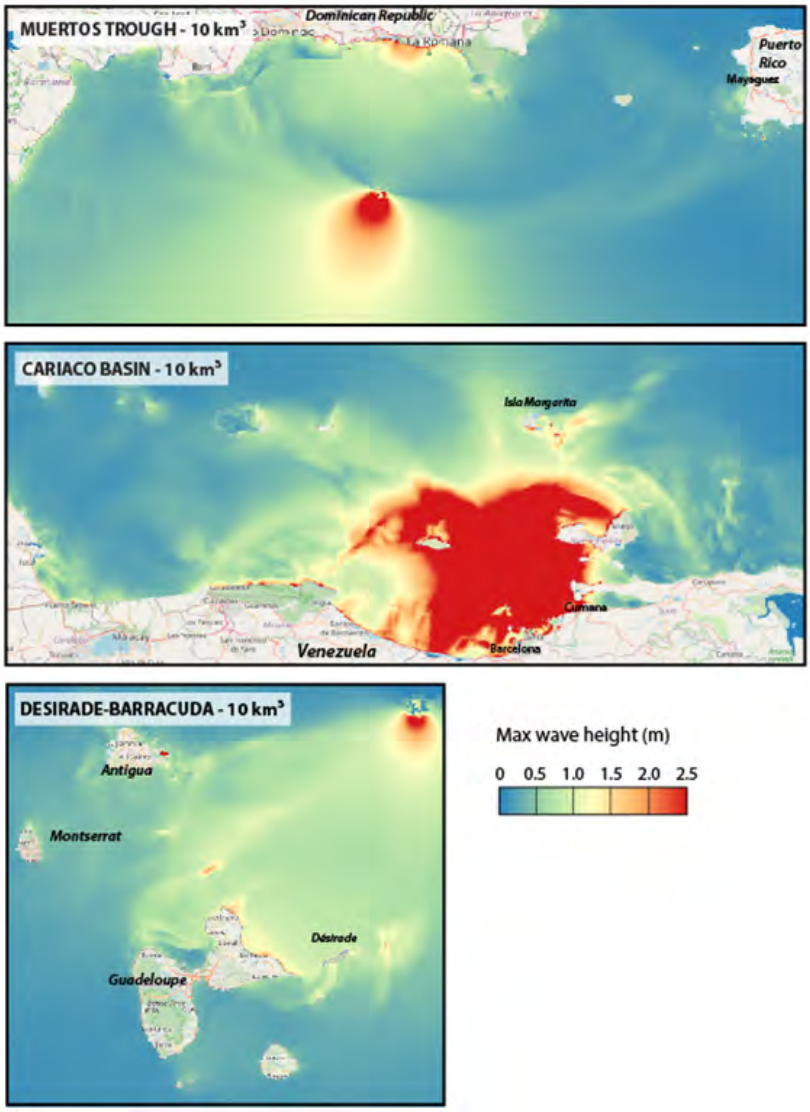

Figure 22. Tsunami arrival times computed for the three cases of submarine landslides: Muertos Trough (top), Cariaco Basin (middle), and Desirade-Barracuda (down), with a volume V = 10 km^3.

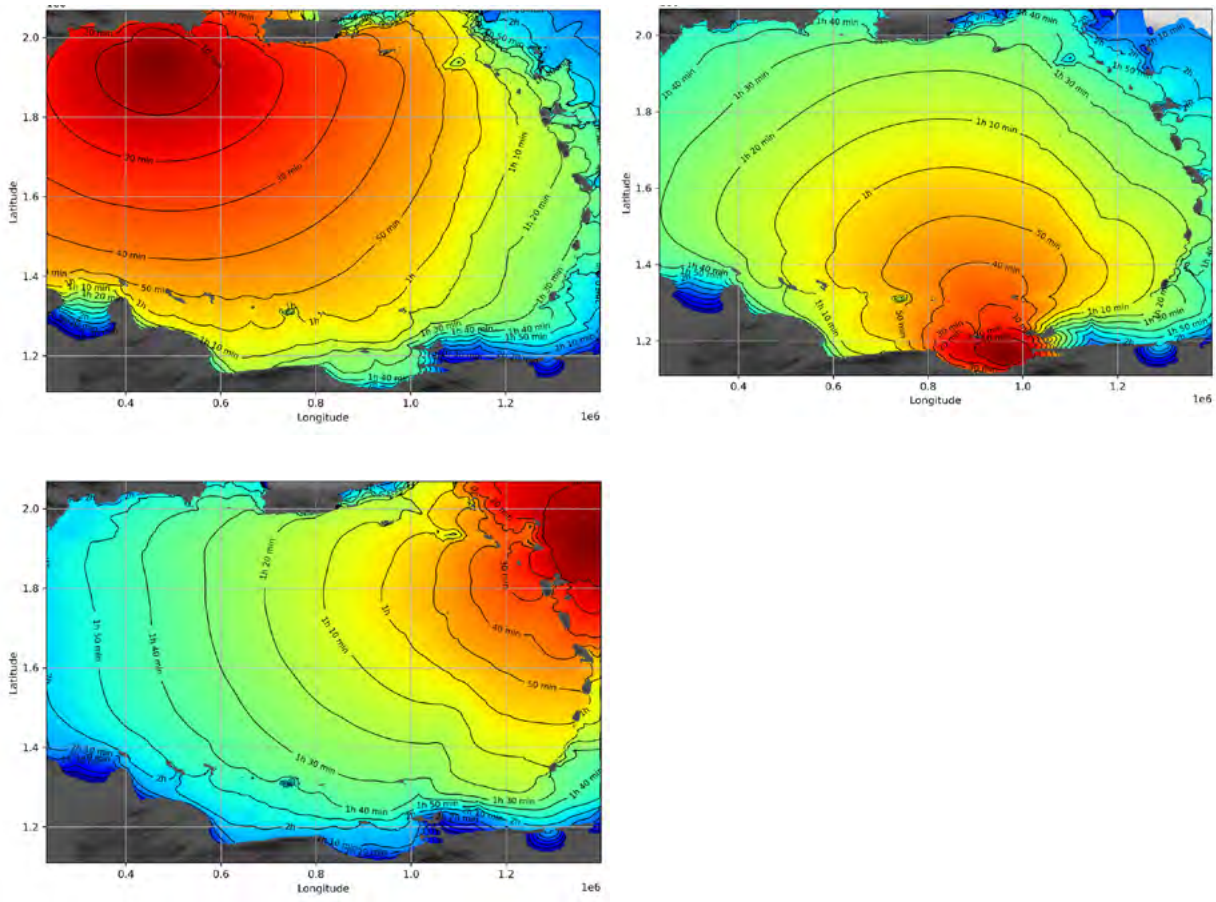

4. Other Topics Discussed

During the meeting several other topics were discussed, and these are summarised in this section. These were mainly related to (1) seismic sources of tsunamis on the south-eastern slope of the Nicaragua Rise (San Andres Rift and Hess escarpment), and (2) the design of a probabilistic tsunami hazard assessment (PTHA) for landslide and volcanic tsunamis in the Caribbean.

4.1 San Andres Rift And Hess Escarpment

More than 183 earthquakes with magnitudes ≥3.95 were recorded since 1972 in the area of the San Andres Rift and Hess Escarpment (Fig. 23). Their crustal depth ranges between 5 and 27 km (Carvajal and Mann, 2018). Focal mechanisms of major events indicate left-lateral strike-slip motion of the Pedro Bank fault zone along with localized normal faulting in the San Andres rift. This is consistent with a pull-apart origin of the basin, which is located between two left-lateral strike-slip fault systems, the Pedro Bank to the north, and the Hess Escarpment to the south. The Hess Escarpment left-lateral strike-slip fault zone becomes less seismically active toward the east and more seismically active toward the west where focal mechanisms also record compression (Fernandez et al., 2007; Symithe et al., 2015).

Figure 23. Earthquake locations (since 1974) and examples of focal mechanisms for events with magnitude ~5 in the area of the San Andres Rift showing major tectonic features, GPS vectors, and other features such as gas and oil wells and seeps, and volcanism (Carvajal and Mann, 2018). Areas (A) and (B) represent the most seismically active areas.

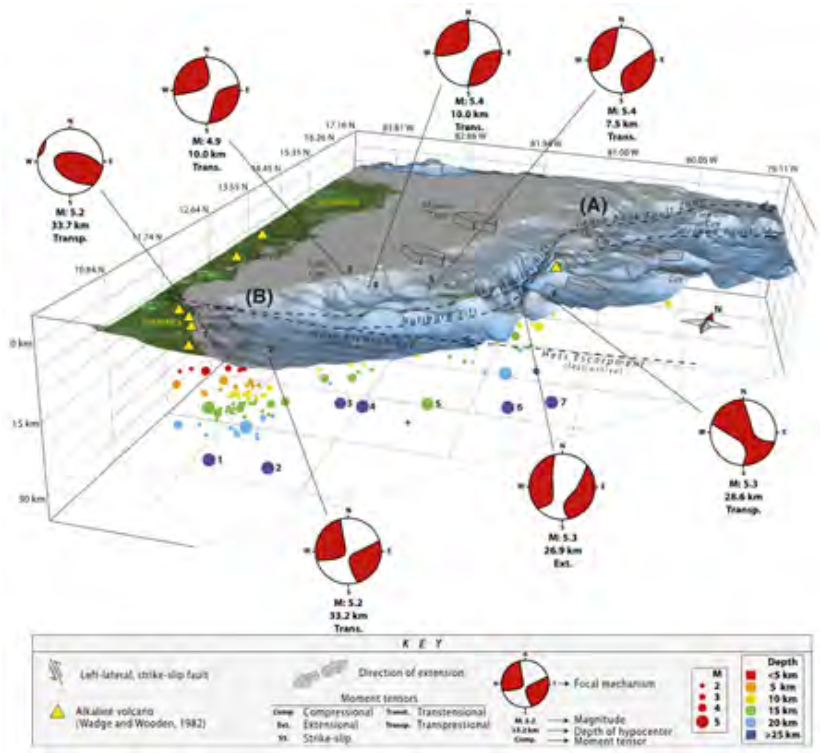

Three original scenarios of seismic rupture, whose main parameters are summarized in Table 2, were discussed during the meeting (Fig. 24): one along the Hess Escarpment, and two on each side of the San Andres Rift. The M_w = 7.6 rupture scenario along the Hess Escarpment (scenario #2 in table 2) has a very limited impact, except at one location in Panama, where a maximum wave amplitude of 0.88 m is recorded (see Annex I). The two other scenarios in the San Andres Rift have almost no impact on the coasts of Central and South America, but waves may reach an amplitude of 1 m on the coast of the San Andres, Providencia, and Maïs islands, which are located very close to the source.

Figure 24. Fault segments selected as potential seismic sources of tsunamis for the San Andres Rift and Hess Escarpment. Numbers refer to the seismic rupture ID as defined in Table 9. Seismicity catalogues : 1904-1964 M5+ events from ISC-GEM (Storchak et al. 2013) and 1964-2017 M3.6+ events from ISC-EHB (Di Giacomo and Storchak, 2016). Epicenters colors are function of depth : red for z from 0 to 29 km, orange 29-74, yellow 74-151 km.

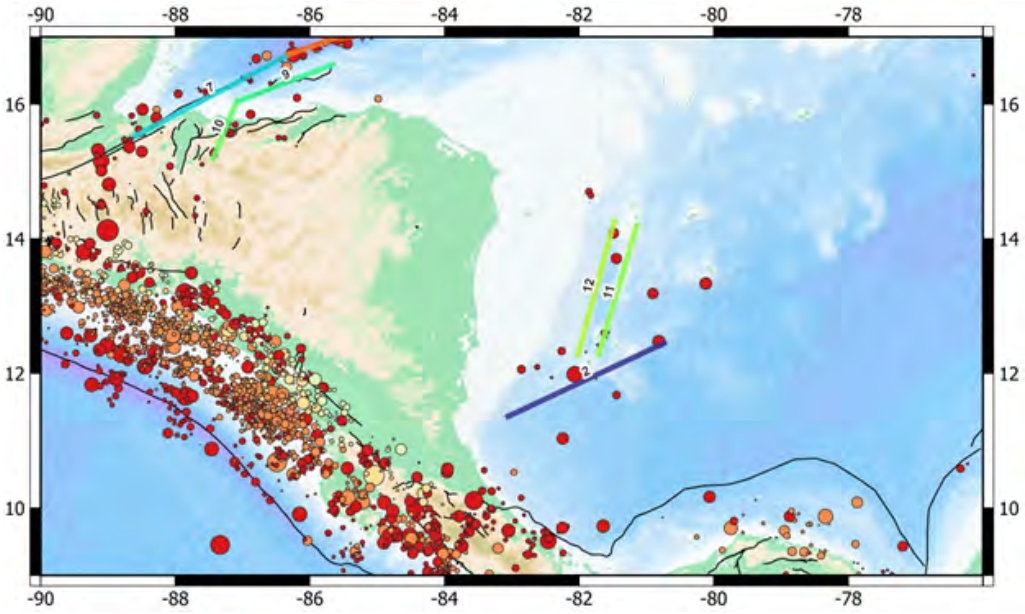

Table 9. Seismic source parameters of tsunamis for the San Andres Rift and Hess Escarpment.

ID	Name	Length (km)	Azimut (°)	LongMin (°)	LongMax (°)	LatMin (°)	LatMax (°)	Strike (°)	Dip (°)	Rake (°)	Width (m)	Sismogenic depth (km)	Slip (m)	Mo	Mw
2	Hess Escarpment	279.1	64.8	-83.051	-80.739	11.361	12.448	262	88	-22	15	15	2.4	3.014E+10	7.6
11	San Andres Rift East	219.8	16.5	-81.709	-81.145	12.283	14.191	169	58	-132	18	15	2.5	2.967E+10	7.6
12	San Andres Rift West	227.2	15.4	-82.02	-81.474	12.283	14.266	71	67	-28	16	15	2.3	2.509E+10	7.5

4.2 Probabilistic non-seismic tsunami hazard assessment

Probabilistic tsunami hazard assessment (PTHA) improves our knowledge of tsunami hazard by estimating the probability of exceeding specific levels of tsunami intensity, expressed through metrics such as the wave height at the shoreline, within a certain period of time and at given areas of interest (e.g., harbours, touristic areas) (Grezio et al., 2017 and references therein). The pioneering work of Parsons and Geist (2009) on tsunami probability in the Caribbean region considered only seismic sources of tsunamis. However, designing a PTHA for landslide or volcanic sources of tsunamis is not a matter of extending an existing PTHA based on seismic sources. There are indeed methodological difficulties linked to the lack of data on landslide and volcanic tsunamis: limited number of events in the historical catalogues, lack of well-documented examples (i.e., including instrumental data), frequent uncertainty about the source of the tsunami itself (e.g., submarine eruptions, co-seismic landslides).

The assessment of landslide tsunami hazard in the Caribbean has so far been developed on deterministic bases, i.e. aiming to reproduce historical tsunamis or proposing future scenarios on empirical grounds (e.g., Harbitz et al., 2012). During the meeting, the experts discussed the feasibility of a probabilistic framework for tsunamis generated by submarine landslide in the Caribbean. As an example, Stephan Grilli (University of Rhode Island) presented a pilot study on landslide tsunami hazard on the east Coast of the United States (Grilli et al., 2009). A Monte Carlo approach is employed, in which distributions of different parameters (recorded seismicity, sediment properties, characteristics of mapped landslide deposits, water depth, etc.) are used to perform large numbers of stochastic stability analyses of submarine slopes. It would be interesting to apply this method to the Caribbean basin, but the experts stressed the need for a homogeneous dataset in terms of bathymetry (slope map), landslide deposit mapping, seismic profiles, sediment mechanical properties, and seismic excitation such as peak ground acceleration (that can be obtained from analyses on sediment cores). As things stand, we are a long way from meeting these conditions for the entire Caribbean basin. An external funding effort gathering multiple partners and human resources is required to address this challenging task. Such a project would also come up against obstacles to data availability (e.g., military data on coastal bathymetry, oil company data). Considering these difficulties, the initiative of developing a PTHA specifically for or including submarine landslides could be handled at a national level, but in the framework of a regional warning system such as CARIBE-EWS, a regional PTHA would be far more relevant.

For volcanic tsunamis, the rationale is a little bit different since the sources, i.e. the volcanoes, are clearly identified. Even if a landslide may occur on the flanks of a volcano that is inactive, due to heavy rains for instance, most volcanic tsunamis are triggered during an eruption or a volcanic unrest. It means that the volcano usually sends us signs that can be translated into pre-warnings. Then it is difficult to determine if the eruption will be tsunamigenic, at which stage of the eruption and which phenomena will be likely to generate a tsunami. Considering these uncertainties, we recommend using a probabilistic approach specifically designed for volcanic tsunamis. Paris et al. (2019) proposed a Bayesian event-tree approach applied to tsunamis generated by submarine explosions in the Campi Flegrei caldera, Italy. The 51 simulations (17 different explosion sites with 3 different explosion energies) are implemented in a Bayesian event tree to produce conditional hazard maps. This approach could be further improved by adding all possible source mechanisms of tsunamis for a given volcano, but it requires a good knowledge of (a) the geology and eruptive history of the volcano, and (b) the conditions that led to the generation of tsunami during past eruptions at a global level.

5. Conclusions And Recommendations

The most significant outcome of the expert meeting was the production of a list of potential tsunami source scenarios, including the numerical simulations of 21 tsunami scenarios generated by seismic ruptures in the NW Caribbean, 9 non-volcanic landslide tsunamis (from 3 different sites), and 3 additional scenarios related to seismic ruptures in the Hess escarpment and San Andres Rift. Numerical simulations of all these new scenarios are now available, thanks to the work of Jean Roger and Jorge Macias following the expert meeting.

The experts also endorsed a number of recommendations**:**

- It will be necessary to update the seismic scenarios included in CATSAM for the NW Caribbean region, based on the 21 new scenarios listed in Table 3 of this report.
- The experts proposed to implement a scenario of landslide offshore Mount Pelée volcano (Martinique, Poulain et al., 2023) in the CATSAM database, together with a landslide in the Mona Passage (Lopez-Venegas et al., 2008).
- Both seismic and non-seismic experts agreed to propose a hybrid scenario combining earthquake and landslide. The Muertos Trough could make a good case study, by combine an existing seismic rupture scenario of CATSAM with one of the new landslide tsunami scenarios proposed in this report (Table 5).
- The experts proposed a list of volcanic tsunamis to be simulated in the near future (Table 6). Some of these simulations are currently being carried out.
- A full probabilistic tsunami hazard study is needed for the Caribbean, as summarized in section 4.2 of the report. This will require finding funding for a collaborative project spanning several years.
- There is a need for more paleotsunami investigations in the NW Caribbean, in order to cover a longer time period (typically the Holocene) based on tsunami deposits preserved in coastal sedimentary sequences.
- One of the two scenarios that were selected for the CaribeWave26 exercise is a tsunami produced by a debris avalanche of Kick'Em jenny volcano. This will be the opportunity to test the tsunami warning procedures in the case of a non-seismic tsunami, as exemplified by the VONUT - volcano notice for tsunami threat - proposed by Clouard et al. (2024).

6. References

Arcement, G.J., Schneider, V.R., 1989. Guide for selecting Manning's roughness coefficients for natural channels and flood plains. [Denver (CO)]: U.S. Geological Survey. Water supply paper 2339. https://doi.org/10.3133/wsp2339

Arnold, D.W.D., Biggs, J., Wadge, G., Ebmeier, S.K., Odbert, H.M., Poland, M.P., 2016. Dome growth, collapse, and valley fill at Soufrière Hills Volcano, Montserrat, from 1995 to 2013. Contributions from satellite radar measurements of topographic change. Geosphere 12 (4), 1300-1315. https://doi.org/10.1130/GES01291.1

Audemard, F.A., Romero, G., Rendón, H., Cano, V., 2005. Quaternary fault kinematics and stress tensors along the southern Caribbean from fault–slip data and focal mechanism solutions. Earth-Science Reviews 69 (3–4), 181–233. https://doi.org/10.1016/j.earscirev.2004.08.001

Authemayou, C., Brocard, G., Teyssier, C., Simon-Labric, T., Guttiérrez, A., Chiquín, E., & Moran, S., 2011. The Caribbean–North America–Cocos Triple Junction and the dynamics of the Polochic–Motagua fault systems: Pull-up and zipper models. Tectonics 30. https://doi.org/10.1029/2010TC002814

Benford, B., DeMets, C., Calais, E., 2012. GPS estimates of microplate motions, northern Caribbean: evidence for a Hispaniola microplate and implications for earthquake hazard. Geophysical Journal International 191, 481–490. https://doi.org/10.1111/j.1365-246X.2012.05662.x

Bonaccorso, A., Calvari, S., Garfì, L., Lodato, L., Patanè, D., 2003. Dynamics of the December 2002 flank failure and tsunami at Stromboli volcano inferred by volcanological and geophysical observations. Geophysical Research Letters 30, 1941. https://doi.org/10.1029/2003GL017702

Borrero, J.C., Cronin, J.C., Helina Latu'ila, F., Tukuafu, P., Heni, N., Maea Tupou, A., et al., 2022. Tsunami Runup and Inundation in Tonga from the January 2022 Eruption of the Hunga Volcano. Pure and Applied Geophysics 180, 1–22. https://doi.org/10.1007/s00024-022-03215-5

Boudon, G. Le Friant, A., Komorowski, J.C., Deplus, C., Semet, M. P. 2007. Volcano flank instability in the Lesser Antilles Arc: Diversity of scale, processes, and temporal recurrence. Journal of Geophysical Research 112, B08205. https://doi.org/10.1029/2006JB004674

Boudon, G., Komorowski, J.C., Villemant, B., Semet, M. P., 2008. A new scenario for the last magmatic eruption of La Soufrière of Guadeloupe (Lesser Antilles) in 1530 A.D. Evidence from stratigraphy radiocarbon dating and magmatic evolution of erupted products. Journal of Volcanology and Geothermal Research 178, 474–49. https://doi.org/10.1016/j.jvolgeores.2008.03.006

Brunet, M. Le Friant, A., Boudon, G., Lafuerza, S., Talling, P., Hornbach, M., et al., 2016. Composition, geometry, and emplacement dynamics of a large volcanic island landslide offshore Martinique: from volcano flank collapse to seafloor sediment failure? Geochemistry, Geophysics, Geosystems 17, 699–724. https://doi.org/10.1002/2015GC006034

Calais, E., Perrot, J., Mercier de Lépinay, B., 1998. Strike-slip tectonics and seismicity along the northern Caribbean plate boundary from Cuba to Hispaniola. Geological Society of America Special Papers 326, 125-169. https://doi.org/10.1130/0-8137-2326-4.125

Calais, E., Gonzalez, O., Arango-Arias, E., Moreno, B., Palau, R., Cutie, M., Diez, E., Montenegro, C., Roche, R., Garcia, J., Castellanos, E., & Symithe, S., 2023. Current deformation along the northern Caribbean plate boundary from GNSS measurements in Cuba. Tectonophysics 868, 230068. https://doi.org/10.1016/j.tecto.2023.230068

Carvajal, L.C., Mann, P., 2018. Western Caribbean intraplate deformation: Defining a continuous and active microplate boundary along the San Andres rift and Hess Escarpment fault zone, Colombian Caribbean Sea. AAPG Bulletin 102 (8), 1523-1563. https://doi.org/10.1306/12081717221

Carvajal, M., Sepúlveda, I., Gubler, A., & Garreaud, R., 2022. Worldwide signature of the 2022 Tonga volcanic tsunami. Geophysical Research Letters 49, e2022GL098153. https://doi.org/10.1029/2022GL098153

Chaytor, J.D., Geist, E.L., Paull, C.K., Caress, D.W., Gwiazda, R., Urrutia Fucugauchi, J., Rebolledo Vieyra, M., 2016. Source Characterization and Tsunami Modeling of Submarine Landslides Along the Yucatán Shelf/Campeche Escarpment, Southern Gulf of Mexico. Pure and Applied Geophysics 173, 4101-4116. https://doi.org/10.1007/s00024-016-1363-3

Cheng, C., Wang, D., 2020. Imaging the rupture process of the 10 January 2018 M_w 7.5 Swan island, Honduras earthquake. Earthquake Science 33, 194-200.

Clouard, V., von Hillebrandt-Andrade, C., McCreery, C., Soto Cortes, J.J., 2024. Implementation of tsunami warning procedures in the Caribbean in case of volcano crisis : use of a Volcano Notice for tsUnami Threat (VONUT). Bulletin of Volcanology 86, 18. https://doi.org/10.1007/s00445-023-01702-8

Collico, S., Arroyo, M., Urgeles, R., Gracia, E., Devincenzi, M., Peréz, N., 2020. Probabilistic mapping of earthquake-induced submarine landslide susceptibility in the South-West Iberian margin. Marine Geology 429, 106296. https://doi.org/10.1016/j.margeo.2020.106296

Coussens, M., Wall-Palmer, D., Talling, P., Watt, S., Cassidy, M., Jutzeler, M., et al., 2016. The relationship between eruptive activity, flank collapse, and sea level at volcanic islands: A long-term (>1 Ma) record offshore Montserrat, Lesser Antilles. Geochemistry, Geophysics, Geosystems 17 (7), 2591–2611. https://doi.org/10.1002/2015GC006053

Cotilla Rodriguez, M.O., Franzke, H.J., Cordoba Barba, D., 2007. Seismicity and seismoactive faults of Cuba. Russian Geology and Geophysics 48, 505-522.

DeMets, C., Jansma, P.E., Mattioli, G.S., Dixon, T.H., Farina, F., Bilham, R., Calais, E., Mann, P., et al., 2000. GPS geodetic constraints on Caribbean-North America plate motion. Geophysical Research Letters 27, 437–440. https://doi.org/10.1029/1999GL005436

DeMets, C., Mattioli, G., Jansma, P., Rogers, R., Tenorio, C., Turner, H.L., 2007. Present motion and deformation of the Caribbean plate: Constraints from new GPS geodetic measurements from Honduras and Nicaragua. In: Mann, P., ed., Geologic and Tectonic Development of the Caribbean Plate in Northern Central America: Geological Society of America Special Paper 428, 21–36. https://doi.org/10.1130/2007.2428(02)

Di Giacomo, D., and D.A. Storchak, 2016. A scheme to set preferred magnitudes in the ISC Bulletin. Journal of Seismology 20, 555-567. https://doi.org/10.1007/s10950-015-9543-7

Dondin, F., Lebrun, J.F., Kelfoun, K., Fournier, N., Randrianasolo, A., 2012. Sector collapse at Kick'em Jenny submarine volcano (Lesser Antilles): numerical simulation and landslide behavior. Bulletin of Volcanology 74, 595-607. https://doi.org/10.1007/s00445-011-0554-0

Elbanna, A., Abdelmeguid, M., Ma, X., Amlani, F., Bhat, H.S., Synolakis, C., Rosakis, A.J., 2021. Anatomy of strike-slip fault tsunami genesis. PNAS 118 (19), e2025632118. https://doi.org/10.1073/pnas.2025632118

Ellis, A., DeMets, C., Briole, P., Cosenza, B., Flores, O., Graham, S.E., Guzmán-Speziale, M., Hernández, D., Kostoglodov, V., LaFemina, P., Lord, N., Lasserre, C., Lyon-Caen, H., Rodriguez Maradiaga, M., McCaffrey, R., Molina, E., Rivera, J., Rogers, R., & Staller, A., 2019. GPS constraints on deformation in northern Central America from 1999 to 2017, Part 1 - Time-dependent modelling of large regional earthquakes and their post-seismic effects. Geophysical Journal International 214, 2177–2194. https://doi.org/10.1093/gji/ggy249

Engel, M., Oetjen, J., May, S.M., Brückner, H., 2016. Tsunami deposits of the Caribbean – Towards an improved coastal hazard assessment. Earth-Science Reviews 163, 260-296. http://dx.doi.org/10.1016/j.earscirev.2016.10.010

Escalona, A., Mann, P., Jaimes, M., 2011. Miocene to recent Cariaco basin, offshore Venezuela: structure, tectonosequences, and basin-forming mechanisms. Marine and Petroleum Geology 28, 177-199. https://doi.org/10.1016/j.marpetgeo.2009.04.001

Fernandez, M., Camacho, E., Molina, E., Marroquin, G., Strauch, W., 2007. Seismicity and neotectonic of Central America. In: Bundschuh, J., Alvarado, G. (Eds.), Central America: Geology, resource and hazards. Andover, United Kingdom, Taylor & Francis Customer Services, 1340 p.

Fritz, H., Hager, W., Minor, H., 2004. Near Field Characteristics of Landslide Generated Impulse Waves. Journal of Waterway Port Coastal and Ocean Engineering 130, 287-302. https://doi.org/10.1061/(ASCE)0733-950X(2004)130:6(287)

Fritz, H.M., Hillaire, J.V., Molière, E., Wei, Y., Mohammed, F., 2013. Twin tsunamis triggered by the 12 January 2010 Haiti earthquake. Pure and Applied Geophysics 170, 1463–1474. https://doi.org/10.1007/s00024-012-0479-3

GEBCO, 2024. GEBCO Bathymetric Compilation Group 2024. The GEBCO_2024 Grid - a continuous terrain model of the global oceans and land. NERC EDS British Oceanographic Data Centre NOC. https://doi:10.5285/1c44ce99-0a0d-5f4f-e063-7086abc0ea0f

González-Vida, J.M., Macías, J., Castro, M.J., Sánchez-Linares, C., de la Asunción, M., Ortega-Acosta, S., Arcas, D., 2019. The Lituya Bay landslide-generated mega-tsunami. Numerical simulation and sensitivity analysis, Natural Hazards and Earth System Sciences 19, 369-388. https://doi.org/10.5194/nhess-19-369-2019

Graham, S.E., DeMets, C., DeShon, H.R., Rogers, R., Maradiaga, M.R., Strauch, W., Wiese, K., Hernandez, D., 2012. GPS and seismic constraints on the M = 7.3 2009 Swan Islands earthquake: implications for stress changes along the Motagua fault and other nearby faults. Geophysical Journal International 190, 1625-1639.

Granja Brunã, J.L., ten Brink, U.S., Carbó-Gorosabel, A., Munõz-Martín, A., Gómez Ballesteros, M., 2009. Morphotectonics of the central Muertos thurst belt and Muertos Trough (northeastern Caribbean). Marine Geology 263, 7-33. https://doi.org/10.1016/j.margeo.2009.03.010

Granja-Bruña, J.L., Gorosabel-Araus, J.M., ten Brink, U., Muñoz-Martín, A., Rodríguez-Zurrunero, A., Leroy, S., López-Venegas, A., Llorente-Isidro, M., Macías Sánchez, J., Sánchez-Linares, C., Carbó-Gorosabel, A., 2022. Seismotectonics and Crustal Structure in the Southern Dominican Republic Offshore Margin : Implications on the Tsunami Potential. Geochemistry, Geophysics, Geosystems 26, e2024GC012092. https://doi.org/10.1029/ 2024GC012092

Grezio, A., Babeyko, A., Baptista, M.A., Behrens, J., Costa, A., Davies, G., Geist, E.L., Glimsdal, S., Gonzàlez, F.I., Griffin, J., Harbitz, C.B., LeVeque, R.J., Lorito, S., Lövholt, F., Omira, R., Mueller, C., Paris, R., Parsons, T., Polet, J., Power, W., Selva, J., Sörensen, M.B., Thio, H.K., 2017. Probabilistic Tsunami Hazard Analysis (PTHA): multiple sources and global applications. Reviews of Geophysics 55, 1158-1198. https://doi.org/10.1002/2017RG000579

Grilli, S.T., Taylor, O.D.S., Baxter, C.D.P., Maretzki, S., 2009. A probabilistic approach for determining submarine landslide tsunami hazard along the upper east coast of the United States. Marine Geology 264, 74-97. https://doi.org/10.1016/j.margeo.2009.02.010

Grilli S.T., Tappin, D.R., Carey, S., Watt, S.F.L., Ward S.N., Grilli, A.R., Engwell, S.L., Zhang C., Kirby J.T., Schambach, L., Muin, M., 2019. Modelling of the tsunami from the December 22, 2018 lateral collapse of Anak Krakatau volcano in the Sunda Straits, Indonesia. Scientific Reports 9, 11946. https://doi.org/doi:10.1038/s41598-019-48327-6

Gueugneau, V., Charbonnier, S., Miller, V.L., Cole, P., Grandin, R., Dualeh, E.W., 2024. Modelling pyroclastic density currents of the April 2021 La Soufrière, St Vincent eruption: from rapid invasion maps to field-constrained numerical simulations. In: Robertson, R.E.A., Joseph, E.P., Barclay, J., Sparks, R.S.J. (eds). The 2020–21 Eruption of La Soufrière Volcano, St Vincent. Geological Society, London, Special Publications, 539, 291–310. https://doi.org/10.1144/SP539-2022-290

Guzman-Speziale, M., 2022. The triple junction of the North America, Cocos, and Caribbean plates. What we know, what we don't. Revista Mexicana de Cienccias Geológicas 39, 190-205.

Harbitz, C.B., Løvholt, F., Pedersen, G., Masson, D.G., 2006. Mechanisms of tsunami generation by submarine landslides: a short review. Norwegian Journal of Geology 86, 255–264. https://doi.org/

Harbitz, C., Glimsdal, S., Bazin, S., Zamora, N., Lóvholt, F., Bungum, H., Smebye, H., Gauer, P., Kjekstad, O., 2012. Tsunami hazard in the Caribbean: regional exposure derived from credible worst case scenarios. Continental Shelf Research 38, 1–23. https://doi.org/10.1016/j.csr.2012.02.006

Heinrich, P., Mangeney, A., Guibourg, S., Roche, R., 1998. Simulation of water waves generated by a potential debris avalanche in Montserrat, Lesser Antilles. Geophysical Research Letters 25 (19), 3697–3700. https://doi.org/10.1029/98GL01407

Herd, R.A., Edmonds, M., Bass, V.A., 2005. Catastrophic lava dome failure at Soufriere Hills Volcano, Montserrat, 12-13 July 2003. Journal of Volcanology and Geothermal Research, 148, 234-252. https://doi.org/10.1016/j.jvolgeores.2005.05.003

Hornbach, M.J., Braudy, N., Briggs, R.W., Cormier, M.H., et al., 2010. High tsunami frequency as a result of combined strike-slip faulting and coastal landslides. Nature Geoscience, 3, 783–789. https://doi.org/10.1038/ngeo975

IOC-UNESCO, 2016. Experts meeting on Sources of tsunamis in the Caribbean with possibility to impact the southern coast of the Dominican Republic. Santo Domingo, Dominican Republic, 6–7 May 2016. Paris, UNESCO, Workshop Report n° 276.

IOC-UNESCO, 2018. Experts meeting on Tsunami hazard in Central America: Historical events and potential sources, San José, Costa Rica, 23-24 June 2016. Paris, UNESCO, Workshop Report n° 278.

IOC-UNESCO, 2020. Experts Meeting on Sources of Tsunamis in the Lesser Antilles. Fort-de-France, Martinique, France, 18–20 March 2019. Paris, UNESCO, Workshop Report n° 291.

IOC-UNESCO, 2023. Monitoring and warning for tsunamis generated by volcanoes. UNESCO, IOC Technical series n° 183.

Komorowski, J.C., Legendre, Y., Caron, B., Boudon, G., 2008. Reconstruction and analysis of sub-plinian tephra dispersal during the 1530 A.D. Soufrière (Guadeloupe) eruption: Implications for scenario definition and hazards assessment. Journal of Volcanology and Geothermal Research 178, 491–515. https://doi.org/10.1016/j.jvolgeores.2007.11.022

Kirby, J.T., Grilli, S.T., Horrillo, J., Liu P.L.F., Nicolsky, D., Abadie, S., Ataie-Ashtiani, B., Castro, M.J., Clous, L., Escalante C., Fine I., Gonzalez-Vida, J.M., Lovholt, F., Lynett, P., Ma, G., Macias, J., Ortega, S., Shi, F., Yavari-Ramshe, S., Zhang, C., 2022. Validation and intercomparison of models for landslide tsunami generation. Ocean Modelling, 170, 101943, doi:10.1016/j.ocemod.2021.101943

Lacroix, A., 1904. La montagne Pelée et ses éruptions. Masson et Cie, Paris, 662 p.

Le Friant, A., Boudon, G., Arnulf, A., Robertson, R.E.A., 2009. Debris avalanche deposits offshore St Vincent (West Indies): impact of flank-collapse events on the morphological evolution of the island. Journal of Volcanology and Geothermal Research 179, 1-10. https://doi.org/10.1016/j.jvolgeores.2008.09.022

Le Friant, A., Ishizuka, O., Boudon, G., Palmer, M. R., Talling, P., Villemant, B., et al., 2015. Submarine record of volcanic island construction and collapse in the Lesser Antilles arc: First scientific drilling of submarine volcanic island landslides by IODP Expedition 340. Geochemistry, Geophysics, Geosystems 16 (2), 420–442. https://doi.org/ 10.1002/2014GC005652

Le Friant, A., Lebas, E., Brunet, M., Lafuerza, S., Hornbach, M., Coussens, M., Watt, S., Cassidy, M., Talling, P.J., and IODP 340 Expedition Science Party, 2020. Submarine Landslides Around Volcanic Islands: A Review of What Can Be Learned From the Lesser Antilles Arc. In: Ogata, K., Festa, A., Pini, G.A., Landslides: Subaqueous Mass Transport Deposits from Outcrops to Seismic Profiles. American Geophysical Union, Geophysical Monograph 246, 277-297. https://doi.org/10.1002/9781119500513.ch17

Lebas, E. , Le Friant, A., Boudon, G., Watt, S.F.L., Talling, P.J., Feuillet, N., Deplus, C., Berndt, C., Vardy, M.E., 2011. Multiple widespread landslides during the long-term evolution of a volcanic island: insights from high-resolution seismic data, Montserrat, Lesser Antilles. Geochemistry, Geophysics, Geosystems 12 (5), Q05006. https://doi.org/10.1029/2010GC003451

de Lépinay, B.M., Deschamps, A., Klingelhoefer, F., Mazabraud, Y., Delouis, B., Clouard, V., Hello, Y., Crozon, J., Marcaillou, B., Graindorge, D., Vallée, M, Perrot, J., Bouin, M.P., Saurel, J.M., Charvis, P., St-Louis, M., 2011. The 2010 Haiti earthquake: A complex fault pattern constrained by seismologic and tectonic observations. Geophysical Research Letters 38, L22305. https://doi.org/10.1029/2011GL049799

Le Roy, S., et al., 2017. Détermination de la submersion marine liée aux tsunamis en Martinique. BRGM (Bureau des Recherches Géologiques et Minières), Public report BRGM/RP-66547-FR, 324 p.

Leslie, S.C., Mann, P., 2016. Giant submarine landslides on the Colombian margin and tsunami risk in the Caribbean Sea. Earth and Planetary Science Letters 449, 382–394. http://dx.doi.org/10.1016/j.epsl.2016.05.040

Lindsay, J. M., Shepherd, J. B., and Wilson, D., 2005. Volcanic and scientific activity at Kick'em Jenny submarine volcano 2001–2002: implications for volcanic hazard in the southern Grenadines, Lesser Antilles. Natural Hazards 34, 1-24.

Liu, P.L.F., Cho, Y.S., Briggs, M.J., Kanoglu, U., Synolakis, C.E., 1995. Runup of solitary waves on a circular island. Journal of Fluid Mechanics. 302:259-285. https://doi.org/10.1017/S0022112095004095

Liu, P.L.F., Woo, S.B., Cho, Y.S., 1998. Computer programs for tsunami propagation and inundation. Ithaca (NY): Cornell University. Technical Report.

López-Venegas, A., ten Brink, U.S. and Geist, E.L. 2008. Submarine landslide as the source for the October 11, 1918 Mona Passage tsunami; observations and modeling. Marine Geology 254, 35–46. https://doi.org/10.1016/j.margeo.2008.05.001

Lyon-Caen, H., Barrier, É., Lasserre, C., Franco, A., Arzu, I., Chiquin, L., Chiquín, M., Duquesnoy, T., Flores, O., Galicia, O., Luna, J., Molina, E., Porras, O., Requena, J., Robles, V., Romero, J., & Wolf, R., 2006. Kinematics of the North American–Caribbean-Cocos plates in Central America from new GPS measurements across the Polochic-Motagua fault system. Geophysical Research Letters 33, L19309. https://doi.org/10.1029/2006GL027694

Macías, J., Escalante, C., and Castro, M.J., 2021a. Multilayer-HySEA model validation for landslide generated tsunamis. Part I Rigid slides. Natural Hazards and Earth System Sciences 21, 775-789. https://doi.org/10.5194/nhess-21-775-2021

Macías, J., Escalante, C., and Castro, M.J., 2021b. Multilayer-HySEA model validation for landslide generated tsunamis. Part II Granular slides. Natural Hazards and Earth System Sciences 21, 791-805. https://doi.org/10.5194/nhess-21-791-2021

Macías, J., Vázquez, J.T., Fernández-Salas, L.M., González-Vida, J.M., Bárcenas, P., Castro, M.J., Díaz-del-Río, V., Alonso, B., 2015. The Al-Boraní submarine landslide and associated tsunami. A modelling approach. Marine Geology 361, 79-95. https://doi.org/10.1016/j.margeo.2014.12.006

Mann, P., Taylor, F.W., Edwards, R.L., Ku, T., 1995. Actively evolving microplate formation by oblique collision and sideways motion along strike-slip faults: an example from the northeastern Caribbean plate margin. Tectonophysics 246, 1–69. https://doi.org/10.1016/0040-1951(94)00268-E

Moscardelli, L., Wood, L., and Mann, P. 2006. Mass-transport complexes and associated processes in the offshore area of Trinidad and Venezuela. AAPG Bulletin 90 (7), 1059–1088. https://doi.org/10.1306/02210605052

Muhari, A., Heidarzadeh, M., Susmoro, H., Nugroho, H.D., Kriswati, E., Supartoyo, et al., 2019. The December 2018 Anak Krakatau Volcano Tsunami as Inferred from Post-Tsunami Field Surveys and Spectral Analysis. Pure Applied Geophysics. 176, 5219–5233. https://doi.org/10.1007/s00024-019-02358-2

Nakata, K., Katsumata, A., Muhari, A., 2020. Submarine landslide source models consistent with multiple tsunami records of the 2018 Palu tsunami, Sulawesi, Indonesia. Earth Planets Space 72, 44. https://doi.org/10.1186/s40623-020-01169-3

Okada, Y., 1985. Surface deformation due to shear and tensile fault in a half-space. Bulletin of the Seismological Society of America 75 (4), 1135-1154. https://doi.org/10.1785/BSSA0750041135

O'Loughlin, K.F., Lander, J.F., 2003. Caribbean Tsunamis: A 500-Year History from 1498-1998. Kluwer Academic Publishers, Dordrecht, The Netherlands. 263 p.

Omira, R., Ramalho, R.S., Kim, J., González, P.J., Kadri, U., Miranda, J.M.,et al., 2022. Global Tonga tsunami explained by a fast-moving atmospheric source. Nature 609, 734–740. https://doi.org/10.1038/s41586-022-04926-4

Paris, R., 2015. Source mechanisms of volcanic tsunamis. Philosophical Transactions of the Royal Society A 373, 20140380. https://doi.org/10.1098/rsta.2014.0380

Paris, R., Switzer, A.D., Belousova, M., Belousov, A., Ontowirjo, B., Whelley, P.L., Ulvrová, M., 2014. Volcanic tsunami: a review of source mechanisms, past events and hazards in Southeast Asia (Indonesia, Philippines, Papua New Guinea). Natural Hazards 70 (1), 447-470. https://doi.org/10.1007/s11069-013-0822-8

Paris, R., Ulvrova, M., Selva, J., Brizuela, B., Costa, A., Grezio, A., Lorito, S., Tonini, R., 2019. Probabilistic hazard analysis for tsunamis generated by subaqueous volcanic explosions in the Campi Flegrei caldera, Italy. Journal of Volcanology and Geothermal Research 379, 106-116. https://doi.org/10.1016/j.jvolgeores.2019.05.010

Paris, R., Ulvrova, M., 2019. Tsunamis generated by subaqueous volcanic explosions in Taal Caldera Lake, Philippines.

Bulletin of Volcanology 81, 14. https://doi.org/10.1007/s00445-019-1272-2

Plafker, G., 1976. Tectonic aspects of the Guatemala Earthquake of 4 February 1976. Science 193, 1201–1208. https://doi.org/10.1126/science.193.4259.1201

Peirce, C., Robinson, A.H., Campbell, A.M., Funnell, M.J., Grevemeyer, I., Hayman, N.W., Van Avendonk, H.J.A. & Castiello, G., 2019. Seismic investigation of an active ocean-continent transform margin: the interaction between the Swan Islands Fault Zone and the ultraslow-spreading Mid-Cayman Spreading Centre. Geophysical Journal International 219, 159–184. https://doi.org/10.1093/gji/ggz283

Pelinovsky, E., Zahibo, N., Dunkley, P., Edmonds, M., Herd, R., Talipova, T., et al., 2004. Tsunamis generated by the volcano eruption on July 12-13, 2003, at Montserrat, Lesser Antilles. Science of Tsunami Hazards, 22, 44-57.

Perrot, J., Calais, E., Mercier de Lépinay, B., 1997. Tectonic and kinematic regime along the Northern Caribbean plate boundary: new insights from broad-band modeling of the May 25, 1992, M_s = 6.9 Cabo Cruz, Cuba, earthquake. Pure and Applied Geophysics 149, 475-487. https://doi.org/10.1007/s000240050036

Peruzzetto, M., Komorowski, J.C., Le Friant, A., Rosas-Carbajal, M., Mangeney, A., Legendre, Y., 2019. Modeling of partial dome collapse of La Soufriere of Guadeloupe volcano: implication for hazard assessment and monitoring. Scientific Reports (2019) 9, 13105. https://doi.org/10.1038/s41598-019-49507-0

Poisson, B. and Pedreros, R., 2010. Numerical modelling of historical landslide-generated tsunamis in the French Lesser Antilles. Natural hazards and Earth System Sciences 10 (6), 1281–1292. https://doi.org/10.5194/nhess-10-1281-2010

Poulain, P., Le Friant, A., Mangeney, A., Viroulet, S., Fernandez-Nieto, E., Castro Diaz M., Peruzzetto, M., Grandjean, G., Bouchut, F., Pedreros, R., Komorowski, J.C., 2023. Performance and limits of a shallow-water model for landslide-generated tsunamis: from laboratory experiments to simulations of flank collapses at Montagne Pelée (Martinique). Geophysical Journal International 233, 796-825. https://doi.org/10.5194/egusphere-egu22-3912

Poupardin, A., Calais, E., Heinrich, P., Hébert, H., Rodriguez, M., Leroy, S., Aochi, H., Douilly,, R., 2020. Deep submarine landslide contribution to the 2010 Haiti earthquake tsunami. Natural Hazards and Earth System Sciences 20, 2055–2065. https://doi.org/10.5194/nhess-20-2055-2020

Robinson, E., Rowe, D.-A.C., Khan, S.A., 2006. Wave-emplaced boulders on Jamaica's rocky shorelines. Zeitschrift für Geomorphologie, Suppl. Band 146, 39–57.

Roger, J., Pelletier, B., Gusman, A., Power, W., Wang, X., Burbidge, D., Duphil, M., 2023. Potential tsunami hazard of the southern Vanuatu subduction zone: tectonics, case study of the Matthew Island tsunami of 10 February 2021 and implication in regional hazard assessment. Natural Hazards and Earth System Sciences 23, 393-414. https://doi.org/10.5194/nhess-23-393-2023

Roger, J., Bull, S., Watson, S.J., Mueller, C., Hillman, J.I.T., Wolter, A., lamarche, G., Power, W., Lane, E., Woelz, S., Davidson, S., 2024. A review of approaches for submarine landslide-tsunami hazard identification and assessment. Marine and Petroleum Geology 162, 106729. https://doi.org/10.1016/j.marpetgeo.2024.106729

Rosencrantz, E. & Mann, P., 1991. SeaMARC II mapping of transform faults in the Cayman Trough, Caribbean Sea. Geology 19, 690–693.

Rowe, D.A., Khan, S., Robinson, E., 2009. Hurricanes or tsunami? Comparative analysis of extensive boulder arrays along the southwest and north coasts of Jamaica: lessons for coastal management. In: McGregor, D., Dodman, D., Barker, D. (Eds.), Global Change and Caribbean Vulnerability. University of the West Indies Press, Kingston, 49–73.

Schambach L., Grilli S.T. and D.R. Tappin 2021. New high-resolution modeling of the 2018 Palu tsunami, based on supershear earthquake mechanisms and mapped coastal landslides, supports a dual source. Frontiers in Earth Sciences 8, 627. https://doi.org/10.3389/feart.2020.598839

Shaw, C.E., Benson, L., 2015. Possible tsunami deposits on the Caribbean coast of the Yucatán peninsula. Journal of Coastal Research 31, 1306–1316. https://doi.org/10.2112/JCOASTRES-D-14-00084.1

Schindelé, F., Kong, L., Lane, E.M., Paris, R., Ripepe, M., Titov, V., Bailey, R., 2024. A review of Tsunamis Generated by Volcanoes (TGV) source mechanism, modelling, monitoring and warning systems. Pure and Applied Geophysics 181, 1745-1792. https://doi.org/10.1007/s00024-024-03515-y

Seibert, C., Feuillet, N., Ratzov, G., Beck, C., Cattaneo, A., 2020. Seafloor morphology and sediment transfer in the mixed carbonate-siliciclastic environment of the Lesser Antilles forearc along Barbuda to St. Lucia. Marine Geology 428, 106242. https://doi.org/10.1016/j.margeo.2020.106242

Seibert, C., Feuillet, N., Ratzov, G., Beck, C., Morena, P., Johannes, L., et al., 2024. Sedimentary records in the Lesser Antilles fore-arc basins provide evidence of large late Quaternary megathrust earthquakes. Geochemistry, Geophysics, Geosystems 25, e2023GC011152. https://doi.org/10.1029/2023GC011152

Smith, M., Shepherd, J.B., 1993. Preliminary investigations of the tsunami hazard of Kick'em Jenny submarine volcano. Natural Hazards 7, 257–277. https://doi.org/10.1007/BF00662650

Smith, M., Shepherd, J.B., 1995. Potential Cauchy-Poisson waves generated by submarine eruptions of Kick'em jenny volcano. Natural Hazards 11, 75-94. https://doi.org/10.1007/BF00613311

Sostre-Cortés, J., Vanacore, E.A., von Hillebrandt-Andrade, C., Watlington, R.A., Clouard, V., Chacón-Barrantes, S., Dourado, F., Gómez-Ramos, O., Joseph, E.P., Paris, R., 2025. Characterizing sea level and barometric disturbances in the Caribbean and adjacent regions from the Hunga Tonga-Hunga Ha'apai 2022 eruption. Ocean and Coastal Research 73, e25010. https://doi.org/10.1590/2675-2824073.23202

Storchak, D.A., Di Giacomo, D., Bondár, I., Engdahl, E. R., Harris, J., Lee, W.H., ..., Bormann, P., 2013. Public release of the ISC–GEM global instrumental earthquake catalogue (1900–2009). Seismological Research Letters 84 (5), 810-815. https://doi.org/10.1785/0220130034

Symithe, S., Calais, E., Chabalier, J.B., Robertson, R., Higgins, M., 2015. Current block motions and strain accumulation on active faults in the Caribbean. Journal of Geophysical Research, Solid Earth 120, 3748-3774. https://doi.org/10.1002/2014JB011779

Tadapansawut, T., Okuwaki, R., Yagi, Y., Yamashita, S., 2021. Rupture process of the 2020 Caribbean earthquake along the Oriente transform fault, involving supershear rupture and geometric complexity of fault. Geophysical Research Letters 48, e2020GL090899. https://doi.org/10.1029/2020GL090899

Tappin, D.R., Watts, P., McMurtry, G.M., Lafoy, Y., Matsumoto, T., 2001. The Sissano, Papua New Guinea tsunami of July 1998 — offshore evidence on the source mechanism. Marine Geology 175, 1-23. https://doi.org/10.1016/S0025-3227(01)00131-1

Tarazona, D.M., Prieto, J., Murphy, W., Naranjo Vesga, J., Rincon, D., Hernandez Munoz, C., Madero Pinzon, H., Mora Mora, A., Acuña-Uribe, M., 2023. Submarine landslide susceptibility assessment along the southern convergent margin of the Colombian Caribbean. The Leading Edge 42 (5), 344-359. https://doi.org/10.1190/tle42050344.1

Tehranirad, B., Harris, J.C., Grilli, A.R., Grilli, S.T., Abadie, S., Kirby, J.T., Shi, F., 2015. Far-field tsunami threat in the north Atlantic basin from large scale flank collapses of the Cumbre Vieja volcano, La Palma. Pure and Applied Geophysics 172, 3589-3616.

ten Brink, U., Coleman, D. & Dillon, W.P., 2002. The nature of the crust under Cayman Trough from gravity. Marine and Petroleum Geology 19, 971–987. https://doi.org/10.1016/S0264-8172(02)00132-0

ten Brink, U., Geist, E.,L., Andrews, B.D., 2006. Size distribution of submarine landslides and its implication to tsunami hazard in Puerto Rico. Geophysical Research Letters 33, L11307. https://doi.org/10.1029/2006GL026125

ten Brink, U., Barkan, R., Andrews, B.D., Chaytor, J.D., 2009. Size distributions and failure initiation of submarine and subaerial landslides. Earth and Planetary Science Letters 287, 31–42. https://doi.org/10.1016/j.epsl.2009.07.031

ten Brink, U., Andrews, B.D., Miller, N.C., 2016. Seismicity and sedimentation rate effects on submarine slope stability. Geology 44 (7), 563-566. https://doi.org/10.1130 /G37866.1

Torsvik, T., Paris, R., Didenkulova, I., Pelinovsky, E., Belousov, A., Belousova, M., 2010. Numerical simulation of a tsunami

event during the 1996 volcanic eruption in Karymskoye Lake, Kamchatka, Russia. Natural Hazards and Earth System Sciences 10, 2359-2369. https://doi.org/10.5194/nhess-10-2359-2010

Urgeles, R., and Camerlenghi, A., 2013. Submarine landslides of the Mediterranean Sea: Trigger mechanisms, dynamics, and frequency-magnitude distribution. Journal of Geophysical Research 118, 2600–2618. https://doi.org/10.1002/2013JF002720

Wang, X., 2008. Numerical modelling of surface and internal waves over shallow and intermediate water [PhD Thesis]. Ithaca (NY): Cornell University. 245 p.

Wang, X., Liu, P.L.F., 2011. An explicit finite difference model for simulating weakly nonlinear and weakly dispersive waves over slowly varying water depth. Coastal Engineering 58 (2), 173-183. https://doi.org/10.1016/j.coastaleng.2010.09.008

Wang, X., Lukovic, B., Power, W.L., Mueller C., 2017. High-resolution inundation modelling with explicit buildings: a case study of Wellington CBD. Lower Hutt (NZ): GNS Science. 27 p. (GNS Science report; 2017/13).

Wang, X., Power, W., 2011. COMCOT: a tsunami generation, propagation and runup model. Lower Hutt (NZ): GNS Science. 121 p. (GNS Science report; 2011/43).

Watt, S.F.L., Talling, P.J., Vardy, M.E., Heller, V., Hühnerbach, V., Urlaub, M., Sarkar, S., Masson, D.G., et al., 2012. Combinations of volcanic-flank and seafloor-sediment failure offshore Montserrat, and their implications for tsunami generation. Earth and Planetary Science Letters 319–320, 228–240. https://doi.org/10.1016/j.epsl.2011.11.032

Williamson, A. L., Melgar, D., Xu, X., Milliner, C., 2020. The 2018 Palu tsunami: Coeval landslide and coseismic sources. Seismological Research Letters 91, 3148–3160. https://doi.org/10.1785/0220200009

Xu, Z., Sun, L., Rahman, M.N.A., Liang, S., Shi, J., Li, H., 2022. Insights on the small tsunami from January 28, 2020, Caribbean Sea M_W7.7 earthquake by numerical simulation and spectral analysis. Natural Hazards 111, 2703–2719. https://doi.org/10.1007/s11069-021-05154-1

Yavari-Ramshe, S., Ataie-Ashtiani, B., 2016. Numerical modelling of subaerial and submarine landslide-generated tsunami waves - recent advances and future challenges. Landslides, 13(6), 1325-1368. https://doi.org/10.1007/s10346-016-0734-2

Ye, L., Zeng, L., Xia, T., Lay, T., Kanamori, H., Hu, Y., 2025. Eastward progression of large strike-slip earthquakes on the western transtensional Caribbean-North America plate boundary. Journal of Geophysical Research, Solid Earth, to be submitted.

Zhang, C., Kirby ,J., Shi, F., Ma, G., Grilli, S.T., 2021a. A two-layer non-hydrostatic landslide model for tsunami generation on irregular bathymetry. 1. Theoretical basis. Ocean Modelling 159, 101749. https://doi.org/0.1016/j.ocemod.2020.101749

Zhang, C., Kirby, J., Shi, F., Ma, G., Grilli, S.T., 2021b. A two-layer non-hydrostatic landslide model for tsunami generation on irregular bathymetry. 2. Numerical discretization and model validation. Ocean Modelling 160, 101769. https://doi.org/10.1016/j.ocemod.2021.101769

Annex I – Numerical Simulations Of Tsunamis Generated By Earthquakes - Max Wave Heigths

This annex contains the results of 24 new seismic rupture scenarios, including 21 scenarios in the NW Caribbean and 3 scenarios near the Hess escarpment (SW Caribbean). Each scenario has an ID listed in the title, identical to that shown in tables 3, 7 and 9. The color scale represents the maximum water surface elevation recorded during the 24 hours of simulated propagation. The purple value corresponds to the highest wave height recorded locally. Red dots indicate virtual tsunami gauges where surface elevation profiles were computed.

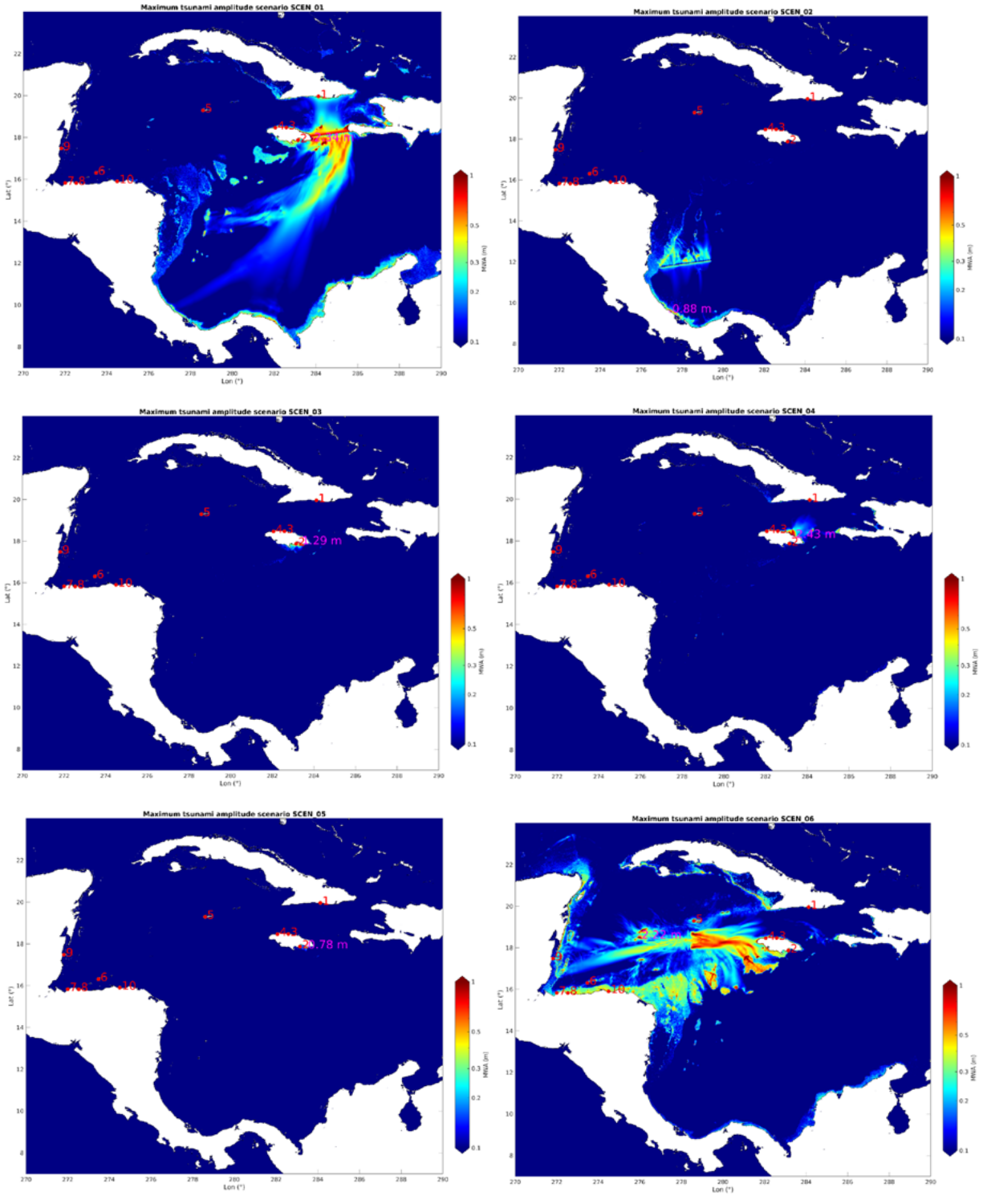

Annex II – Numerical Simulations Of Tsunamis Generated By Earthquakes – Tsunami Travel Times

This annex contains the results of 24 new seismic rupture scenarios, including 21 scenarios in the NW Caribbean and 3 scenarios near the Hess escarpment (SW Caribbean). Each scenario has an ID listed in the title, identical to that shown in tables 3, 7 and 9. The color scale represents the computed tsunami travel times with a detection threshold of 1 cm (i.e., if the wave amplitude shows less than 1 cm, there is no TTT shown on the map).

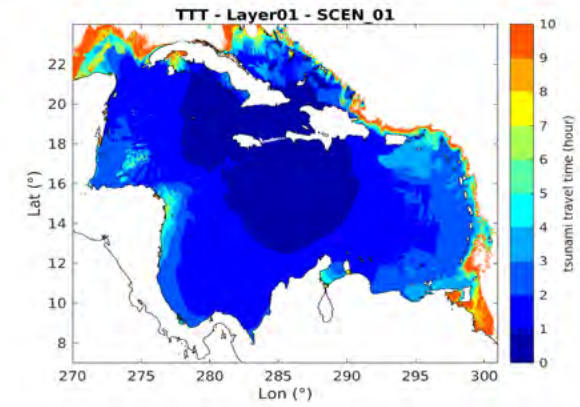

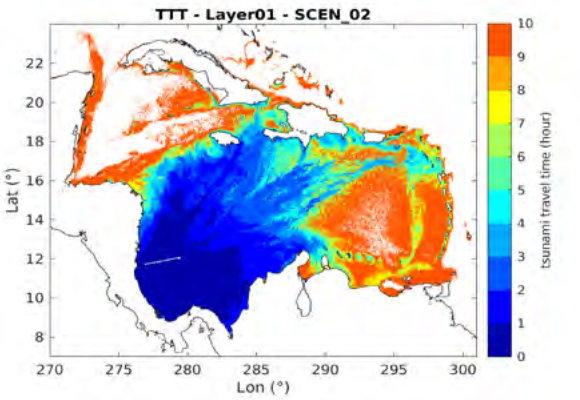

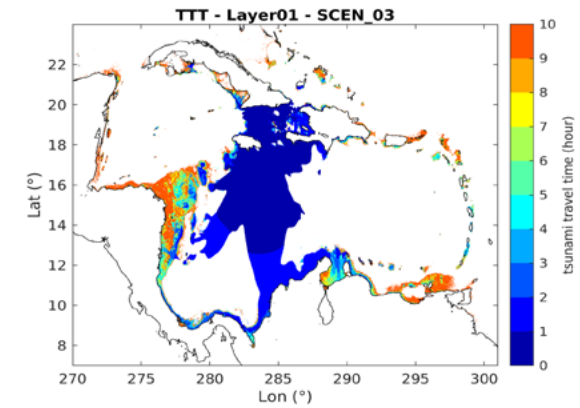

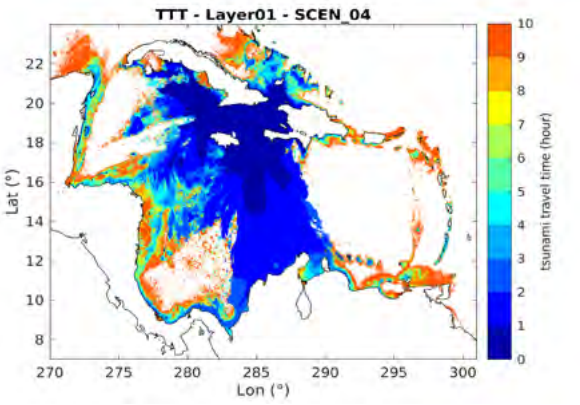

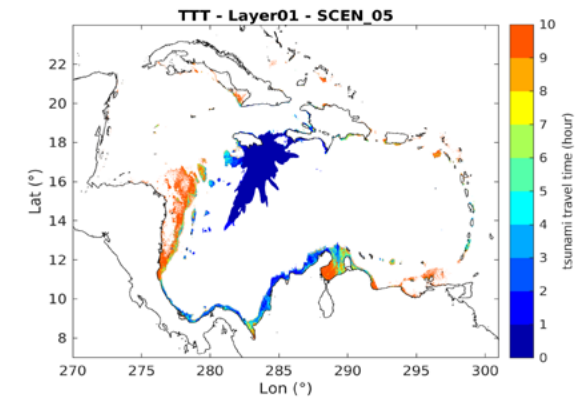

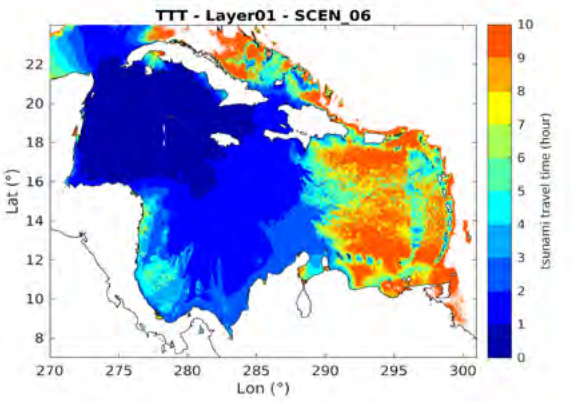

Annex III - Calibrated Submarine Landslide Method

The Calibrated Submarine Landslide (CSL) method is designed to model the initial conditions of submarine landslides for tsunami simulations. This methodology integrates (a) the slope and gradient analysis to determine optimal orientation, (b) a Gaussian height distribution calibrated to match desired volumes, and (c) elliptical or arbitrary shapes to approximate landslide geometry.

CSL method steps overview

1. Slope and Gradient Calculation:
    - Extract local topography from bathymetric data.
    - Compute slopes and gradients to identify high-slope areas.
2. Optimal Ellipse Orientation:
    - Rotate ellipse to align with high-slope areas.
    - Maximize points of interest inside the ellipse.
3. Height Distribution:
    - Use a Gaussian profile to distribute heights inside the shape.
    - Ensure total volume matches desired landslide volume.

Ellipse construction

1. Input Parameters:
    - Coordinates of the center of the ellipse (lon, lat).
    - Length of semi-axes (L, W).
    - Orientation (angle).
2. Optimization Criteria:
    - Maximize overlap with steep slopes.
    - Align with gradient directions.
3. Objective:
    - Rotate the ellipse to maximize the number of high-slope pixels inside it.

Gaussian Distribution of the slide volume

- Landslide mass follows a semi-elliptical Gaussian distribution.
- Volume calibration ensures consistency with field observations.
- This iterative approach ensures that the prescribed volume is distributed homogeneously within the ellipse.
- The total volume V of the sliding mass is then calculated by integrating h(x, y) over the area of the ellipse.
- This volume is compared to the target volume specified in the model. To achieve exact calibration, H is iteratively adjusted until the computed volume matches the target volume within a predefined tolerance.

Figure S1. Equations used to calibrate the submarine landslide geometry and illustrations of the number of iterations required to reach the targeted landslide volume.

Volume Constraint:

$$V = \int_{\text{Shape}} h(x, y)\, dx\, dy.$$

Height Distribution:

$$h(x, y) = H \cdot \exp\left(-\frac{r(x, y)^2}{2\sigma^2}\right),$$

where:

- H: Maximum height (calibrated to match V).
- $r(x, y)$: Distance from the center.
- σ: Spread parameter (controls steepness).

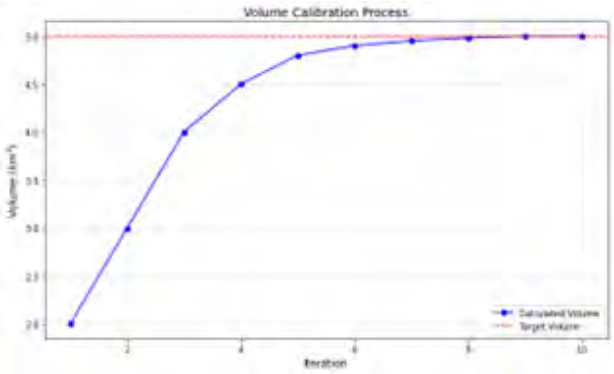

Figure S2. Comparison of the initial (left) and final (right) distribution of the thickness of the sliding mass. The initial state shows the predefined configuration of the slide, while the final state reflects its distribution after the simulation.

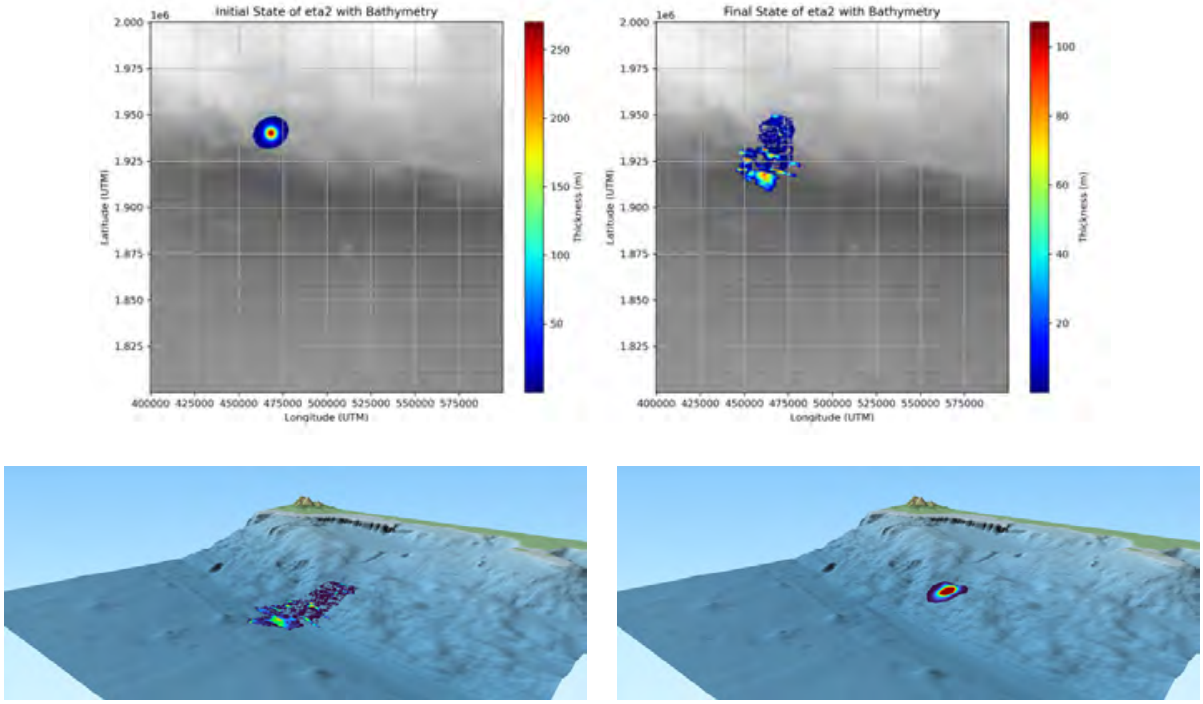

Figure S3. Topographic profiles of submarine landslides (volume V = 10 km^3) obtained using the CSL method).

A – Muertos Trough

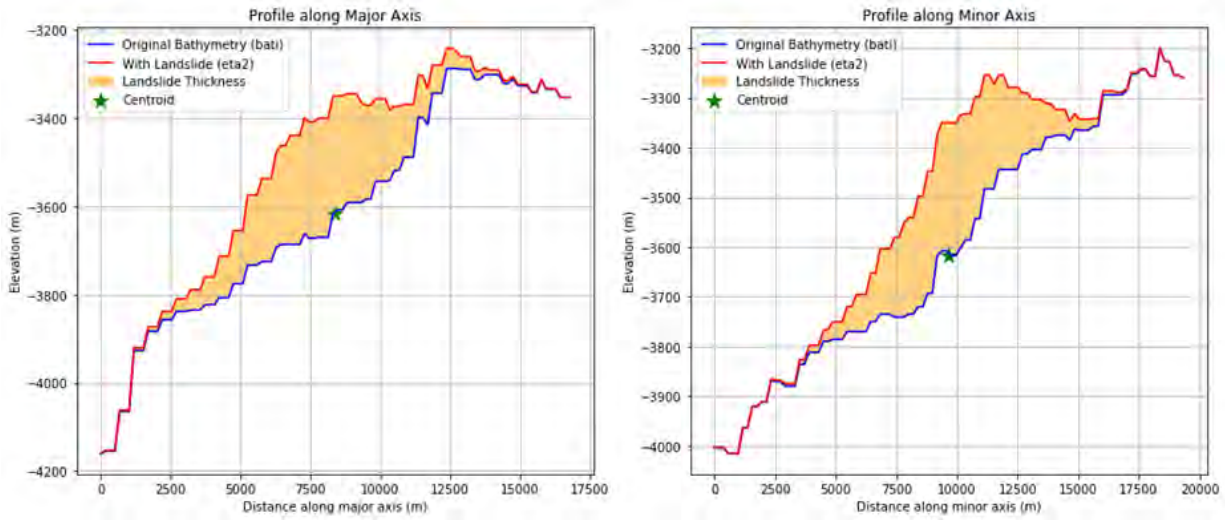

B- Cariaco Basin

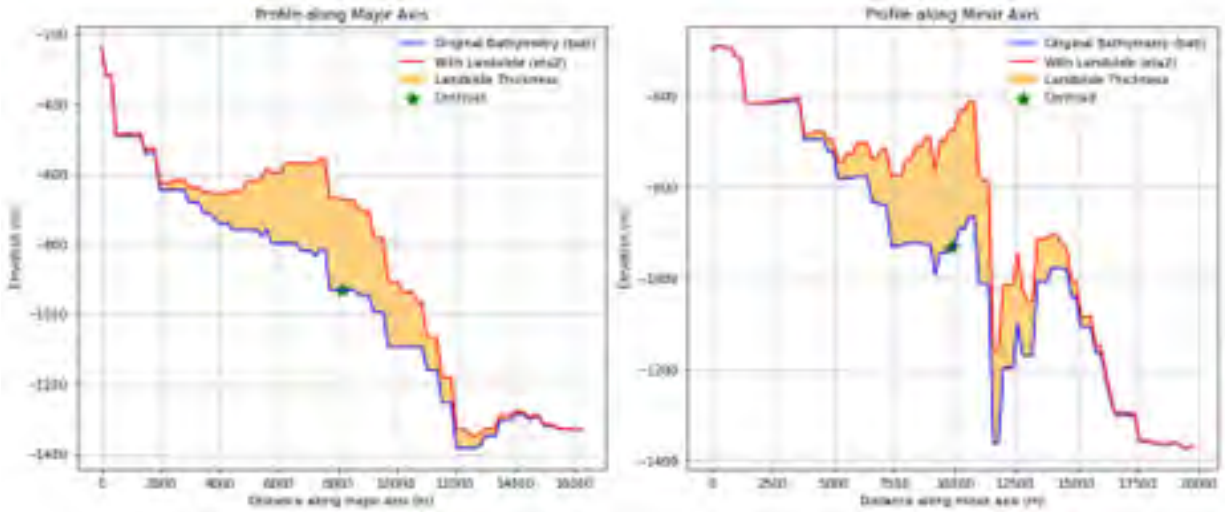

C- Desirade-Barracuda

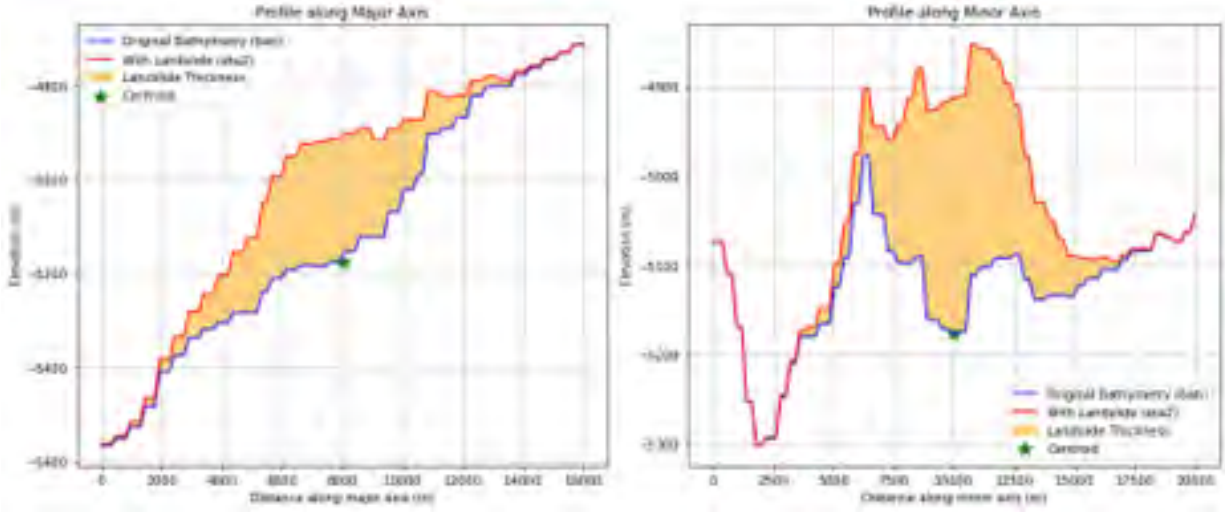

Annex IV - List of Acronyms

CATSAM	Caribbean and Adjacent Regions Tsunamis Sources and Models (NOAA)
ICG/CARIBE-EWS	Intergovernmental Coordination Group for Tsunami and Other Coastal Hazards Warning System for the Caribbean and Adjacent Regions (IOC)
ICG/NEAMTWS	Intergovernmental Coordination Group for the Tsunami Early Warning and Mitigation System in the North-Eastern Atlantic (IOC)
IPGP	Institut de Physique du Globe de Paris (France)
IOC	Intergovernmental Oceanographic Commission (UNESCO)
IODP	Integrated Ocean Drilling Program
ML	Local magnitude of an earthquake based on Richter scale
M_s	Magnitude of an earthquake calculated from surface waves
M_w	Moment magnitude of an earthquake
MVO	Montserrat volcano observatory
NOAA	National Oceanic and Atmospheric Administration (USA)
NCEI	National Center for Environmental Information (USA)
OVSICORI	Observatorio Vulcanológico y Sismológico de Costa Rica
PTHA	Probabilistic Tsunami Hazard Assessment
PTWC	Pacific Tsunami Warning Center
SCR-UWI	Seismic Research Center, University of the West Indies
SINAMOT	Sistema Nacional de Monitoreo de Tsunamis, Costa Rica
TGV	Tsunamis generated by Volcanoes
TOWS	Tsunamis and Other hazards related to sea level Warning and mitigation Systems
TT-TWO (UNESCO)	Task Team on Tsunami Watch Operations (UNESCO)
UNESCO	United Nations Educational, Scientific and Cultural Organization

Annex V - List Of Participants

Alberto Lopez (online)
University of Puerto Rico
Mayaguez, USA
alberto.lopez3@upr.edu

Anne Le Friant
Institut de Physique du Globe, CNRS
Paris, France
lefriant@ipgp.fr

Anne Lemoine
Bureau des Recherches Géologiques et Minières
Orléans, France
a.lemoine@brgm.fr

Elizabeth Vanacore
University of Puerto Rico
Mayaguez, USA
elizabeth.vanacore@upr.edu

Emile Okal
Northwestern University
Illinois, USA
e-okal@northwestern.edu

Erouscilla Joseph
University of the West Indies,
Seismological Research Center
Trinidad-and-Tobago
erouscilla.joseph@sta.uwi.edu

Frédéric Dondin
Bureau des Recherches Géologiques et Minières
Martinique, France
f.dondin@brgm.fr

Guillermo Alvarado-Induni
galvaradoinduni15@gmail.com

Jean Roger
Earth Sciences Institute of New Zealand (formerly GNS Science)
Lower Hutt, New Zealand
j.roger@gns.cri.nz

Jorge Macias
Universidad de Málaga, EDANYA
Málaga, Spain
jmacias@uma.es

Natalia Zamora (online)
Barcelona Supercomputing Center
Barcelona, Spain
nzamora@bsc.es

Nicolas Arcos
NOAA
Asheville, USA
nicolas.arcos@noaa.gov

Raphaël Paris
Université Clermont-Auvergne, LMV-CNRS, France
raphael.paris@uca.fr

Silvia Chacon-Barrantes
Universidad Nacional, SINAMOT
Heredia, Costa Rica
silvia.chacon.barrantes@una.ac.cr

Stephan Grilli
University of Rhode Island
Narragansett, USA
grilli@uri.edu

Thorne Lay (online)
University of California
Santa Cruz, USA
tlay@ucsc.edu

Uri Ten Brink
USGS
Woods Hole, USA
utenbrink@usgs.gov

Valérie Clouard
Géosciences Environnement Toulouse
Toulouse, France
valerie.clouard@get.omp.eu

Carl Bonnevie Harbitz (online)
Norwegian Geotechnical Institute
Oslo, Norway
carl.bonnevie.harbitz@ngi.no

Finn Lovholt (online)
Norwegian Geotechnical Institute
Oslo, Norway
finn.lovholt@ngi.no

Stefano Lorito (online)
Instituto Nazionale di Geofisica e Vulcanologia
Roma, Italy
stefano.lorito@ingv.it

Observers

Esteban Chaves
OVSICORI
Costa Rica
esteban.j.chaves@una.ac.cr

Fabio Rivera Cerdas
Universidad Nacional, SINAMOT
Heredia, Costa Rica
fabio.rivera.cerdas@una.ac.cr

Pedro Sandoval Alvarado
Universidad Nacional, SINAMOT
Heredia, Costa Rica
pedro.sandoval.alvarado@una.ac.cr

Secretariat

Öcal NECMIOGLU
Technical Secretary of ICG/PTWS and ICG/CARIBE EWS
IOC-UNESCO
Email: o.necmioglu@unesco.org

Annex VI - Meeting Agenda

Time	Tuesday 03/12/2024	
08:30 - 10:30	**Joint session**	
	Welcoming remarks (Ocal Necmioglu, Silvia Chacon Barrantes) **Purpose of the meeting and overview of past expert meetings** (Frédéric Dondin, Raphaël Paris) **Introduction of participants** **Presentation of CATSAM** (Nicolas Arcos, online) **Introduction to TRR program** (Silvia Chacon Barrantes)	
10:30 - 11:00	**Coffee Break**	
11:00 - 12:30	**Presentation of the Global Tsunami Model** (Finn Lovholt, online) **Tsunami hazard assessment opportunities for the Caribbean** (Natalia Zamora, online) **The example of the NEAM PTHA** (Stefano Lorito and Hong Kie Thio, on line)	
12:30 - 13:30	**Lunch Break**	
13:30 - 15:30	**Parallel sessions**	
	NW Caribbean earthquake sources	Non-seismic sources
	Overview of seismic sources of tsunamis in the NW Caribbean Region: tectonic setting and historical events (Emile Okal)	***Overview of non-seismic sources in the Caribbean Region: a state of the art from the last Expert meeting in Martinique (2019)*** (Raphaël Paris)
15:30 –16:00	**Coffee Break**	
16:00 – 17:30	All participants are then invited to present slides of their choice to illustrate the discussion	All participants are then invited to present slides of their choice to illustrate the discussion

Time	Wednesday 04/12/2024	
08:30 - 10:30	**Parallel sessions**	
	NW Caribbean earthquake sources **Discussion on the sources of tsunamis and credible scenarios** (all participants)	**Non-seismic sources** **Results of preliminary simulations of landslide tsunamis** (Jorge Macias)
10:30 - 11:00	**Coffee Break**	
11:00 - 12:30	**Definition of the parameters of new or updated scenarios to be modelled** (all participants)	**Discussion on the new sources of landslide and volcanic tsunamis to be simulated** (all participants)
12:30 - 13:30	**Lunch Break**	
13:30 - 15:30	**Parallel sessions**	
	Implementation of the input parameters for numerical models and grid parameterization (all participants)	**Designing a probabilistic submarine landslide tsunami hazard assessment for the Caribbean** (all participants)
15:30 - 16:00	**Coffee Break**	
16:00 - 17:30	**Numerical modelling session** (Jean Roger and all participants) *NB – it would be good to start preliminary simulations at this stage so that the models can run at night.*	**Designing a probabilistic volcanic tsunami hazard assessment for the Caribbean** (all participants)

Time	Thursday 05/12/2024
08:30 - 10:30	**Joint sessions**
	Summary Presentations from Parallel Sessions **Discussion on the preliminary results of numerical modelling and further improvements** (all **Discussion on the selection of new volcanic tsunami scenarios** (all participants) *NB – volcanic tsunami models are already available in the literature and could be used as reference scenarios*
10:30 - 11:00	**Coffee Break**
11:00 - 12:30	**Joint session**
	Discussion on hybrid scenarios combining earthquake and landslide sources (all participants)
12:30 - 13:30	**Lunch Break**
13:30 - 15:30	**Joint session**
	Summary Report of the session on seismic sources **Summary Report of the session on non-seismic sources**
15:30 - 16:00	**Coffee Break**
16:00 - 17:30	**Final joint session**
	Joint review and discussion on the outcomes of the parallel sessions **Deadlines for the preparation of the report** **Conclusions**

IOC Workshop Reports

The Scientific Workshops of the Intergovernmental Oceanographic Commission are sometimes jointly sponsored with other intergovernmental or non-governmental bodies. In most cases, IOC assures responsibility for printing, and copies may be requested from:

Intergovernmental Oceanographic Commission – UNESCO
1, rue Miollis, 75732 Paris Cedex 15, France

No.	Title	Languages
1	CCOP-IOC, 1974, Metallogenesis, Hydrocarbons and Tectonic Patterns in Eastern Asia (Report of the IDOE Workshop on); Bangkok, Thailand, 24-29 September 1973 UNDP (CCOP),	E (out of stock)
2	CICAR Ichthyoplankton Workshop, Mexico City, 16-27 July 1974 (UNESCO Technical Paper in Marine Sciences, No. 20).	E (out of stock) S (out of stock)
3	Report of the IOC/GFCM/ICSEM International Workshop on Marine Pollution in the Mediterranean; Monte Carlo, 9-14 September 1974.	E,F E (out of stock)
4	Report of the Workshop on the Phenomenon known as 'El Niño'; Guayaquil, Ecuador, 4-12 December 1974.	E (out of stock) S (out of stock)
5	IDOE International Workshop on Marine Geology and Geophysics of the Caribbean Region and its Resources; Kingston, Jamaica, 17-22 February 1975	E (out of stock) S
6	Report of the CCOP/SOPAC-IOC IDOE International Workshop on Geology, Mineral Resources and Geophysics of the South Pacific; Suva, Fiji, 1-6 September 1975.	E
7	Report of the Scientific Workshop to Initiate Planning for a Co-operative Investigation in the North and Central Western Indian Ocean, organized within the IDOE under the sponsorship of IOC/FAO (IOFC)/UNESCO/ EAC; Nairobi, Kenya, 25 March-2 April 1976.	E, F,S, R
8	Joint IOC/FAO (IPFC)/UNEP International Workshop on Marine Pollution in East Asian Waters; Penang, 7-13 April 1976	E (out of stock)
9	IOC/CMG/SCOR Second International Workshop on Marine Geoscience; Mauritius 9-13 August 1976.	E, F, S, R
10	IOC/WMO Second Workshop on Marine Pollution (Petroleum) Monitoring; Monaco, 14-18 June 1976	E, F E (out of stock) R
11	Report of the IOC/FAO/UNEP International Workshop on Marine Pollution in the Caribbean and Adjacent Regions; Port of Spain, Trinidad, 13-17 December 1976.	E, S (out of stock)
11 Suppl.	Collected contributions of invited lecturers and authors to the IOC/FAO/UNEP International Workshop on Marine Pollution in the Caribbean and Adjacent Regions; Port of Spain, Trinidad, 13-17 December 1976	E (out of stock), S
12	Report of the IOCARIBE Interdisciplinary Workshop on Scientific Programmes in Support of Fisheries Projects; Fort-de-France, Martinique, 28 November-2 December 1977.	E, F, S
13	Report of the IOCARIBE Workshop on Environmental Geology of the Caribbean Coastal Area; Port of Spain, Trinidad, 16-18 January 1978.	E, S
14	IOC/FAO/WHO/UNEP International Workshop on Marine Pollution in the Gulf of Guinea and Adjacent Areas; Abidjan, Côte d'Ivoire, 2-9 May 1978	E, F
15	CPPS/FAO/IOC/UNEP International Workshop on Marine Pollution in the South-East Pacific; Santiago de Chile, 6-10 November 1978.	E (out of stock)
16	Workshop on the Western Pacific, Tokyo, 19-20 February 1979.	E, F, R
17	Joint IOC/WMO Workshop on Oceanographic Products and the IGOSS Data Processing and Services System (IDPSS); Moscow, 9-11 April 1979.	E
17 suppl.	Papers submitted to the Joint IOC/WMO Seminar on Oceano-graphic Products and the IGOSS Data Processing and Services System; Moscow, 2-6 April 1979.	E
18	IOC/UNESCO Workshop on Syllabus for Training Marine Technicians; Miami, U.S.A., 22-26 May 1978 (UNESCO reports in marine sciences, No. 4 published by the Division of Marine Sciences, UNESCO).	E (out of stock), F, S (out of tock), R
19	IOC Workshop on Marine Science Syllabus for Secondary Schools; Llantwit Major, Wales, U.K., 5-9 June 1978 (UNESCO reports in marine sciences, No. 5, published by the Division of Marine Sciences, UNESCO).	E (out of stock), S, R, Ar
20	Second CCOP-IOC Workshop on IDOE Studies of East Asia Tectonics and Resources; Bandung, Indonesia, 17-21 October 1978	E
21	Second IDOE Symposium on Turbulence in the Ocean; Liège, Belgium, 7-18 May 1979.	E, F, S, R
22	Third IOC/WMO Workshop on Marine Pollution Monitoring; New Delhi, 11-15 February 1980.	E, F, S, R
23	WESTPAC Workshop on the Marine Geology and Geophysics of the North-West Pacific; Tokyo, 27-31 March 1980.	E, R
24	WESTPAC Workshop on Coastal Transport of Pollutants; Tokyo, Japan, 27-31 March 1980.	E (out of stock)
25	Workshop on the Inter-calibration of Sampling Procedures of the IOC/ WMO UNEP Pilot Project on Monitoring Background Levels of Selected Pollutants in Open-Ocean Waters; Bermuda, 11-26 January 1980.	E (Superseded by IOC Technical Series No.22)
26	IOC Workshop on Coastal Area Management in the Caribbean Region; Mexico City, 24 September- 5 October 1979.	E, S
27	CCOP/SOPAC-IOC Second International Workshop on Geology, Mineral Resources and Geophysics of the South Pacific; Nouméa, New Caledonia, 9-15 October 1980.	E
28	FAO/IOC Workshop on the effects of environmental variation on the survival of larval pelagic fishes. Lima, 20 April-5 May 1980.	E
29	WESTPAC Workshop on Marine Biological Methodology; Tokyo, 9-14 February 1981.	E
30	International Workshop on Marine Pollution in the South-West Atlantic; Montevideo, 10-14 November 1980.	E (out of stock) S
31	Third International Workshop on Marine Geoscience; Heidelberg, 19-24 July 1982.	E, F, S
32	UNU/IOC/UNESCO Workshop on International Co-operation in the Development of Marine Science and the Transfer of Technology in the context of the New Ocean Regime; Paris, France, 27 September-1 October 1982.	E, F, S
32 Suppl.	Papers submitted to the UNU/IOC/ UNESCO Workshop on International Co-operation in the Development of Marine Science and the Transfer of Technology in the Context of the New Ocean Regime; Paris, France, 27 September-1 October 1982.	E
33	Workshop on the IREP Component of the IOC Programme on Ocean Science in Relation to Living Resources (OSLR); Halifax, 26-30 September 1963.	E
34	IOC Workshop on Regional Co-operation in Marine Science in the Central Eastern Atlantic (Western Africa); Tenerife, 12-17 December 1963.	E, F, S
35	CCOP/SOPAC-IOC-UNU Workshop on Basic Geo-scientific Marine Research Required for Assessment of Minerals and Hydrocarbons in the South Pacific; Suva, Fiji, 3-7 October 1983.	E
36	IOC/FAO Workshop on the Improved Uses of Research Vessels; Lisbon, Portugal, 28 May-2 June 1984.	E
36 Suppl.	Papers submitted to the IOC/FAO Workshop on the Improved Uses of Research Vessels; Lisbon, 28 May-2 June 1984	E
37	IOC/UNESCO Workshop on Regional Co-operation in Marine Science in the Central Indian Ocean and Adjacent Seas and Gulfs; Colombo, 8-13 July 1985.	E
38	IOC/ROPME/UNEP Symposium on Fate and Fluxes of Oil Pollutants in the Kuwait Action Plan Region; Basrah, Iraq, 8-12 January 1984.	E
39	CCOP (SOPAC)-IOC-IFREMER-ORSTOM Workshop on the Uses of Submersibles and Remotely Operated Vehicles in the South Pacific; Suva, Fiji, 24-29 September 1985.	E
40	IOC Workshop on the Technical Aspects of Tsunami Analysis, Prediction and Communications; Sidney, B.C., Canada, 29-31 July 1985.	E
40 Suppl.	First International Tsunami Workshop on Tsunami Analysis, Prediction and Communications, Submitted Papers; Sidney, B.C., Canada, 29 July-1 August 1985.	E
41	First Workshop of Participants in the Joint FAO/IOC/WHO/IAEA/UNEP Project on Monitoring of Pollution in the Marine Environment of the West and Central African Region (WACAF/2); Dakar, Senegal, 28 October- 1 November 1985.	E
43	IOC Workshop on the Results of MEDALPEX and Future Oceano-graphic Programmes in the Western Mediterranean; Venice, Italy, 23-25 October 1985.	E
44	IOC-FAO Workshop on Recruitment in Tropical Coastal Demersal Communities; Ciudad del Carmen, Campeche, Mexico, 21-25 April 1986.	E (out of stock) S
44 Suppl.	IOC-FAO Workshop on Recruitment in Tropical Coastal Demersal Communities, Submitted Papers; Ciudad del Carmen, Campeche, Mexico, 21-25 April 1986.	E
45	IOCARIBE Workshop on Physical Oceanography and Climate; Cartagena, Colombia, 19-22 August 1986.	E
46	Reunión de Trabajo para Desarrollo del Programa "Ciencia Oceánica en Relación a los Recursos No Vivos en la Región del Atlántico Sud-occidental"; Porto Alegre, Brasil, 7-11 de abril de 1986.	S
47	IOC Symposium on Marine Science in the Western Pacific: The Indo-Pacific Convergence; Townsville, 1-6 December 1966	E
48	IOCARIBE Mini-Symposium for the Regional Development of the IOC-UN (OETB) Programme on 'Ocean Science in Relation to Non-Living Resources (OSNLR)'; Havana, Cuba, 4-7 December 1986.	E, S
49	AGU-IOC-WMO-CPPS Chapman Conference: An International Symposium on 'El Niño'; Guayaquil, Ecuador, 27-31 October 1986.	E
50	CCALR-IOC Scientific Seminar on Antarctic Ocean Variability and its Influence on Marine Living Resources, particularly Krill (organized in collaboration with SCAR and SCOR); Paris, France, 2-6 June 1987.	E
51	CCOP/SOPAC-IOC Workshop on Coastal Processes in the South Pacific Island Nations; Lae, Papua-New Guinea, 1-8 October 1987.	E
52	SCOR-IOC-UNESCO Symposium on Vertical Motion in the Equatorial Upper Ocean and its Effects upon Living Resources and the Atmosphere; Paris, France, 6-10 May 1985.	E
53	IOC Workshop on the Biological Effects of Pollutants; Oslo, 11-29 August 1986.	E
54	Workshop on Sea-Level Measurements in Hostile Conditions; Bidston, UK, 28-31 March 1988.	E
55	IBCCA Workshop on Data Sources and Compilation, Boulder, Colorado, 18-19 July 1988.	E
56	IOC-FAO Workshop on Recruitment of Penaeid Prawns in the Indo-West Pacific Region (PREP); Cleveland, Australia, 24-30 July 1988.	E
57	IOC Workshop on International Co-operation in the Study of Red Tides and Ocean Blooms; Takamatsu, Japan, 16-17 November 1987.	E
58	International Workshop on the Technical Aspects of the Tsunami Warning System; Novosibirsk, USSR, 4-5 August 1989.	E
58 Suppl.	Second International Workshop on the Technical Aspects of Tsunami Warning Systems, Tsunami Analysis, Preparedness,	E

No.	Title	Languages
	Observation and Instrumentation. Submitted Papers; Novosibirsk, USSR, 4-5 August 1989.	
59	IOC-UNEP Regional Workshop to Review Priorities for Marine Pollution Monitoring Research, Control and Abatement in the Wider Caribbean; San José, Costa Rica, 24-30 August 1989.	E, F, S
60	IOC Workshop to Define IOCARIBE-TRODERP proposals; Caracas, Venezuela, 12-16 September 1989.	E
61	Second IOC Workshop on the Biological Effects of Pollutants; Bermuda, 10 September-2 October 1988.	E
62	Second Workshop of Participants in the Joint FAO-IOC-WHO-IAEA-UNEP Project on Monitoring of Pollution in the Marine Environment of the West and Central African Region; Accra, Ghana, 13-17 June 1988.	E
63	IOC/WESTPAC Workshop on Co-operative Study of the Continental Shelf Circulation in the Western Pacific; Bangkok, Thailand, 31 October-3 November 1989.	E
64	Second IOC-FAO Workshop on Recruitment of Penaeid Prawns in the Indo-West Pacific Region (PREP); Phuket, Thailand, 25-31 September 1989.	E
65	Second IOC Workshop on Sardine/Anchovy Recruitment Project (SARP) in the Southwest Atlantic; Montevideo, Uruguay, 21-23 August 1989.	E
66	IOC ad hoc Expert Consultation on Sardine/ Anchovy Recruitment Programme; La Jolla, California, U.S.A., 1989	E
67	Interdisciplinary Seminar on Research Problems in the IOCARIBE Region; Caracas, Venezuela, 28 November-1 December 1989.	E (out of stock)
68	International Workshop on Marine Acoustics; Beijing, China, 26-30 March 1990.	E
69	IOC-SCAR Workshop on Sea-Level Measurements in the Antarctica; Leningrad, USSR, 28-31 May 1990.	E
69 Suppl.	IOC-SCAR Workshop on Sea-Level Measurements in the Antarctica; Submitted Papers; Leningrad, USSR, 28-31 May 1990.	E
70	IOC-SAREC-UNEP-FAO-IAEA-WHO Workshop on Regional Aspects of Marine Pollution; Mauritius, 29 October - 9 November 1990.	E
71	IOC-FAO Workshop on the Identification of Penaeid Prawn Larvae and Postlarvae; Cleveland, Australia, 23-28 September 1990.	E
72	IOC/WESTPAC Scientific Steering Group Meeting on Co-Operative Study of the Continental Shelf Circulation in the Western Pacific; Kuala Lumpur; Malaysia, 9-11 October 1990.	E
73	Expert Consultation for the IOC Programme on Coastal Ocean Advanced Science and Technology Study; Liège, Belgium, 11-13 May 1991.	E
74	IOC-UNEP Review Meeting on Oceanographic Processes of Transport and Distribution of Pollutants in the Sea; Zagreb, Yugoslavia, 15-18 May 1989.	E
75	IOC-SCOR Workshop on Global Ocean Ecosystem Dynamics; Solomons, Maryland, U.S.A., 29 April-2 May 1991.	E
76	IOC/WESTPAC Scientific Symposium on Marine Science and Management of Marine Areas of the Western Pacific; Penang, Malaysia, 2-6 December 1991.	E
77	IOC-SAREC-KMFRI Regional Workshop on Causes and Consequences of Sea-Level Changes on the Western Indian Ocean Coasts and Islands; Mombasa, Kenya, 24-28 June 1991.	E
78	IOC-CEC-ICES-WMO-ICSU Ocean Climate Data Workshop Goddard Space Flight Center; Greenbelt, Maryland, U.S.A., 18-21 February 1992.	E
79	IOC/WESTPAC Workshop on River Inputs of Nutrients to the Marine Environment in the WESTPAC Region; Penang, Malaysia, 26-29 November 1991.	E
80	IOC-SCOR Workshop on Programme Development for Harmful Algae Blooms; Newport, U.S.A. 2-3 November 1991.	E
81	Joint IAPSO-IOC Workshop on Sea Level Measurements and Quality Control; Paris, France, 12-13 October 1992.	E
82	BORDOMER 92: International Convention on Rational Use of Coastal Zones. A Preparatory Meeting for the Organization of an International Conference on Coastal Change; Bordeaux, France, 30 September-2 October 1992.	E
83	IOC Workshop on Donor Collaboration in the Development of Marine Scientific Research Capabilities in the Western Indian Ocean Region; Brussels, Belgium, 12-13 October 1992.	E
84	Workshop on Atlantic Ocean Climate Variability; Moscow, Russian Federation, 13-17 July 1992	E
85	IOC Workshop on Coastal Oceanography in Relation to Integrated Coastal Zone Management; Kona, Hawaii, 1-5 June 1992.	E
86	International Workshop on the Black Sea; Varna, Bulgaria, 30 September – 4 October 1991	E
87	Taller de trabajo sobre efectos biológicos del fenómeno «El Niño» en ecosistemas costeros del Pacífico Sudeste; Santa Cruz, Galápagos, Ecuador, 5-14 de octubre de 1989.	S only (summary in E, F, S)
88	IOC-CEC-ICSU-ICES Regional Workshop for Member States of Eastern and Northern Europe (GODAR Project); Obninsk, Russia, 17-20 May 1993.	E
89	IOC-ICSEM Workshop on Ocean Sciences in Non-Living Resources; Perpignan, France, 15-20 October 1990.	E
90	IOC Seminar on Integrated Coastal Management; New Orleans, U.S.A., 17-18 July 1993.	E
91	Hydroblack'91 CTD Intercalibration Workshop; Woods Hole, U.S.A., 1-10 December 1991.	E
92	Réunion de travail IOCEA-OSNLR sur le Projet « Budgets sédimentaires le long de la côte occidentale d'Afrique » Abidjan, côte d'Ivoire, 26-28 juin 1991.	E
93	IOC-UNEP Workshop on Impacts of Sea-Level Rise due to Global Warming. Dhaka, Bangladesh, 16-19 November 1992.	E
94	BMTC-IOC-POLARMAR International Workshop on Training Requirements in the Field of Eutrophication in Semi-enclosed Seas and Harmful Algal Blooms, Bremerhaven, Germany, 29 September-3 October 1992.	E
95	SAREC-IOC Workshop on Donor Collaboration in the Development of Marine Scientific Research Capabilities in the Western Indian Ocean Region; Brussels, Belgium, 23-25 November 1993.	E
96	IOC-UNEP-WMO-SAREC Planning Workshop on an Integrated Approach to Coastal Erosion, Sea Level Changes and their Impacts; Zanzibar, United Republic of Tanzania, 17-21 January 1994.	E
96 Suppl.	IOC-UNEP-WMO-SAREC Planning Workshop on an Integrated Approach to Coastal Erosion, Sea Level Changes and their Impacts; Submitted Papers 1. Coastal Erosion; Zanzibar, United Republic of Tanzania 17-21 January 1994.	E
96 Suppl	IOC-UNEP-WMO-SAREC Planning Workshop on an Integrated Approach to Coastal Erosion, Sea Level Changes and their Impacts; Submitted Papers 2. Sea Level; Zanzibar, United Republic of Tanzania 17-21 January 1994.	E
97	IOC Workshop on Small Island Oceanography in Relation to Sustainable Economic Development and Coastal Area Management of Small Island Development States; Fort-de-France, Martinique, 8-10 November, 1993.	E
98	CoMSBlack '92A Physical and Chemical Intercalibration Workshop; Erdemli, Turkey, 15-29 January 1993.	E
99	IOC-SAREC Field Study Exercise on Nutrients in Tropical Marine Waters; Mombasa, Kenya, 5-15 April 1994.	E
100	IOC-SOA-NOAA Regional Workshop for Member States of the Western Pacific - GODAR-II (Global Oceanographic Data Archeology and Rescue Project); Tianjin, China, 8-11 March 1994.	E
101	IOC Regional Science Planning Workshop on Harmful Algal Blooms; Montevideo, Uruguay, 15-17 June 1994.	E
102	First IOC Workshop on Coastal Ocean Advanced Science and Technology Study (COASTS); Liège, Belgium, 5-9 May 1994.	E
103	IOC Workshop on GIS Applications in the Coastal Zone Management of Small Island Developing States; Barbados, 20-22 April 1994.	E
104	Workshop on Integrated Coastal Management; Dartmouth, Canada, 19-20 September 1994.	E
105	BORDOMER 95: Conference on Coastal Change; Bordeaux, France, 6-10 February 1995.	E
105 Suppl.	Conference on Coastal Change: Proceedings; Bordeaux, France, 6-10 February 1995	E
106	IOC/WESTPAC Workshop on the Paleographic Map; Bali, Indonesia, 20-21 October 1994.	E
107	IOC-ICSU-NIO-NOAA Regional Workshop for Member States of the Indian Ocean - GODAR-III; Dona Paula, Goa, India, 6-9 December 1994.	E
108	UNESCO-IHP-IOC-IAEA Workshop on Sea-Level Rise and the Multidisciplinary Studies of Environmental Processes in the Caspian Sea Region; Paris, France, 9-12 May 1995.	E
108 Suppl.	UNESCO-IHP-IOC-IAEA Workshop on Sea-Level Rise and the Multidisciplinary Studies of Environmental Processes in the Caspian Sea Region; Submitted Papers; Paris, France, 9-12 May 1995.	E
109	First IOC-UNEP CEPPOL Symposium; San José, Costa Rica, 14-15 April 1993.	E
110	IOC-ICSU-CEC regional Workshop for Member States of the Mediterranean - GODAR-IV (Global Oceanographic Data Archeology and Rescue Project) Foundation for International Studies, University of Malta, Valletta, Malta, 25-28 April 1995.	E
111	Chapman Conference on the Circulation of the Intra-Americas Sea; La Parguera, Puerto Rico, 22-26 January 1995.	E
112	IOC-IAEA-UNEP Group of Experts on Standards and Reference Materials (GESREM) Workshop; Miami, U.S.A., 7-8 December 1993.	E
113	IOC Regional Workshop on Marine Debris and Waste Management in the Gulf of Guinea; Lagos, Nigeria, 14-16 December 1994.	E
114	International Workshop on Integrated Coastal Zone Management (ICZM) Karachi, Pakistan; 10-14 October 1994.	E
115	IOC/GLOSS-IAPSO Workshop on Sea Level Variability and Southern Ocean Dynamics; Bordeaux, France, 31 January 1995	E
116	IOC/WESTPAC International Scientific Symposium on Sustainability of Marine Environment: Review of the WESTPAC Programme, with Particular Reference to ICAM, Bali, Indonesia, 22-26 November 1994.	E
117	Joint IOC-CIDA-Sida (SAREC) Workshop on the Benefits of Improved Relationships between International Development Agencies, the IOC and other Multilateral Inter-governmental Organizations in the Delivery of Ocean, Marine Affairs and Fisheries Programmes; Sidney B.C., Canada, 26-28 September 1995.	E
118	IOC-UNEP-NOAA-Sea Grant Fourth Caribbean Marine Debris Workshop; La Romana, Santo Domingo, 21-24 August 1995.	E
119	IOC Workshop on Ocean Colour Data Requirements and Utilization; Sydney B.C., Canada, 21-22 September 1995.	E
120	International Training Workshop on Integrated Coastal Management; Tampa, Florida, U.S.A., 15-17 July 1995.	E
121	Atelier régional IOC-CERESCOR sur la gestion intégrée des zones littorales (ICAM), Conakry, Guinée, 18–22 décembre 1995	F
122	IOC-EU-BSH-NOAA-(WDC-A) International Workshop on Oceanographic Biological and Chemical Data Management, Hamburg, Germany, 20-23 May 1996	E
123	Second IOC Regional Science Planning Workshop on Harmful Algal Blooms in South America; Mar del Plata, Argentina, 30 October–1 November 1995.	E, S
124	GLOBEC-IOC-SAHFOS-MBA Workshop on the Analysis of Time Series with Particular Reference to the Continuous Plankton Recorder Survey; Plymouth, U.K.,4-7 May 1993.	E
125	Atelier sous-régional de la COI sur les ressources marines vivantes du Golfe de Guinée ; Cotonou, Bénin, 1-4 juillet 1996.	E

No.	Title	Languages
126	IOC-UNEP-PERSGA-ACOPS-IUCN Workshop on Oceanographic Input to Integrated Coastal Zone Management in the Red Sea and Gulf of Aden. Jeddah, Saudi Arabia, 8 October 1995.	E
127	IOC Regional Workshop for Member States of the Caribbean and South America GODAR-V (Global Oceanographic Data Archeology and Rescue Project); Cartagena de Indias, Colombia, 8-11 October 1996.	E
128	Atelier IOC-Banque Mondiale-Sida/SAREC-ONE sur la Gestion Intégrée des Zones Côtières ; Nosy Bé, Madagascar, 14-18 octobre 1996.	E
129	Gas and Fluids in Marine Sediments, Amsterdam, the Netherlands; 27-29 January 1997.	E
130	Atelier régional de la COI sur l'océanographie côtière et la gestion de la zone côtière ;Moroni, RFI des Comores, 16-19 décembre 1996.	E
131	GOOS Coastal Module Planning Workshop; Miami, USA, 24-28 February 1997	E
132	Third IOC-FANSA Workshop; Punta-Arenas, Chile, 28-30 July 1997	S/E
133	Joint IOC-CIESM Training Workshop on Sea-level Observations and Analysis for the Countries of the Mediterranean and Black Seas; Birkenhead, U.K., 16-27 June 1997.	E
134	IOC/WESTPAC-CCOP Workshop on Paleogeographic Mapping (Holocene Optimum); Shanghai, China, 27-29 May 1997.	E
135	Regional Workshop on Integrated Coastal Zone Management; Chabahar, Iran; February 1996.	E
136	IOC Regional Workshop for Member States of Western Africa (GODAR-VI); Accra, Ghana, 22-25 April 1997.	E
137	GOOS Planning Workshop for Living Marine Resources, Dartmouth, USA; 1-5 March 1996.	E
138	Gestión de Sistemas Oceanográficos del Pacífico Oriental; Concepción, Chile, 9-16 de abril de 1996.	S
139	Sistemas Oceanográficos del Atlántico Sudoccidental, Taller, TEMA;Furg, Rio Grande, Brasil, 3-11 de noviembre de 1997	S
140	IOC Workshop on GOOS Capacity Building for the Mediterranean Region; Valletta, Malta, 26-29 November 1997.	E
141	IOC/WESTPAC Workshop on Co-operative Study in the Gulf of Thailand: A Science Plan; Bangkok, Thailand, 25-28 February 1997.	E
142	Pelagic Biogeography ICoPB II. Proceedings of the 2nd International Conference. Final Report of SCOR/IOC Working Group 93; Noordwijkerhout, The Netherlands, 9-14 July 1995.	E
143	Geosphere-biosphere coupling: Carbonate Mud Mounds and Cold Water Reefs; Gent, Belgium, 7–11 February 1998.	E
144	IOC-SOPAC Workshop Report on Pacific Regional Global Ocean Observing Systems; Suva, Fiji, 13-17 February 1998.	E
145	IOC-Black Sea Regional Committee Workshop: 'Black Sea Fluxes' Istanbul, Turkey, 10-12 June 1997.	E
146	Taller Internacional sobre Formacíon de Capacidades para el Manejo de las Costas y los Oéanos en le Gran Caribe, La Habana, – Cuba, 7–10 de Julio de 1998 / International Workshop on Management Capacity-Building for Coasts and Oceans in the Wider Caribbean, Havana, Cuba, 7–10 July 1998	S/E
147	IOC-SOA International Training Workshop on the Intregration of Marine Sciences into the Process of Integrated Coastal Management, Dalian, China, 19-24 May 1997.	E
148	IOC/WESTPAC International Scientific Symposium – Role of Ocean Sciences for Sustainable Development Okinawa, Japan, 2-7 February 1998.	E
149	Workshops on Marine Debris & Waste Management in the Gulf of Guinea, 1995-97.	E
150	Primera Sesión del Grupo de Trabajo COI sobre Algas Nocivas en el Caribe y Regiones Adyacentes (IOCARIBE-ANCA)/First Meeting of the IOC Working Group on Harmful Algae in the Caribbean and Adjacent Region (IOCARIBE-ANCA), 29 June – 1 July 1998, Havana, Cuba.	S/E ***(electronic copy only)***
151	Taller Pluridisciplinario TEMA sobre Redes del Gran Caribe en Gestión Integrada de Áreas Costeras Cartagena de Indias, Colombia, 7-12 de septiembre de 1998.	S
152	Workshop on Data for Sustainable Integrated Coastal Management (SICOM) Maputo, Mozambique, 18-22 July 1998	E
153	IOC/WESTPAC-Sida (SAREC) Workshop on Atmospheric Inputs of Pollutants to the Marine Environment Qingdao, China, 24-26 June 1998	E
154	IOC-Sida-Flanders-SFRI Workshop on Ocean Data Management in the IOCINCWIO Region (ODINEA project) Capetown, South Africa, 30 November-11 December 1998.	E
155	Science of the Mediterranean Sea and its applications UNESCO, Paris 29-31 July 1997	E
156	IOC-LUC-KMFRI Workshop on RECOSCIX-WIO in the Year 2000 and Beyond, Mombasa, Kenya, 12-16 April 1999	E
157	'98 IOC-KMI International Workshop on Integrated Coastal Management (ICM), Seoul, Republic of Korea 16-18 April 1998	E
158	The IOCARIBE Users and the Global Ocean Observing System (GOOS) Capacity Building Workshop, San José, Costa Rica, 22-24 April 1999	E
159	Oceanic Fronts and Related Phenomena (Konstantin Fedorov Memorial Symposium) – Proceedings, Pushkin, Russian Federation, 18-22 May 1998	E
160	Under preparation	
161	Under preparation	
162	Workshop report on the Transports and Linkages of the Intra-americas Sea (IAS), Cozumel, Mexico, 1-5 November 1997	E
163	Under preparation	
164	IOC-Sida-Flanders-MCM Third Workshop on Ocean Data Management in the IOCINCWIO Region (ODINEA Project), Cape Town, South Africa, 29 November – 11 December 1999	E
165	An African Conference on Sustainable Integrated Management; Proceedings of the Workshops. An Integrated Approach, (PACSICOM), Maputo, Mozambique, 18 –25 July 1998	E, F
166	IOC-SOA International Workshop on Coastal Megacities: Challenges of Growing Urbanization of the World's Coastal Areas; Hangzhou, P.R. China, 27 –30 September 1999	E
167	IOC-Flanders First ODINAFRICA-II Planning Workshop, Dakar, Senegal, 2-4 May 2000	E
168	Geological Processes on European Continental Margins; International Conference and Eight Post-cruise Meeting of the Training-Through-Research Programme, Granada, Spain, 31 January – 3 February 2000	E
169	International Conference on the International Oceanographic Data & Information Exchange in the Western Pacific (IODE-WESTPAC) 1999, ICIWP '99, Langkawi, Malaysia, 1-4 November 1999	E ***(electronic copy only)***
170	IOCARIBE-GODAR-I Cartagenas, Colombia, February 2000	***under preparation***
171	Ocean Circulation Science derived from the Atlantic, Indian and Arctic Sea Level Networks, Toulouse, France, 10-11 May 1999	E
172	(*Under preparation*)	
173	The Benefits of the Implementation of the GOOS in the Mediterranean Region, Rabat, Morocco, 1-3 November 1999	E, F
174	IOC-SOPAC Regional Workshop on Coastal Global Ocean Observing System (GOOS) for the Pacific Region, Apia, Samoa, 16-17 August 2000	E
175	Geological Processes on Deep-water European Margins, Moscow-Mozhenka, 28 Jan.-2 Feb. 2001	E
176	MedGLOSS Workshop and Coordination Meeting for the Pilot Monitoring Network System of Systematic Sea Level Measurements in the Mediterranean and Black Seas, Haifa, Israel, 15-17 May 2000	E
177	*(Under preparation)*	
178	*(Under preparation)*	
179	*(Under preparation)*	
180	Abstracts of Presentations at Workshops during the 7th session of the IOC Group of Experts on the Global Sea Level Observing System (GLOSS), Honolulu, USA, 23-27 April 2001	E
181	*(Under preparation)*	
182	*(Under preparation)*	
183	Geosphere/Biosphere/Hydrosphere Coupling Process, Fluid Escape Structures and Tectonics at Continental Margins and Ocean Ridges, International Conference & Tenth Post-cruise Meeting of the Training-through-Research Programme, Aveiro, Portugal, 30 January-2 February 2002	E
184	*(Under preparation)*	
185	*(Under preparation)*	
186	*(Under preparation)*	
186	*(Under preparation)*	E
187	Geological and Biological Processes at deep-sea European Margins and Oceanic Basins, Bologna, Italy, 2–6 February 2003	E
188	Proceedings of 'The Ocean Colour Data' Symposium, Brussels, Belgium, 25-27 November 2002	E
189	Workshop for the Formulation of a Draft Project on Integrated Coastal Management (ICM) in Latin America and the Caribbean (LAC), Cartagena, Colombia, 23–25 October 2003	E F ***(electronic copy only)***
	Taller de Formulación de un Anteproyecto de Manejo Costero Integrado (MCI) en América Latina y el Caribe (ALC), Cartagena, Colombia, 23–25 de Octubre de 2003	
190	First ODINCARSA Planning Workshop for Caribbean Islands, Christchurch, Barbados, 15–18 December 2003	E ***(electronic copy only)***
191	North Atlantic and Labrador Sea Margin Architecture and Sedimentary Processes — International Conference and Twelfth Post-cruise Meeting of the Training-through-research Programme, Copenhagen, Denmark, 29–31 January 2004	E
192	Regional Workshop on Coral Reefs Monitoring and Management in the ROPME Sea Area, Iran I.R., 14–17 December 2003	E ***(under preparation)***
193	Workshop on New Technical Developments in Sea and Land Level Observing Systems, Paris, France, 14–16 October 2003	E ***(electronic copy only)***
194	IOC/ROPME Planning Meeting for the Ocean Data and Information Network for the Central Indian Ocean Region	***(under preparation)***
195	Workshop on Indicators of Stress in the Marine Benthos, Torregrande-Oristano, Italy, 8–9 October 2004	E
196	International Coordination Meeting for the Development of a Tsunami Warning and Mitigation System for the Indian Ocean within a Global Framework, Paris, France, 3–8 March 2005	E
197	Geosphere-Biosphere Coupling Processes: The TTR Interdisciplinary Approach Towards Studies of the European and North African Margins; International Conference and Post-cruise Meeting of the Training-Through-Research Programme, Morocco, 2-5 February 2005	E
198	Second International Coordination Meeting for the Development of a Tsunami Warning and Mitigation System for the Indian Ocean, Grand Baie, Mauritius, 14–16 April 2005	E
199	International Conference for the Establishment of a Tsunami and Coastal Hazards Warning System for the Caribbean and Adjacent Regions, Mexico, 1–3 June 2005	E
200	Lagoons and Coastal Wetlands in the Global Change Context: Impacts and Management Issues — Proceedings of the International Conference, Venice, 26–28 April 2004 (*ICAM Dossier N° 3)*	E
201	Geological processes on deep-water European margins - International Conference and 15th Anniversary Post-cruise Meeting of the Training-Through-Research Programme, Moscow/Zvenigorod, Russian Federation, 29 January–4 February 2006	E
202	Proceedings of 'Ocean Biodiversity Informatics': an international conference on marine biodiversity data management Hamburg, Germany, 29 November–1 December 2004	E
203	IOC-Flanders Planning Workshop for the formulation of a regional Pilot Project on Integrated Coastal Area Management in Latin America, Cartagena de Indias, Colombia, 16–18 January 2007	***E (electronic copy only)***
204	Geo-marine Research along European Continental Margins, International Conference and Post-cruise Meeting of the Training-through-research Programme, Bremen, Germany, 29 January–1 February 2007	E
205	IODE/ICAM Workshop on the development of the Caribbean marine atlas (CMA), United Nations House, Bridgetown, Barbados, 8–10 October 2007	E ***(electronic copy only)***
206	IODE/JCOMM Forum on Oceanographic Data Management and Exchange Standards, Ostend, Belgium, 21–25 January 2008	*(Under preparation)*
207	SCOR/IODE Workshop on Data Publishing, Ostend, Belgium, 17–18 June 2008	*(Under preparation)*

No.	Title	Languages
208	JCOMM Technical Workshop on Wave Measurements from Buoys, New York, USA, 2–3 October 2008 (IOC-WMO publication)	*(Under preparation)*
209	Collaboration between IOC and OBIS towards the Long-term Management Archival and Accessibility of Ocean Biogeographic Data, Ostend, Belgium, 24–26 November 2008	*(Under preparation)*
210	Ocean Carbon Observations from Ships of Opportunity and Repeat Hydrographic Sections (IOCCP Reports, 1), Paris, France, 13–15 January 2003	E ***(electronic copy only)***
211	Ocean Surface pCO_2 Data Integration and Database Development (IOCCP Reports, 2), Tsukuba, Japan, 14–17 January 2004	E ***(electronic copy only)***
212	International Ocean Carbon Stakeholders' Meeting, Paris, France, 6–7 December 2004	E ***(electronic copy only)***
213	International Repeat Hydrography and Carbon Workshop (IOCCP Reports, 4), Shonan Village, Japan, 14–16 November 2005	E ***(electronic copy only)***
214	Initial Atlantic Ocean Carbon Synthesis Meeting (IOCCP Reports, 5), Laugavatn, Iceland, 28–30 June 2006	E ***(electronic copy only)***
215	Surface Ocean Variability and Vulnerability Workshop (IOCCP Reports, 7), Paris, France, 11–14 April 2007	E ***(electronic copy only)***
216	Surface Ocean CO2 Atlas Project (SOCAT) 2nd Technical Meeting Report (IOCCP Reports, 9), Paris, France, 16–17 June 2008	E ***(electronic copy only)***
217	Changing Times: An International Ocean Biogeochemical Time-Series Workshop (IOCCP Reports, 11), La Jolla, California, USA, 5–7 November 2008	E ***(electronic copy only)***
218	Second Joint GOSUD/SAMOS Workshop, Seattle, Washington, USA, 10–12 June 2008	E ***(electronic copy only)***
219	International Conference on Marine Data management and Information Systems (IMDIS), Athens, Greece, 31 March–2 April 2008	E
220	Geo-marine Research on the Mediterranean and European-Atlantic Margins. International Conference and TTR-17 Post-cruise Meeting of the Training-through-research Programme, Granada, Spain, 2–5 February 2009	E ***(electronic copy only)***
221	Surface Ocean CO_2 Atlas Project Pacific Regional Workshop, Tsukuba, Japan, 18-20 March, 2009 (IOCCP Report Number 12)	E ***(electronic copy only)***
222	Surface Ocean CO_2 Atlas Project Atlantic and Southern Oceans Regional Meeting, Norwich, UK, 25-26 June, 2009 (IOCCP Report Number 13)	E ***(electronic copy only)***
223	Advisory Workshop on enhancing forecasting capabilities for North Indian Ocean Storm Surges, Indian Institute of Technology (IIT), New Delhi, India, 14–17 July 2009	E ***(electronic copy only)***
224	2009 International Nutrients Scale System (INSS) Workshop Report, Paris, France, 10–12 February 2009	E ***(electronic copy only)***
225	Reunión subregional de planificación de ODINCARSA (Red de Datos e Información Oceanográficos para las Regiones del Caribe y América del Sur)/ ODINCARSA (Ocean Data and Information Network for the Caribbean and South America region) Latin America sub-regional Planning Meeting, Universidad Autónoma de Baja California (UABC), Ensenada (México), 7-10 December 2009. 2010	E/S ***(electronic copy only)***
226	OBIS (Ocean Biogeographic Information System) Strategy and Work plan Meeting, IOC Project Office for IODE, Oostende, Belgium, 18–20 November 2009	E ***(electronic copy only)***
227	ODINAFRICA-IV Project Steering Committee, First Session, Ostend, Belgium, 20–22 January 2010. 2010	E ***(electronic copy only)***
228	First IODE Workshop on Quality Control of Chemical Oceanographic Data Collections, Ostend, Belgium, 8–11 February 2010. 2010	E ***(electronic copy only)***
229	Surface Ocean CO_2 Atlas Project Equatorial Pacific, North Pacific, and Indian Ocean Regional Workshop, Tokyo, Japan, 8–11 February 2010. 2010 (IOCCP Report Number 18)	E ***(electronic copy only)***
230	SCOR/IODE/MBLWHOI Library Workshop on Data Publication, Paris, France, 2 April 2010	E ***(electronic copy only)***
231	First ODINAFRICA Coastal and Marine Atlases Planning Meeting, Ostend, Belgium, 12–14 October 2009	E ***(electronic copy only)***
232	Eleventh International Workshop on Wave Hindcasting and Forecasting and Second Coastal Hazard Symposium, Halifax, Canada, 18–23 October 2009	E ***(electronic copy only)***
233	2010 Meeting of the Joint IODE-JCOMM Steering Group on the Global Temperature-Salinity Profile Programme Ostend, Belgium, 5–7 May 2010	E ***(electronic copy only)***
234	Southern and Indian Surface Ocean CO_2 Atlas (SOCAT) Workshop, CSIRO Marine Laboratories, Hobart, Tasmania 16-18 June 2010	E ***(electronic copy only)***
235	The Caribbean Marine Atlas (CMA) Review and Planning Workshop and Saint Lucia National Coastal Atlas Stakeholder Event, Bay Gardens Inn, Rodney Bay, Saint Lucia, 2–6 August 2010	E ***(electronic copy only)***
236	First Session of the IODE Steering Group for the IODE OceanDataPortal (SG-ODP-I), 20–22 September 2010, Ostend, Belgium	E ***(electronic copy only)***
237.	Ad hoc meeting of the IODE Steering Group for OBIS, Ostend, Belgium 18-19 November 2010	E ***(electronic copy only)***
238.	Implementing Adaptation to Climate Change in Western and Eastern Africa, Nairobi, Kenya, 3-5 November 2010	E ***(electronic copy only)***
239.	2nd Advisory Workshop on enhancing forecasting capabilities for North Indian Ocean Storm Surges, 11-15 February 2011, New Delhi, India	E ***(electronic copy only)***
240.	Ocean Biogeographic Information System (OBIS) Infrastructure Meeting, INCOIS, Hyderabad, India, 2–4 March 2011.	E ***(electronic copy only)***
241.	Best Practice on Tsunami and Coastal Hazards Community Preparedness and Readiness in Central America and the Caribbean, 11–13 August 2008, Panama City, Panama	E ***(electronic copy only)***
242.	Integrated Coastal Area Management (ICAM) Training Workshop for the English Speaking Caribbean States, 16–18 March 2011, Bridgetown, Barbados	E ***(electronic copy only)***
243.	Implementing Adaptation to Climate Change in Western and Eastern Africa: Targeting the Adaptation Fund. Nairobi, Kenya, 3–5 November 2010	*cancelled*
244.	SCOR/IODE/MBLWHOI Library Workshop on Data Publication, 4th Session, British Oceanographic Data Centre, Liverpool, United Kingdom, 3-4 November 2011	E ***(electronic copy only)***
245.	Surface Ocean CO2 Data-to-Flux Workshop, UNESCO, Paris, 12-14 September 2011	*cancelled*
246.	NEAMTIC/ICAM Workshop on Coastal Management Approaches for Sea-Level Related Hazards, Paris, UNESCO, 5–7 December 2011	E ***(electronic copy only)***
247.	Technical Workshop on the IODE OceanDataPortal, IOC Project Office for IODE, Ostend, Belgium, 27-29 February 2012	E ***(electronic copy only)***
248.	Inter-sessional working group for updating the IOC Strategic Plan for Oceanographic Data and Information Exchange (2012-2015), Ostend, Belgium, 1-2 March 2012	E ***(electronic copy only)***
249.	Operational Oceanography of IOC (for Group II Member States), 20–22 March 2012 Paris, UNESCO (Advisory Workshop)	E ***(electronic copy only)***
250.	Advisory Workshop on The Future of IOC towards next ten years and its Implications for Member States, Varna, Bulgaria, 19 March 2012	E ***(electronic copy only)***
251	Second Technical Meeting of Ocean Biogeographic Information System (OBIS), Ostend, Belgium, 21–22 June 2012	E ***(electronic copy only)***
252.	SCOR/IODE/MBLWHOI Library Workshop on Data Publication, 5th Session, Woods Hole Oceanographic Institution, Woods Hole, USA, 9-10 October 2012	E ***(electronic copy only)***
253.	Second IODE Workshop on Quality Control of Chemical and Biological Oceanographic Data Collections, 22-24 October 2012, IOC Project Office for IODE, Ostend, Belgium	E ***(electronic copy only)***
254.	Consultation on Scientific and Technical Aspects of Sustained Ocean Observations and Services, 5th March, 2013, Rio de Janeiro, Brazil	E ***(electronic copy only)***
255.	Earthquake and tsunami hazard in Northern Haiti: Historical events and potential sources (Meeting of experts)	E ***(electronic copy only)***
256	Sexto Taller Regional de Planificación Científica sobre Floraciones de Algas Nocivas en Sudamérica, Guayaquil, Ecuador, 22-24 Octubre 2003	S ***(electronic copy only)***
257	*(Under preparation)*	
258	*(Under preparation)*	
259	Noveno Taller Regional-COI de Planificación Científica sobre Florecimientos de Algas Nocivas en Sudamérica, 11-13 enero 2011, Puerto Varas, Chile	S ***(electronic copy only)*** *(Summary in E)*
260	*Caribbean Marine Atlas Review and Planning Meeting, Miami, USA, 10-13 December 2013*	
261	Indo-Pacific Ocean Forum on "Charting the Future of Sustained Ocean Observations and Services", Bangkok, Thailand, 25-28 Nov. 2013	E ***(electronic copy only)***
262	*First Planning Workshop For The Ocean Data And Information Network For The Westpac Region (ODINWESTPAC), Tianjin, China, 4-7 March 2014*	
263	*International Coastal Atlas Network Workshop 6: Expanding Participation in Coastal Web Atlas Development and Use, 16–17 June 2013, University of Victoria, British Columbia, Canada*	
264	9th WESTPAC International Scientific Symposium, Research Directors' Forum: A Healthy and Safe Ocean for Prosperity in the Indo-Pacific region, Nha Trang, Viet Nam, 22 April 2014	E ***(electronic copy only)***
265	Electoral Group 1 Consultation on the Future of the IOC, Utrecht, The Netherlands, 26–27 May 2014	E ***(electronic copy only)***
266	IOC-UNESCO-ISESCO workshop on Improving Tsunami Warning and Emergency Response in the North-Eastern Atlantic, Mediterranean and connected seas Rabat, 23-24 September 2014	A/E/F ***(electronic copy only)***
267	Proceedings of the First IOCAFRICA Ocean Forecasting workshop for the Western Indian Ocean region, Nairobi, Kenya, 11–15 August 2014	E ***(electronic copy only)***
268	Proceedings of the African Summer School on Application of Ocean Data and Modelling Products, Ghana, Kenya, April–September 2014	E ***(electronic copy only)***
269.	*Forum on Sustained Ocean Observations and Services in IOC Group V (Africa and Arab countries)*	E
270.	*Second China-Africa Forum on Marine Science and Technology, 9-10 April 2015, Nairobi, Kenya*	*Under preparation*
271.	WESTPAC Workshop on Research and Monitoring of the Ecological Impacts of Ocean Acidification on Coral Reef Ecosystems. Phuket, Thailand, 19–21 January 2015	E ***(electronic copy only)***
272.	Second IOCAFRICA Planning Meeting for the Second International Indian Ocean Expedition (IIOE-2), 6-8 October 2015, Catembe, Mozambique	E ***(electronic copy only)***
273.	Initiative de LOANGO : Atelier de la sous-région sur l'érosion côtière en Afrique centrale, Loango, République du Congo, 6–10 octobre 2008	F
274.	First Session of the Advisory Group for the Ocean Data and Information Network for the WESTPAC Region (ODINWESTPAC), Tianjin, China, 27-28 January 2016	E
275.	Scientific meeting of experts for coordinated scenario analysis of future tsunami events and hazard mitigation schemes for the South China Sea region, Xiamen, China, 16–18 November 2015	E
276.	Sources of Tsunamis in the Caribbean with Possibility to Impact the Southern Coast of the Dominican Republic, Santo Domingo, Dominican Republic, 6–7 May 2016	E & S
277.	VI IOC Regional Science Planning Workshop on Harmful Algae in the Caribbean and Adjacent Regions, Santo Domingo, Dominican Republic, 26-30 October 2015 / COI – VI Taller Regional de Planificación Científica sobre Algas Nocivas en el Caribe y Regiones Adyacentes, Santo Domingo, República Dominicana, 26-30 Octubre 2015	E/S
278.	Tsunami Hazard in Central America: Historical Events and Potential Sources. Meeting of Experts, San José, Costa Rica, 23-24 June 2016	E
279.	2nd International Conference on Marine/Maritime Spatial Planning, 15-17 March 2017, UNESCO, Paris	E
280.	Information Meeting on North-Eastern Atlantic, the Mediterranean and Connected Seas Tsunami Early Warning and Mitigation System (NEAMTWS) and NEAMWave 17 Tsunami Exercise: Summary Recommendations, Tunis, Tunisia, 13-14 September 2017	E/F/Ar
281.	Workshop on Sea-Level Measurements in Hostile Conditions, Moscow, Russian Federation, 13–15 March 2018	E/R
282.	IODE/OBIS-Event-Data workshop on animal tagging and tracking, Ostend, Belgium, 23–26 April 2018	E
283.	Sixth International XBT Science Workshop, Ostend, Belgium, 18–20 April 2018	E
284.	Sargassum and Oil Spills Monitoring Pilot Project for the Caribbean and Adjacent Regions Workshop, Mexico DF, Mexico, 2–4 May 2018	E
285	Drafting Workshop for the development of a training and Repository Portal for the Caribbean Large Marine Ecosystem	E

No.	Title	Languages
286.	Preparing for the Next Tsunami: Reducing Losses and Damages in the Coastal Western Mediterranean Areas: Summary Recommendations, Rabat, Morocco, 15-16 November 2018	E/F/Ar
287	Workshop on Sea level Data Archaeology, UNESCO, Paris, 10–12 March 2020	E
288	Workshop on data sharing between UN agencies as a contribution to the UN decade of ocean science for sustainable development, Online meeting, 20 April 2020, 14:00-16:30	E
289	Expert meeting on Tsunami sources, hazards, risk and uncertainties associated with the Tonga-Kermadec Subduction Zone. Wellington, New Zealand. 29 October – 3 November 2018.	E
290	International data sharing workshop for non-UN IGOs, Global and Regional organizations and projects, NGOs and private sector, Online meeting, 12 October 2020.	E
291	Experts Meeting on Sources of Tsunamis in the Lesser Antilles. Fort-de-France, Martinique (France), 18–20 March 2019	E
292	Italian Digital Mobilization Event for the United Nations Decade of Ocean Science for Sustainable Development: “Towards the Generation Ocean”, 22 October 2020, Milan, Italy	E/I
295	Expert Meeting on Tsunami Sources, Hazards, Risk and Uncertainties Associated with the Colombia-Ecuador Subduction Zone. Guayaquil, Ecuador, 27–29 January 2020	E
296	Engaging blue fishing ports in marine spatial planning: key findings of regional workshops	E
297	Best Practices in Aquaculture, EATIP-OBPS Workshop, Tuesday, 5 April 2022, (Online) – Proceedings	E
298	*Blue Curriculum: a training session – Final results and report, 1st July 2022, Lisbon*	*Under preparation*
299	*Best Practices Workshop VI, 5–19 October 2023 (online)*	*Under preparation*
300	International Forum for Marine/Maritime Spatial Planning (MSPForum), Kick-off event, 24–25 May 2018, Brussels	E
301	Marine Spatial Planning Forum (MSPForum), 26–29 March 2019, La Réunion, France	E
302	Third Marine Spatial Planning Forum (MSPForum), 12–15 May 2019, Vigo, Spain	E
303	Fourth Marine Spatial Planning Forum (MSPForum), 19–21 November 2019; Riga, Latvia	E
304	Regional MSPforum for Africa (1st edition), 8–9 December 2022 (online)	E
305	Regional MSPforum for Latin America and The Caribbean (1st edition), 12–13 December 2022 (online)	E
306	Regional MSPforum for Western Pacific and its Adjacent Areas (1st edition), 16 December 2022 (online)	E
307	Fifth international Forum on Marine/Maritime Spatial Planning (MSPforum), 21 November 2022, Barcelona, Spain	E
308	Third International Conference on Marine/Maritime Spatial Planning, 22–23 November 2022, Barcelona, Spain + Supplement: Abstracts	E
309	MSPglobal 2.0 Online Kick-off Conference, 6 September 2023	
310	Feuille de route d’un Plan d’Espace Marin aux Comores : Initialiser le processus (Atelier du 22 au 25 novembre 2021, Moroni)	F
311	*First IODE/GOOS Data Workshop Ostend, Belgium, 30 September – 2 October 2024*	*Under preparation*
312	OceanPractices: Ocean Best Practices Workshop VII & Focus Sessions, 9-20 October 2023. Proceedings	E
313	Second MSPforum for Africa; 5th – 6th November 2023, Dar-es-Salaam, Tanzania	E
314	Sixth international Forum on Marine/Maritime Spatial Planning (MSPforum), 8–11 October 2024, Bali, Republic of Indonesia	E
315	Expert Meeting on Tsunami Sources, Hazards, Risk and Uncertainties Associated with the Vanuatu, Solomon and New Britain Subduction Zones, 14–17 May 2024	E
316	Stimulating Ocean Best Practices: Dialogues across Science and Technology for Innovative Solutions and Effective Governance. Ocean Best Practices Workshop VIII, 14–18 October 2024 [online]. Proceedings	E
317	MSPglobal Online Conference: 2.0 Closing & 3.0 Kick-off, 4 September 2025	E
318	Expert meeting on seismic sources of tsunamis in the NW Caribbean and non-seismic sources in the Caribbean Region, Heredia, Costa Rica, 3–5 December 2024	E

Expert meeting on seismic sources of tsunamis in the NW Caribbean and non-seismic sources in the Caribbean Region

WORKSHOP REPORT NO. 318

unesco
Intergovernmental
Oceanographic
Commission

Tsunami Ready